New Weapon from an Ancient Tree

- Antifungal protein ginkbilobin binds actin

Zur Erlangung des akademischen Grades eines

DOKTORS DER NATURWISSENSCHAFTEN

(Dr. rer. nat.)

Fakultät für Chemie und Biowissenschaften

Karlsruher Institut für Technologie (KIT)-Universitätsbereich

genehmigte

DISSERTATION

von

Ningning Gao

aus

Weifang, China

Dekan: Prof. Dr. Peter Roesky

Referent: Prof. Dr. Peter Nick

Korreferent: Prof. Dr. Anne S. Ulrich

Tag der mündlichen Prüfung: 11. Juli. 2014

Die vorliegende Dissertation wurde am Botanischen Institut des Karlsruher Instituts für Technologie (KIT), Botanisches Institut, Lehrstuhl 1 für Molekulare Zellbiologe, im Zeitraum von September 2011 bis Juli 2014 angefertigt.

Hiermit erkläre ich, dass ich die vorliegende Dissertation, abgesehen von der Benutzung der angegebenen Hilfsmittel, selbständig verfasst habe.

Alle Stellen, die gemäß Wortlaut oder Inhalt aus anderen Arbeiten entnommen sind, wurden durch Angabe der Quelle als Entlehnungen kenntlich gemacht.

Diese Dissertation liegt in gleicher oder ähnlicher Form keiner anderen Prüfungsbehörde vor.

Karlsruhe, im Juni 2014

Ningning Gao

Acknowledgments

The dissertation was conducted in Botanical Institute 1 from September 2011 to July 2014. I would like to take this opportunity to thank all those who helped me during my study.

First of all, I would like to thank Prof. Peter Nick to give me the precious opportunity to challenge and enhance myself. I really appreciate all the time, patience and trust he devoted, all the suggestions and ideas he provided in supervising me on this project. His enthusiasm, optimism, kindness, courage and insight will inspire me for the rest of my life.

I am grateful that Prof. Anne S. Ulrich agreed to be my co-examiner immediately and I really appreciate her time, devotion and expertise.

My special thanks to Prof. Dr. Anne S. Ulrich, Dr. Parvesh Wadhwani and Philipp Mühlhäuser from Institute of Biological Interfaces (IBG-2), Karlsruhe Institute of Technology for synthesizing the cell-penetrating peptides for us.

I especially thank Dr. Michael Riemann, Dr. Jan Maisch and Dr. Kai Eggenberger for their help and suggestions during my work as well as Dr. Michael Riemann for critical reading of this thesis. I appreciate the excellent work of our lab technician Sabine Purper and Sybille Wörner.

My thanks also go to all the members working in Botanical Institute 1 for such a friendly and helpful working atmosphere. I sincerely thank Qiong Liu for her support and accompany and she always helps me to tide over my difficulties. My heartfelt thanks extend to Mohamed, Rita, Katharina, Fan, Natalie, Sebastian, Thomas, Sahar and Max whom I always get help and learn from so many times. And thanks to my Chinese colleagues for their constant help and encouragement

in my daily life.

Finally, I would like to thank my parents, my brother and my husband for their unconditional love, support and understanding through all these years.

This work was supported by the DFG-Center of Functional Nanostructure (CFN, projects E1.2 and E1.5) and the China Scholarship Council (CSC).

Ningning Gao

Table of Contents

Abbreviations

2, 4-D: 2, 4-dichlorophenoxyacetic acid

ASB: Actin stabilizing buffer

BY-2: Tobacco *Nicotiana tabacum* L. cv. bright yellow 2

CPPs: Cell-penetrating peptides

Cys: Cysteine

DMSO: Dimethyl sulfoxide

ETI: Effector-triggered immunity

FABD2: Fimbrin actin-binding domain 2

FL: Full length

GFP: Green fluorescent protein

Gnk: Ginkbilobin

HR: Hypersensitive response

IAA: Indolyl-3-acetic acid

Lat B: Latrunculin B

MS-Medium: Murashige and Skoog medium

MT: Microtubule

NSP: Non-signal peptide

NP: Nuclear position

NPA: 1-N-naphthylphthalamic acid

PBS: Phosphate buffered saline

PCD: Programmed cell death

Pha: Phalloidin

PTI: PAMP-triggered immunity

RFP: Red fluorescent protein

RhB: Rhodamine B

RLKs: Receptor-like kinase

SP: Signal peptide

ΔSP: Full-length ginkbilobin-2 without the signal peptide

TRITC: Tetramethylrhodamine B isothiocyanate

Zusammenfassung

Ginkbilobin ist ein kurzes, fungizides Protein, das aus Samen des lebenden Fossils *Ginkgo biloba* gereinigt und kloniert wurde. Homologe dieses Proteins kommen in allen Samenpflanzen und dem Farn *Selaginella* vor. Die Anordnung von Domänen, Peptidmotiven und spezifischen Cysteinsignaturen sind in den unterschiedlichen Homologen konserviert.

Um einen Einblick in die zelluläre Funktion der konservierten Motive zu erlangen, haben wir GFP-Fusionen des vollständigen und Teilen des Proteins Ginkbilobin transient und stabil in Tabak BY-2 Zellen experimiert. Das Signalpeptid des vollständigen Proteins bewirkt seinen effizienten Export aus der Zelle. Wird das Signalpeptid verdeckt oder abgespalten, bindet Ginkbilobin-GFP ans Aktinzellskelett und kann es so indirekt sichtbar machen. Wir konnten die Aktin-bindende Aktivität von Ginkbilobin auf eine spezifische Subdomäne hinter dem Signalpeptid eingrenzen. Wird diese Unterdomäne stabil überexprimiert, kann man eine spezifische Verzögerung in der prämitotischen Positionierung des Zellkerns beobachten, was auf eine eingeschränkte Dynamik von perinukleären Aktinbündeln hinweist. Die durch diese Domäne verursachte Aktinbündelung beeinträchtigt die Synchronizität der Zellteilung, ein Effekt, der durch Zugabe des polar transportierten Auxins Indol-3-Essigsäure (IAA) aufgehoben werden kann.

Um die zelluläre Reaktion der Bindung dieser Subdomäne an Aktin aufzuklären, verwenden wir Chemical Engineering, basierend auf synthetischen Peptiden, die aus Konjugaten von unterschiedlichen Teilen der Aktin-bindenden Subdomäne mit dem zellpermeierenden Peptid BP100 und Rhodamin B als fluoreszenten Marker bestehen. Durch die Bindung dieses synthetischen Konstrukts an Aktin wird sehr wirksam Zelltod induziert. Bei geringeren Konzentrationen wird das Konjugat von BP100 mit der spezifischen Domäne in die lebende Zelle transportiert und bindet dort an Aktin. Die Aufnahme des konjugierten Peptids in

die Zelle wird durch Phytotropine wie IAA und NPA so wie durch Aktindrogen (Latrunculin B and Phalloidin) beeinflusst. Wir entwickeln aus diesen Ergebnissen ein Arbeitsmodell, in dem Ginkbilobin das Aktinzellskelett der Zielzelle behindern kann und auf diese Weise einen evolutionär konservierten Apoptoseweg aktiviert.

Abstract

Ginkbilobin is a short antifungal protein that had been purified and cloned from the seeds of the living fossil *Ginkgo biloba*. Homologues of this protein can be detected in all seed plants and the heterosporic fern *Selaginella*, and are conserved with respect to domain structures, peptide motifs, and specific cysteine signatures.

To get insight into the cellular functions of these conserved motifs we expressed GFP fusions of full-length and truncated ginkbilobin in tobacco BY-2 cells. We show that the signal peptide confers efficient secretion of ginkbilobin. When this signal peptide is either cleaved or masked, ginkbilobin binds and visualizes the actin cytoskeleton. We can locate this actin-binding activity of ginkbilobin to a specific subdomain just downstream of the signal peptide. Upon stable overexpression of this domain, we observe a specific delay in premitotic nuclear positioning indicative of a reduced dynamicity of perinuclear actin cables. And the actin-bundling of this domain impairs the synchrony of cell division, whereas in addition of the polarly transported auxin indole-3-acetic acid restored the synchrony.

To elucidate the cellular response of the binding of this subdomain to actin, we use chemical engineering based on synthetic peptides comprising different parts of the actin-binding subdomain conjugated with the cell-penetrating peptide BP100 and with rhodamine B as a fluorescent reporter. Binding of this synthetic construct to actin efficiently induces cell death. At lower concentrations, the specific domain peptide in fusion with BP100 can be delivered into the living cells and binds to actin. The cellular uptake of the conjugated peptides is affected by phytotropins (IAA and NPA) and actin drugs (latrunculin B and phalloidin). We discuss these findings in terms of a working model, where ginkbilobin can interfere with the actin cytoskeleton of the target cell to activate an evolutionarily conserved apoptotic pathway.

1. Introduction

1.1 Ginkbilobin: a new weapon from *Ginkgo biloba*

Ginkgo biloba is one of the most primitive extant seed plants and is regarded as a 'living fossil'. It harbours a broad spectrum of resistance or tolerance to many pathogens and herbivores. *Ginkgo* anatomy, structure and growth of the shoot apex and internal secretory structures have been studied since the beginning of the last century (Shaw, 1908; Mundry and Stutzel, 2006). This unique tree and the antifungal protein ginkbilobin cloned from the seed of it will be described in the following paragraphs.

1.1.1 The *Ginkgo* tree

Dating back more than 270 million years, *Ginkgo biloba*, the only species remaining from the family Ginkgoaceae, is one of the most ancestral lines in the gymnosperms often referred to as a 'living fossil' because it is known to have existed early in the Jurassic period. Because its leaves resemble the maidenhair fern, it is also known as the maidenhair tree (Jacobs and Browner, 2000). The key identifying features of *Ginkgo biloba* are motile sperm within the pollen tube and archegonia in the megagametophyte within ovule (Friedman, 1993; Zhang, 1998; An *et al.*, 2007). These specific structures define *Ginkgo* as primitive living gymnosperms and highlight their unique male and female gametophyte development and fertilization. And the gametophytes must undergo an elaborate maturation process taking 4.5 months (Zhang *et al.*, 2013). Unrelated to any other living plant species, it grows throughout China, Korea, Japan, Europe, and the United States. *Ginkgo* trees can be up to 100 feet tall, 50 feet in circumference, and can live up to 2500 years. After the nuclear bomb was detonated in Hiroshima, they were the first plants to re-grow and were free of signs of genetic mutation (Jacobs and Browner, 2000).

In fact, *Ginkgo* seems to be highly resistant or tolerant to many pathogens and herbivores, which may be the reason why this unique tree can live up to thousand years. This species is rich in pharmacologically active compounds that are also exploited for medical applications, including antioxidant, neurotransmitter/ receptor modulator and anti-platelet activating activities (for review see Diamond et al., 2000). A jasmonate-dependent defensin gene (Shen *et al.*, 2005), and a chitin binding antimicrobial protein (Huang *et al.*, 2000) cloned and purified from *Ginkgo biloba* leaves provide further evidence for efficient inducible basal immunity in this species. In fact, seeds of *Ginkgo biloba* contain high levels of the antifungal protein ginkbilobin (Wang and Ng, 2000) that exhibits sequence similarity to embryo-abundant proteins mainly from gymnosperms, and a homology with the extracellular domain of angiosperm cysteine-rich receptor-like kinases (Sawano *et al.*, 2007; Liu *et al.*, 2010).

1.1.2 Ginkbilobin homology to extracellular domain of receptor-like kinase

Receptor-like kinases are key pattern-recognition receptors (PRRs) for microbe- and plant-derived molecular patterns that are associated with pathogen attack (Wu and Zhou, 2013). Last several years, substantial efforts have been conducted to investigate the function of the RLKs. RLKs participate in a wide range of processes, including self-incompatibility, disease resistance, regulation of development and hormone perception (Shiu and Bleecker, 2001). RLKs are one of the largest protein families in plant. Normally, they contain a signal peptide at the N-terminus, an extracellular domain, a transmembrane region, and a C-terminal domain with eukaryotic protein kinase signatures (van der Geer *et al.*, 1994). The *Arabidopsis* genome contains more than 600 RLKs members, and rice has nearly twice as many such members as *Arabidopsis* does (Shiu *et al.*, 2004). Plant RLKs are grouped into four classes according to sequence motifs of their extracellular receptor domains (Hardie, 1999). The first class of RLKs is characterized by the Leu-rich repeat (LRR) which is involved in protein to protein interaction (Walker, 1994). The second class represents homologues of S-domain

RLKs (SRKs) of Brassicaceae with a characteristic array of Cys residues and other conserved motifs that are presumably involved in self-incompatibility (Stein *et al.*, 1991; Walker, 1994). The third class contains a lectin-like extracellular domain that may bind oligosaccharides, such as the elicitors derived from breakdown of the cell wall (Herve *et al.*, 1996). Wak1 from *Arabidopsis* is the only gene present in the fourth class that contains extracellular sequence repeats related to mammalian epidermal growth factors (Kohorn *et al.*, 1992). Other types of extracellular domains of *Arabidopsis* RLKs such as PR5 proteins that accumulate in the extracellular space are expressed in response to infection by microbial pathogens (Wang *et al.*, 1996). Studies of phytopathogenic molecular structures and their receptors have provided crucial insight into the co-evolution between plants and pathogens.

The angiosperm homologues of ginkbilobin share the characteristic feature of receptor-like kinases, such as the N-terminal signal peptide, an extracellular domain (which is the domain exhibiting the homology with ginkbilobin), a transmembrane region, and a C-terminal domain with eukaryotic kinase signatures (for review see van der Geer et al., 1994). Ginkbilobin has been purified in two versions – the full-length protein contains a signal peptide and is termed ginkbilobin-2, while the first discovered ginkbilobin-1 is a fragment lacking the signal peptide and the C-terminal half of the protein harbouring a characteristic cysteine signature, which is conserved between all plant homologues of ginkbilobin including the angiosperm receptor-like kinases (Wang and Ng, 2000; Sawano *et al.*, 2007).

1.2 Evolution of plant defence

Due to expose to a large number of threatening pathogens and insects, plants have evolved different mechanisms for self-defence, such as the production of secondary metabolites or defence-related proteins. *Ginkgo* as the ancient seed plant would serve as a precious model to address the question about the

evolution of seed immunity. General concepts of plant immunity and the evolution of defence mechanisms in lower plants will be discussed in the following sections.

1.2.1 Plant immunity

Plants as sessile organisms cannot run away when they are attacked, nor can they rely on mobile defence cells that constitute the core of animal immunity. Instead, plant defence, is based upon the innate immunity of individual cells. This innate immunity is composed of two layers (Jones and Dangl, 2006): on the one side is a very general basal defence which can be triggered by microbial associated molecular patterns (MAMPs) and activate the production of secondary metabolites or proteins with antimicrobial activity. Specialized pathogens have adapted to this host response by so-called effector molecules which can suppress this basal defence, such that the pathogen can invade the host cell. On the other side, during the co-evolution with these pathogens, some host plants have acquired specific receptors that can recognize the microbial effectors and reactivate defence. As final response to microbial invasion, this effector-triggered immunity (ETI) can culminate in programmed cell death (PCD). Cell-death related immunity is a very effective strategy to kill or at least to contain the intruder, but it is a meaningful strategy only in organisms, where cells have developed a high degree of functional cooperation. Cell-death related immunity is therefore not expected in most of the algae, where true multicellularity has not been fully unfolded, but must have evolved later, during the evolution of terrestrial plants. Nonetheless, there is evidence for a second, possibly independent development of cell-death related immunity in the kelps, macroalgae that have developed true multicellularity as well (for review see Weinberger, 2007).

1.2.2 Defence tools in early land plants

During evolution, plants have developed mechanisms to cope with different stress, including pathogen infection. Secretion of toxic compounds is considered to be the primary and most ancient tool of defence. In fact, there is a rich literature

describing such compounds from lower plants including mosses, ferns, and algae. Production and secretion of these compounds is expected to be inducible for mainly two reasons: (a) It sequesters considerable metabolic activity, which is thus not available for normal growth and development, and (b) these compounds are toxic, so one strategy to evade auto-intoxication of the producer cell or tissue is to strictly confine the production of these compounds to the time when they are needed, and to the location where they are needed.

Mosses are one of the oldest land plants that are rarely infected by bacteria and fungi. They lack shields like cuticle or bark to protect themselves against microbial infections, but they use chemical weapons to defend themselves. Fungistatic and fungitoxic compounds are released when a fungal spore falls on bryophyte thallus or leaf, inhibiting spore germination. This chemical weapon is one of their life strategies to be survived for more than 350 million years (Frahm, 2004). Mosses are known to contain a range of secondary metabolites. The *P. patens* genome has been duplicated 30 and 60 million years ago, and metabolic genes seem to have been retained in excess following duplication, leading probably, in part, to the high versatility of moss metabolism (Rensing *et al.*, 2007). Some of these metabolites, such as flavonoids, have played important roles in the adaptation of plants to land, to cope with a variety of stresses, including ultraviolet-B (UV-B) radiation, desiccation stress and co-evolving herbivores and pathogens (Ponce de Leon and Montesano, 2013).

Pteridophytes are not infected by microbial pathogens, which may be one of the important factors for the evolutionary success of pteridophytes and the fact that they survived for more than 350 million years (Sharma and Vyas, 1985). Many ferns have been used as medicinal plants since ancient times. The extensive survey of antibiotic activity among the ferns conducted and about a hundred species could be used in preparation of improved herbal or drug formulations (Banerjee and Sen, 1980). Phytochemicals from pteridophytes show very potent

antimicrobial properties. Many species of *Selaginella* have cytotoxic activity and each species with such activity contains bioflavonoids (Lin *et al.*, 2000; Zhang *et al.*, 2012). Ferns collected from the Aravalli hills (Rajasthan, India) have antibacterial activity against the phytopathogen, *Agrobacterium tumefaciens*, and human pathogens, *Salmonella arizonae*, *E. coli* and *Salmonella typhi* (all MTCC strains) (Parihar *et al.*, 2010).

Macroalgae which lack cell-based inducible immune responses, enhance their fitness via chemical defences against microbes. This hypothesis could explain why macroscopic algae are rarely infected, despite constant exposure to potentially deleterious microorganisms (Kohlmeyer, 1971). The antimicrobial compounds produced from algae provide an effective chemical defence against ecologically important microbes (Hornsey and Hide, 1974; Kubanek *et al.*, 2003). Animals and vascular plants defend pathogens with innate receptors mediating their resistance. Macroalgae defend microbes mainly using their chemical compounds. While pathogen-activated or pathogen-induced macroalgal defence was detected two decades ago, it revealed major functional similarities among the defence systems of distant macroalgal clades and the innate immune systems of vascular plants and metazoans. However, the molecular concept of macroalgal receptor-mediated immunity needs to be complemented to develop a joint ecological perspective on seaweed-microbe interactions (Weinberger, 2007).

The invention of seeds as mobile and robust means for gene has flow confronted plant defence with a new challenge: as an adaptation to propagation function, maturating seeds shut down metabolic activity almost completely. A structure that is densely packed with rich biological resources and at the same time is metabolically inactive, represents a very attractive target for microbial attack. Since, under these circumstances, inducible defence does not provide an efficient strategy to ward off pathogens from seeds, seed plants (and possibly already the heterosporic ferns, such as *Selaginella*) must have evolved constitutive protection

against fungal attack. *Ginkgo biloba* as a 'living fossil' represents one of the most ancestral lines in the gymnosperms and therefore might serve as an interesting model to address the question about the evolution of seed immunity. The general question of seed immunity is even accentuated in *Ginkgo biloba*, because the immature seed is shed several months before fertilization actually takes place, which means that the delicate gametophytes have to survive for a long period a midst the progressively rotten fleshy tissue.

1.3 Fungal growth and responses

1.3.1 Role of actin in hyphal growth

Fungi are divided into two big groups: yeasts and moulds. Yeasts are solitary rounded forms that reproduce by making more rounded forms through mechanisms such as budding or fission. Moulds, on the other hand, have bodies composed of thread-like long cells called hyphae. Thus, moulds are also known as filamentous fungi.

Fungi form long, tube-like hyphae, which show extreme polarized growth from the tip. A continuous flow of secretion vesicles from the hyphal cell body to the growing hyphal tip is essential for cell wall and membrane extension. Microtubules (MT) and actin, together with their corresponding motor proteins, are involved in the process. And the arrangement of the cytoskeleton is a crucial step to establish and maintain polarity. In *Saccharomyces cerevisiae* and *Schizosaccharomyces pombe*, actin-mediated vesicle transportation is sufficient for polar cell extension, but in *S. pombe*, MTs are in addition required for the establishment of polarity (Fischer *et al.*, 2008). In single cell yeasts, such as in budding yeast *Saccharomyces cerevisiae* and in fission yeast *Schizosaccharomyces pombe*, polarized growth is restricted to certain times during the cell cycle, whereas in filamentous fungi, such as *Aspergillus nidulans* or *Neurospora crassa*, cell extension is a continuous and indefinite process (Snell

and Nurse, 1994; Pringle *et al.*, 1995; Riquelme *et al.*, 2003).

Polarized growth depends on the actin cytoskeleton, which consists of cortical actin patches and actin cables (Pruyne and Bretscher, 2000a). The polymerization of actin to form the patch ultrastructure is considered to be the driving force for generating endocytic vesicles by pulling the membrane inwards, but the formation also serves well as a structural scaffold (Ayscough *et al.*, 1997; Kaksonen *et al.*, 2003; Huckaba *et al.*, 2004). Actin cables are targeted specifically to polarity sites, which are protein assemblies that direct new cell growth (Casamayor and Snyder, 2002), and which facilitate appropriate endocytosis and exocytosis in these regions (Pruyne and Bretscher, 2000b). Actin cables are thought to form tracks along which the class V myosin, Myo2, and its regulatory light chain, Mlc1, transport secretory vesicles that contain the raw materials and enzymes for the synthesis of new cell walls and cell membranes in the growing bud (Johnston *et al.*, 1991; Schott *et al.*, 1999; Karpova *et al.*, 2000). Polarization of the actin cytoskeleton is ultimately by the Cdc42 GTPase, which localizes to the incipient bud site and the bud tip (Wendland and Philippsen, 2001; Bassilana and Arkowitz, 2006).

1.3.2 Actin mediated apoptosis in fungi

In fungi the actin cytoskeleton is involved in numerous cellular processes including: cell polarity, cytokinesis, endocytosis, exocytosis, bud site selection, cell wall remodelling and cell shape determination (Drubin *et al.*, 1988; Kubler and Riezman, 1993; Karpova *et al.*, 1998; Torralba *et al.*, 1998; Pruyne and Bretscher, 2000a; Harris, 2006). The regulation of actin assembly and disassembly is under the control of complex signaling systems that link external signals to remodeling events, which result in altered cellular activities that adapt cell shape or behaviour to suit new environmental conditions. Actin and ABPs are convincingly placed within signaling networks regulating commitment to apoptosis.

A range of studies have revealed that actin plays a key role in apoptosis/PCD regulation from the animal, plant and fungal Kingdoms. Recent data suggests that the activity of actin regulatory proteins such as gelsolin, cofilin/ADF (actin-depolymerization factor), coronin and β-thymosins play a crucial role in the regulation of apoptosis in animal cells (Franklin-Tong and Gourlay, 2008). Inhibitors of actin polymerization, such as cytochalasin, which causes depolymerization of actin microfilaments, have been demonstrated to prevent defence responses, alterations in actin polymerization status can be a general mechanism used by plants to mediate PCD (Tomiyama *et al.*, 1982; Skalamera and Heath, 1998). It has been reported that, as has been found in many mammalian and plant cells, the stabilization of cortical actin structures induces apoptosis in yeast (Gourlay *et al.*, 2004). Mutations in actin regulatory proteins that lead to the accumulation of aggregates of stabilized F-actin have been shown to trigger a process termed 'actin mediated apoptosis' in *Saccharomyces cerevisiae* (Gourlay and Ayscough, 2005, 2006). It has been proposed that the dynamics of actin polymerization may be responsible for modulating apoptotic signaling cascades.

Ras signaling may be a conserved mechanism by which yeasts are able to regulate cell death. The production of the secondary messenger cAMP is carried out by an adenylyl cyclase, Cyr1p, and can be stimulated by two mechanisms. One is the G protein-coupled receptor GPR1-GPA2 system (Thevelein *et al.*, 2005). The second is through binding of GTP-bound Ras and adenylyl cyclase-associated (Srv2p/CAP) proteins (Toda *et al.*, 1985). Elevation of cAMP levels leads to dissociation of the protein kinase A (PKA) regulator Bcy1p to yield active A kinases which elicit alterations in processes such as cell cycle progression and stress responses (Thevelein, 1992). A strong correlation between ROS accumulation, apoptosis, and the dynamic state of the actin cytoskeleton exists in yeast (Gourlay *et al.*, 2004). Evidence to support this from data showing that the pathogenic yeast *Candida albicans* has been shown

regulate apoptosis via Ras/cAMP signaling (Phillips *et al.*, 2003; Phillips *et al.*, 2006). And an actin-mediated apoptosis pathway also exists in *Saccharomyces cerevisiae* which is likely to arise from a tight interaction between the cytoskeleton and the Ras signaling pathway (Gourlay and Ayscough, 2006).

1.4 Bypassing the membrane barrier by BP100

Cell-penetrating peptides (CPPs) are generally short cationic peptides, such as β-peptides or peptoids, which have amphipathic α-helical conformations that are attracted by the anionic cell surface and can eventually penetrate through the hydrophobic lipid bilayer (Eggenberger *et al.*, 2011).

Peptide-based gene delivery systems have been well established that certain potential peptide carriers are able to penetrate membranes of mammalian cells (Fawell *et al.*, 1994; Simeoni *et al.*, 2003; Numata and Kaplan, 2010). These so-called CPPs are able to enter cells seemingly independent of energy and classic receptor mediated endocytosis (Lindgren *et al.*, 2000; Zorko and Langel, 2005). For plant cells, however, this new technology is still in its early stage, with several studies reporting the use of CPPs to deliver plasmid DNA into permeabilized wheat embryo (Chugh and Eudes, 2008), mung bean and soy bean roots (Chen *et al.*, 2007), and others using double-stranded RNA to induce post-transcriptional gene silencing in tobacco suspension cells (Unnamalai *et al.*, 2004). The CPP BP100 has been developed as an efficient cell penetrating tool to introduce functional cargoes such as the actin-binding Lifeact peptide (MGVADLIKKFESISKEE) into tobacco cells (Eggenberger *et al.*, 2011).

BP100 (KKLFKKILKYL-amide) is an antimicrobial peptide that was obtained by systematic mutation of Pep3 (WKLFKKILKVL-amide), a hybrid peptide derived from the naturally occurring cecropin-A (an antimicrobial peptide from the moth Hyalophora cecropia) and melittin (a membrane permeabilizing component of bee venom) (Wade *et al.*, 1992; Ferre *et al.*, 2006; Ferre *et al.*, 2009). It has

already been demonstrated that BP100 has antimicrobial activity against *Erwinia amylovora*, *Pseudomonas syringae* and *Xanthomonas vesicatoria* in vivo and in vitro (Badosa *et al.*, 2007). CPPs share two common important features: a net positive charge and the ability to assume an amphipathic structure. The net positive charge promotes their binding to the anionic cell surface, while the amphipathic structure favors peptide insertion into the membrane.

Several models have been proposed to account for the morphological changes involved in antimicrobial peptides (AMPs)-mediated membrane disruption, such as pore formation (Yang *et al.*, 2001), cell lysis (Shai, 1999), peptide translocation into the cytoplasm (Kobayashi *et al.*, 2004) or intracellular targets without membrane damage (Yeaman and Yount, 2003; Brogden, 2005; Hancock and Sahl, 2006). In such mechanisms, peptides would stress the cell membrane to traverse and reach their site of action (Ferre *et al.*, 2009). BP100 is a multifunctional membrane-active peptide of only 11 amino acids, with a high antimicrobial activity, an efficient cell-penetrating ability and low hemolytic side-effects. It forms an amphiphilic α-helix that is similar to other antimicrobial peptides like magainin (Wadhwani *et al.*, 2014). However, BP100 is not long enough to span the lipid bilayer to form transmembrane pores and can be taken up into BY-2 cells without being toxic, hence it represents an ideal test candidate for the targeted cargo delivery into plant cells (Eggenberger *et al.*, 2011).

1.5 Scope of this study

To defend against pathogen attacks, seed plants have evolved efficient strategies to protect themselves. *Ginkgo* as the ancient seed plant would provide a precious model to figure out the evolution of seed immunity. Seeds of *Ginkgo biloba* contain high levels of the antifungal protein ginkbilobin which is resistant to different fungi such as *Fusarium oxysporum*, *Trichoderma reesei*, or *Candida albicans* (Wang and Ng, 2000; Sawano *et al.*, 2007). But the cellular mechanism of growth inhibition is not clear. In this study, we put forward two main questions to work on

the antifungal protein ginkbilobin.

1. Where dose ginkbilobin and its truncated versions target in tobacco BY-2 cells?

To get insight into potential cellular targets of ginkbilobin, we expressed GFP fusions of full-length and various truncated ginkbilobin in tobacco BY-2 suspension cells. We show that the signal peptide confers efficient secretion of ginkbilobin. When this secretion is prevented by cleaving off or masking the signal peptide, ginkbilobin decorates filamentous structures. Via different covisualization strategies, it is shown that these structures are actin filaments, and that the actin-binding activity of ginkbilobin is located in a specific subdomain (termed as A1), just downstream of the signal peptide. Upon stable overexpression of this domain, we observe a specific delay in premitotic nuclear positioning indicative of a reduced dynamicity of perinuclear actin cables.

2. What is the biological function of ginkbilobin?

To get insight into the cellular events evoked by the binding of this subdomain to actin, we employ a strategy based on chemical engineering using synthetic peptides. They comprise of different parts of the actin-binding subdomain conjugated with the cell-penetrating peptide BP100 and with rhodamine B (RhB) as a fluorescent reporter. We observe that the binding of specific subdomain motifs to actin filaments is followed by rapid and efficient induction of cell death, leading to a working model for the mode of action of ginkbilobin, where ginkbilobin can interfere with the actin cytoskeleton of the target cell to activate an evolutionarily conserved apoptotic pathway.

2. Materials and Methods

2.1 Cell lines and cultivation

Suspension cell lines of BY-2 (*Nicotiana tabacum* L. cv Bright Yellow-2; Nagata et al., 1992) were cultivated in liquid medium containing 4.3 g l^{-1} Murashige and Skoog salts (Duchefa Biochemie, Haarlem, Netherlands), 30 g l^{-1} sucrose, 200 mg l^{-1} KH2PO4 , 100 mg l^{-1} inositol, 1 mg l^{-1} thiamine, and 0.2 mg l^{-1} 2,4-D, pH 5.8. The cells were subcultivated weekly inoculating 1.0 to 1.5 ml of stationary cells into 30 ml fresh medium in 100 ml Erlenmeyer flasks. The cells were incubated at 27°C under constant shaking on an orbital shaker (IKA Labortechnik, Staufen, Germany) at 150 rpm. Stock BY-2 calli were maintained on MS medium solidified with 0.8 % (w/v) agar (Roth, Karlsruhe, Germany) and subcultivated monthly. In addition to the BY-2 wild type (WT) (Nagata *et al.*, 1992), two transgenic cell lines, GF11 (Sano *et al.*, 2005) and FABD2 (Klotz and Nick, 2012) were used in this study which express the actin-binding domain 2 of plant fimbrin in fusion with GFP and RFP, respectively, under the control of the constitutive cauliflower mosaic virus (CaMV) 35S promoter. Several stable transgenic cell lines expressing different domains of ginkbilobin in fusion with GFP were generated in the current work. Transgenic cell lines and calli were cultivated on the same medium as non-transformed BY-2 WT cell culture, but complemented with the respective antibiotics (100 mg l^{-1} kanamycin for the ginkbilobin lines and FABD2, 30 mg l^{-1} hygromycin for GF11, respectively).

2.2 Cloning of full-length and truncated versions of ginkbilobin-2

2.2.1 RNA extraction and cDNA preparation

Mature seeds of *Ginkgo biloba* were collected in Freiburg (Germany) in December and kept at -80°C. The material was ground in liquid nitrogen using a mortar and total RNA extracted following the improved RNA extraction method

developed by Liu *et al.* (2010) (see Appendix 5.1, P. 77, for an overview of the improved RNA extraction method). Genomic DNA was digested by incubating the samples with RNase-free DNAse I (Qiagen, Hilden, Germany) on column for 30 min at 37°C. The integrity of RNA was checked by electrophoresis. cDNA synthesis was performed using the Dynamo cDNA Synthesis Kit (Finnzymes, Vantaa, Finland), according to the instruction of the manufacturer, taking 1 µg of RNA as template for reverse transcription.

2.2.2 TA cloning and Gateway® cloning

To generate transgenic cell lines overexpressing full-length or truncated versions of ginkbilobin-2, binary vectors were constructed using TA cloning and Gateway®-Cloning technology (Invitrogen Corporation, Paisley, UK). Gateway primers were designed according to the manufacturer's instruction amplifying either full length, signal peptide, full length without signal peptide, subdomain A1, subdomain A1+A2, subdomain A1+A2+A3, and subdomain B of ginkbilobin-2 from the cDNA of *Ginkgo biloba* (see the coding sequence of ginkbilobin-2 and its subdomains in Appendix 5.2, P. 78). The primer sequences are specified in Appendix 5.3, P. 78. For the preparatory PCR standard conditions and the Phusion Polymerase (NEB, Frankfurt, Germany; 0.4 U for a total volume of 20 µl) were used with 35 cycles (pre-heating at 98°C for 30 s; denaturation at 98°C for 10 s, annealing at 58°C for 20 s, and extension at 72°C for 20 s), followed by final extension at 72°C for 5 min. The PCR products were excised from the gel and purified using the NucleoSpin® Extract II (Macherey-Nagel, Dueren, Germany) kit according to the manufacturer instructions. A-overhangs were added to the PCR product by A-tailing (purified PCR product 15 µl; Taq Polymerase 0.2 µl; 10x ThermoPol buffer 5 µl; 10 mM dATP 1 µl; dd H2O 28.8 µl; total volume 50 µl) at 72°C for 10-30 min, and the A-tailing product was directly purified using the NucleoSpin® Extract II, then inserted into vector pGEM-T® Easy (Promega Corporation, USA). Destination vectors were constructed following Gateway® cloning technology instructions (see Appendix 5.4 and 5.5, P. 79 and P. 81, for an

overview of TA-cloning technology and the Gateway® cloning technology) with TA-cloning products and the binary vector pK7WGF2 (Karimi *et al.*, 2002) (C-terminal fusion GFP, kanamycin resistance) and pK7FWG2 (Karimi *et al.*, 2002) (N-terminal fusion GFP, kanamycin resistance). The structure of the different domains is shown in Figure 3.1B, P. 27 and all the generated Gateway® destination vector maps can be found in Appendix 5.6, P. 81.

2.3 Establishment of biolistic and stable transformation of tobacco BY-2 cells

2.3.1 Biolistic transformation

Gold particles (1.5-3.0 µm; Sigma-Aldrich, Taufkirchen, Germany) were coated with the corresponding plasmid DNA according to the standard manual of Bio-Rad (PDS-1000/He Particle Delivery System manual; for details, see Appendix 5.7, P. 83) with the following modifications. Gold particles (1.5-3.0 µM; Sigma-Aldrich, Germany) were suspended in 1 ml 50% (v/v) sterile glycerol by mixing on a bench-top vortexer (Bender & Hobein Zurich, Switzerland). For each sample, 12.5 µl of gold suspension were added to a 1.5 ml reaction tube. While mixing vigorously, the following components were added successively: 1 µg of plasmid DNA, 12.5 µl of 2.5 M sterile $CaCl_2$ and 5 µl of 0.1 M sterile spermidine (Roth, Karlsruhe, Germany), and then mixed for 3 min, spun down briefly, the supernatant was then discarded. Subsequently, the gold particles were washed with 125 µl of ice-cold absolute ethanol and resuspended in 40 µl of ice-cold absolute ethanol. The coated gold particles were loaded on macrocarriers (BIO-RAD Hercules, CA, USA) in 10µl step wise. 750 µl 3-day-old tobacco BY-2 WT cells were placed on PetriSlides™ (Millipore, Billerica, USA) containing a thin layer of solid MS medium (0.8% w/v Danish agar). These loaded PetriSlides™ were transferred into a custom-made chamber (Finer *et al.*, 1992), and bombarded by three shots at a pressure of 1.5 bar in a vacuum chamber of -0.8 bar. After the bombardment, the cells were incubated for 18-48 h in the dark at

27°C, and then inspected by microscopy. For the cotransformation of two constructs, 500 ng of each plasmid were mixed before coating the gold particles.

2.3.2 *Agrobacterium*-mediated transformation

BY-2 cells were transformed via *Agrobacterium*-mediated transformation following the improved protocol by Buschmann *et al.* (2011) to get both transient and stable transformation. Chemo-competent *Agrobacteria* were prepared using a freeze-thaw transformation protocol: competent LBA 4404 cells (strain LBA 4404; Invitrogen Corporation, Paisley, UK) were thawed at room temperature, gently mixed with 500-1000 ng of plasmid DNA, frozen in liquid nitrogen for 1 min, and rethawed for 5 min at 37°C. 500 µl of LB medium (Lennox Broth, Roth, Karlsruhe, Germany) were added and the mixture was then incubated at 28°C for 1-2 hours under continuous shaking. Subsequently, 100-200 µl of bacteria were plated onto solidified LB containing 50 mg l^{-1} rifampicin, 300 mg l^{-1} streptomycin, and 100 mg l^{-1} spectinomycin and incubated for 2-3 days at 28°C.

Single colonies were picked and inoculated into 5 ml of liquid LB medium containing the same antibiotics and shaken at 28°C for further 24 hours. From this suspension, 1 ml were transferred into 5 ml of fresh LB medium and cultivated in a shaker up to an OD_{600} of 0.8. Then, the *Agrobacteria* were harvested by centrifugation at 8,000 rpm (Heraeus Pico 17 Centrifuge, Thermo Scientific, Langenselbold, Germany) for 7 min in a 50-ml Falcon tube. The supernatant was discarded, and the sediment resuspended thoroughly with 180 µl of Paul's medium (4.3 g l^{-1} Murashige and Skoog salts with 1% sucrose, pH 5.8) to yield the cocultivation inoculum. For cocultivation, 90ml of 3-day-old BY-2 cells were washed with Paul's medium using a Scientific Nalgene® Filter Holder (Thermo Scientific, Langenselbold, Germany) combined with Nylon mesh with pores of diameter of 70 µm and resuspended in 1/5 of the starting volume, and this five-fold concentrated suspension cells were mixed with the cocultivation inoculum on an orbitary shaker for 5 min at 100 rpm. The mixture of transformed

bacteria and BY-2 cells was plated on Paul's agar (Paul's media with 0.5% Phytagel), and kept at 22°C in the dark for 3-4 days before microscopical analysis.

To obtain stably transformed lines, the calli were further cultivated on solid MS medium (0.8% w/v Danish agar) with 100 mg l^{-1} kanamycin and 100-300 mg l^{-1} cefotaxime. Transformed calli appeared after 2-3 weeks. For cotransformation, the cocultivation inoculum was prepared as mixture of the respective transformed *Agrobacterium* strains.

2.4 Phalloidin-based actin staining

To visualize actin, the modified method by Maisch *et al.* (2009) based on the protocol by Olyslaegers and Verbelen (1998) was used. 120 µl of cells were fixed for 10 min in 1.8 % (w/v) paraformaldehyde freshly prepared in actin stabilizing buffer (ASB, 0.1 M PIPES, 5 mM $MgCl_2$, and 10 mM EGTA, pH 7.0), and then transferred to ASB with fixative, but supplemented with 1% glycerol for additional 10 min to permeabalize the cell membrane. Subsequently, the cells were incubated for 30 min with 500 µl of 0.66 µM TRITC-phalloidin (Sigma-Aldrich, Taufkirchen, Germany) prepared from a stock solution in 96% (w/v) ethanol by dilution (1:100, v/v) with phosphate-buffered saline (0.15 M NaCl, 2.7 mM KCl, 1.2 mM KH_2PO_4, 6.5 mM Na_2HPO_4, pH 7.2). Finally, the cells were washed three times for 10 min in phosphate-buffered saline and directly viewed under the microscope.

2.5 Ginkbilobin-2 subdomain peptide conjugates treatment of tobacco BY-2 cells

To test the vivo localization of Ginkbilobin-2 subdomain peptide conjugates Rhodamine B-BP100-domain A1; Rhodamine B-BP100-domain A2; Rhodamine B-BP100-domain A3) and unconjugated BP100 (Rhodamine B-BP100) (Ferre *et*

al., 2009) (see the sequences of the peptide conjugates in Appendix 5.8, P. 83) as a control, 50 µl of 4 day old BY-2 WT cell suspension and 950 µl of culture medium were mixed in a 1.5 ml reaction tube. Each peptide was added to a final concentration of 0.5 µM and incubated for 6 hours up to 24 hours in the dark under continuous shaking. Following incubation, the cells were transferred to custom-made staining chambers and thoroughly washed 3 times with 15 ml of fresh sterile culture medium and viewed the uptake of the cells at 6 hours, 12 hours, and 24 hours under microscope.

To assess the localization of RBA1, RBA2 and RBA3 in relation to actin filaments in vivo, the conjugated peptides and BP100 were incubated with the 4 day old transgenic tobacco BY-2 cell line GF-11 for 24 hours, washed as described above and viewed under a microscope immediately.

2.6 Drug Treatment of tobacco BY-2 cells

2.6.1 Auxin and phytotropin treatment

The natural auxin indole-3-acetic acid (IAA, Sigma-Aldrich) or the auxin-transport inhibitors 1-*N*-naphthylphthalamic acid (NPA, Sigma-Aldrich) were added to the 3 days old actin maker line GF-11 at final concentrations of 2 µM for IAA (diluted from a stock solution of 100 mM IAA in 96 % (v/v) ethanol) and 12 µM for NPA (diluted from a stock solution of 10 mM NPA in DMSO) and incubated 10 min, and followed under a microscope. Following this pre-incubation, 2 µM ginkbilobin conjugates and BP100 was added and incubated for 30 min. During this incubation step the response of the cells were followed under a microscope.

2.6.2 Actin inhibitors latrunculin B and phalloidin treatment

To eliminate actin filaments, 1 µM of Latrunculin B (Sigma-Aldrich, Deisenhofen, Germany) (stock solution 1 mM in DMSO) were added to 3-day-old BY-2 cells (overexpressors of ginkbilobin subdomain A1, full length ginkbilobin without signal

peptide and actin marker line GF11) and the response was followed under a microscope.

For the actin inhibitor treatment, 1 µM latrunculin B or 1 µM Phalloidin from *Amanita phalloides* (Sigma-Aldrich; stock solution 1mM in 96 % (v/v) ethanol) was added into 3 days old actin maker line GF-11 and incubated for 30 min. The response was followed under a microscope. Following this pre-incubation, 2 µM ginkbilobin conjugates and BP100 was added and incubated for 30 min. During this incubation step the response of the cells were followed under a microscope.

2.6.3 Peptide conjugates treatment to GF-11 cell line preincubated with drugs

Following the preincubation of the drugs (2 µM IAA and 12 µM NPA for 10 min, 1 µM Lat B and 1 µM phalloidin for 30 min as described above), 2 µM Ginkbilobin-2 subdomain peptide conjugates and BP100 were added and viewed the following 30 min under a microscope.

2.7 Phenotyping cellular responses

2.7.1 Determination of nuclear positioning, division synchrony, cell length and width

The different ginkbilobin-2 based overexpressor lines were phenotyped as described in Kühn *et al.* (2013). Nuclear positioning (NP) was quantified from 500 individual 3 days old cells were measured from three independent experimental series. To determine the response of division synchrony, cell length and width the natural auxin indole acetic acid (IAA, 2 µM, diluted from a stock solution of 100 mM IAA in ethanol) and the auxin-efflux inhibitor 1-N-naphthyl phthalamic acid (NPA, 10 µM, diluted from a stock solution of 10 mM NPA in dimethyl sulfoxide), cells were either scored at day 4 (division synchrony) or day 7 (cell length and width) after subcultivation. 20 µl aliquot of cells viewed under AxioImager Z.1

microscope (Zeiss, Jena, Germany) and images taken using the MosaiX module of the AxioVision software to cover a 4x4 mm area with 121 single pictures at an overlay of 10 % to monitor division synchrony and measure the NP, the cell length and width (Campanoni *et al.*, 2003; Maisch and Nick, 2007). Each experiment was accompanied by a corresponding solvent control. For division synchrony around 3000 cell files were recorded from at least three independent experimental series. For cell length and width, 1500 individual cells were measured from three independent experimental series.

2.7.2 Determination of cell mortality

To evaluate the cell mortality of Ginkbilobin-2 subdomain peptide conjugates and unconjugated BP100, each peptide was added to 4 day old tobacco BY-2 WT cell line with different concentrations of 0.5 µM, 1 µM, 2 µM or 3 µM. The cells were incubated at 27 °C under continuous shaking up to 24 hours. And the cell mortality was recorded at 1 hour, 6 hours, 12 hours and 24 hours. To check for a possible influence of drug treatment on cell mortality, following 30 min drug treatment (2 µM IAA, 12 µM NPA , 1 µM Lat B and 1 µM phalloidin), 1 µM subdomain conjugates and BP100 were added to GF11 cell line, respectively, and continued to incubate for 6 hours to record the cell mortality.

Mortality in response to ginkbilobin-2 subdomain peptide conjugates was quantified by 1 ml of 2.5 % Evans Blue (w/v) (Sigma-Aldrich) dissolved in millipore water for 1 min and filtered the cells using custom-made staining chamber with a pore-size of 70 µm mesh bottom (Nick *et al.*, 2000). Following 3 times washing with Millipore water the cells were viewed under AxioImager Z.1 microscope (Zeiss, Jena, Germany) and mosaic pictures were obtained as described above. 1000 cells were counted from three independent experimental series.

2.8 Synthesis of ginkbilobin-subdomain peptide conjugates

The subdomains A1, A2, and A3 from the putative actin-binding domain of

ginkbilobin-2 were synthetically generated as fusions with the cell-penetrating peptide BP100 and rhodamine B, following the strategy previously described in (Eggenberger *et al.*, 2011). All peptides were synthesized by using standard 9-fluorenylmethoxycarbonyl (Fmoc) solid-phase peptide synthesis (Fields and Noble, 1990). Rhodamine B was used as a fluorescent marker and BP100 as the cell-penetrating carrier. Rhodamine B was coupled at the N-terminus of BP100, and the different ginkbilobin-2 subdomain peptides were coupled at the C-termini of the constructs (see the sequences of the peptide conjugates in Appendix 5.8, P. 83). The peptides were purified by HPLC using acetonitrile/water gradients as previously described (Wadhwani *et al.*, 2006; Wadhwani *et al.*, 2008), and the purified peptides were characterized by analytical liquid chromatography combined with ESI-mass spectrometry (Eggenberger *et al.*, 2011).

2.9 Microscopy

To phenotype cellular responses, cells were observed and recorded under an AxioImager Z.1 microscope (Zeiss, Jena, Germany) equipped with an ApoTome microscope slider for optical sectioning and a cooled digital CCD camera (AxioCam MRm; Zeiss). TRITC-/RFP- and GFP-/Alexa-Fluor® 488-fluorescence were observed through the filter sets 43 HE (excitation: 550 nm, beamsplitter: 570 nm, and emission: 605 nm) and 38 HE (excitation: 470 nm, beamsplitter: 495 nm, and emission: 525 nm), respectively (Zeiss). For cell mortality, cell division synchrony and cell size, samples were observed in the differential interference contrast (DIC) using a 20x objective (Plan-Apochromat 20x/0.75) and the MosaiX module of the imaging software (Zeiss). And images were analysed using the AxioVision (Rel. 4.8.2) software or Image J (NIH, Bethesda, USA).

To observe the cellular details of the transformed cells, images of RFP-/TRITC and GFP-/Alexa-Fluor® 488-fluorescence were examined with an AxioObserver Z1 (Zeiss, Jena, Germany) using a 63 × LCI-Neofluar Imm Corr DIC oil objective (NA 1.3), the 561nm and 488 nm emission line of the Ar-Kr laser, a cooled digital

CCD camera (AxioCam MRm; Zeiss) and a spinning-disc device (Yokogawa CSU-X1 Spinning Disk Unit, Yokogawa Electric Corporation, Tokyo, Japan).

3. Results

In this chapter, the results from this work are separated into three main parts. In the first part, divergent phylogeny of proteins containing a ginkbilobin-2 domain is analyzed. Following that, the generation of new transgenic tobacco BY-2 cell lines is described. Firstly, the localization of the transgenic cell lines and their colocalization with actin marker cell line FABD2 are visualized. Secondly, morphologic studies of overexpressing subdomain A1, full length without signal peptide (NSP) and subdomain B of ginkbilobin-2 with auxin treatment are analyzed. In the third part, the work deals with the cellular response of ginkbilobin-2. Truncated subdomain A coupled with the cell-penetrating carrier BP100 and rhodamine B were introduced into BY-2 cells firstly to get insight into cellular response. Secondly, the uptake of subdomain conjugates pretreated with actin drugs and auxin into the cell should be studied.

3.1 Divergent phylogeny of proteins containing a ginkbilobin-2 domain

To get access to putative functions of ginkbilobin-2, a phylogenetic tree was constructed based on the neighbour-joining algorithm of homologous proteins (Figure 3.1 A). Homologues of ginkbilobin-2 could be identified only in seed plants, and in the heterosporic fern *Selaginella*. These homologues clustered into two classes (Figure 3.1 B) – one class contained proteins just composed of the ginkbilobin-2 domain and along with N-terminal putative signal peptide for secretion, while the other class contained proteins harbouring, in addition, a long C-terminal extension of usually ~180 amino acids. Both classes occurred in all taxa, but there was a clear dominance of the version without extension in the gymnosperms, whereas the version with extension dominated in the angiosperms. In *Selaginella*, eight ginkbilobin-2 homologues could be identified; three with, and five without this C-terminal extension. Within each of the two classes of

ginkbilobin-2 domain proteins, the members clustered mostly in accordance with taxonomic relationship, i.e. dicot and monocot, as well as the gymnosperm members formed separate subclades. However, those homologues from *Selaginella* that lacked the C-terminal extension were split into two groups, one was basal to the clade, and one was closer to the monocot members. Alignment of the sequences revealed specific cysteine signatures that were conserved throughout, even between the accessions with and without the C-terminal extension. In this extension, further cysteine signatures could be detected that were preserved as well (Figure 3.1 B). The closest relatives of ginkbilobin-2 with approximately 85% identity were embryo-abundant proteins from conifers. In *Ginkgo*, a closely matching second protein, designated as ginkbilobin-1, had been described as well (Wang and Ng, 2000). However, since this protein was lacking a signal peptide and even a start codon, we considered ginkbilobin-1 as a fragment and did not analyse it further. Based on the conservation in the alignment, the ginkbilobin-2 domain could be subdivided into subdomains A1, A2, A3, B1, and B2. Among those subdomains, especially B1 and A2 were conserved throughout the evolution of vascular plants, whereas A3 appeared to be more variable. The domain B contained a conserved cysteine signature C-X_8-C-X_2-C, which is a characteristic feature of a receptor superfamily described for *Arabidopsis thaliana* and rice and was proposed to participate in defence signalling (Chen, 2001). However, these receptors do not share a ginkbilobin-2 domain.

The conservation of the cysteine signatures along with numerous other motifs of the ginkbilobin-2 domain throughout the evolution of vascular plants suggests that these motifs confer important biological functions. Since the ginkbilobin-2 domain as an entity, to our knowledge, does not occur outside the vascular plants, we were wondering whether the isolated subdomains (A1, A2, A3, B1 and B2) might have additional homologues. For this purpose, we conducted a Blast-search with the isolated subdomains at reduced stringency of the e-value threshold (100) to

recover such additional, partial, homologues whose functional assignments might give us an idea about potential cellular functions of ginkbilobin-2.

For the A1 motif, among 12 recovered hits, three of the homologues were part of the so-called CLASP-N-like/armadillo fold proteins (see the alignments in Appendix 5.9, P. 84). These cytoskeletal proteins are known to mediate interactions between actin filaments and microtubules. Two of those proteins were from insects, one from an oomycete with up to 65% similarity that remained confined to the A1 motif. A search with the A2 motif yielded 13 hits, whereby six were two-component histidine kinases of plant-interacting bacteria. The homology was located to the start of the histidine-kinase homodimerization domain and reached up to 80% similarity, again remaining confined to this motif on both sides. Whereas a search with the A3 motif did not uncover any homologues, the search with the B1 motif produced a couple of angiosperm sequences (both mono- and dicots) in addition to the previously known ginkbilobin-2 containing proteins. These additional sequences also possess the above-mentioned specific cysteine signatures, and showed homologies of 50-60% similarity in most cases that were, however, confined to the B1 motif. For most of them no function was assigned. Three of these hits belonged to a plant receptor-like kinase superfamily involved in pathogen sensing (Chen, 2001). A search with the B2 domain yielded homologues in bacterial proteins related to phytopathogenicity, but also one plant DUF26 domain protein that had already been picked up by the search for B1 homologues. It should be noted that the hits recovered by this strategy shared only similarity with individual subdomains of ginkbilobin-2, not with ginkbilobin-2 as an entity. Nevertheless, these motifs indicate a putative relationship with defence on the one hand, and with the cytoskeleton on the other.

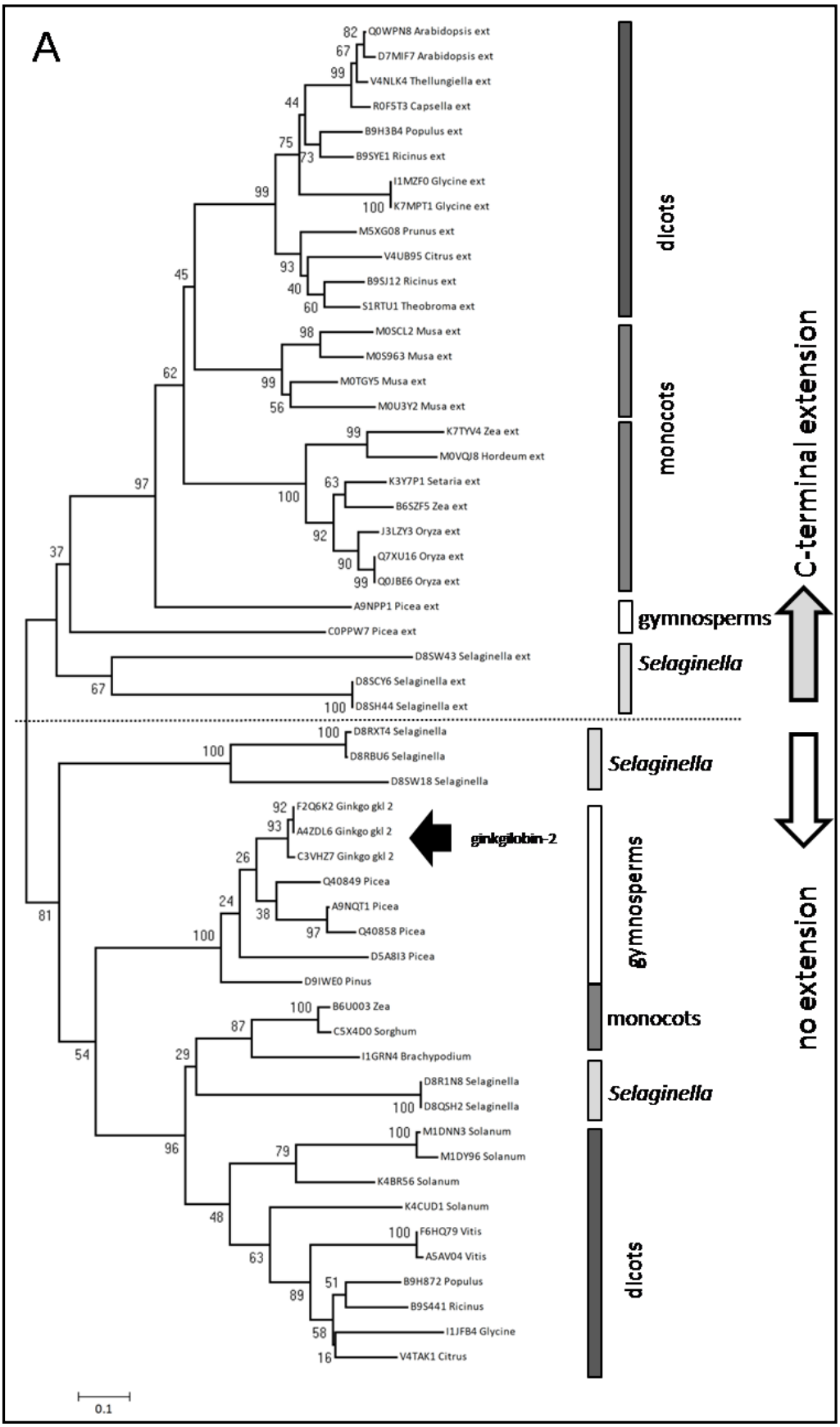
A
Q0WPN8 Arabidopsis ext
D7MIF7 Arabidopsis ext
V4NLK4 Thellungiella ext
R0F5T3 Capsella ext
B9H3B4 Populus ext
B9SYE1 Ricinus ext
I1MZF0 Glycine ext
K7MPT1 Glycine ext
M5XG08 Prunus ext
V4UB95 Citrus ext
B9SJ12 Ricinus ext
S1RTU1 Theobroma ext
M0SCL2 Musa ext
M0S963 Musa ext
M0TGY5 Musa ext
M0U3Y2 Musa ext
K7TYV4 Zea ext
M0VQJ8 Hordeum ext
K3Y7P1 Setaria ext
B6SZF5 Zea ext
J3LZY3 Oryza ext
Q7XU16 Oryza ext
Q0JBE6 Oryza ext
A9NPP1 Picea ext
C0PPW7 Picea ext
D8SW43 Selaginella ext
D8SCY6 Selaginella ext
D8SH44 Selaginella ext
D8RXT4 Selaginella
D8RBU6 Selaginella
D8SW18 Selaginella
F2Q6K2 Ginkgo gkl 2
A4ZDL6 Ginkgo gkl 2
C3VHZ7 Ginkgo gkl 2
ginkgobin-2
Q40849 Picea
A9NQT1 Picea
Q40858 Picea
D5A8I3 Picea
D9IWE0 Pinus
B6U003 Zea
C5X4D0 Sorghum
I1GRN4 Brachypodium
D8R1N8 Selaginella
D8QSH2 Selaginella
M1DNN3 Solanum
M1DY96 Solanum
K4BR56 Solanum
K4CUD1 Solanum
F6HQ79 Vitis
A5AV04 Vitis
B9H872 Populus
B9S441 Ricinus
I1JFB4 Glycine
V4TAK1 Citrus
0.1
dicots
monocots
gymnosperms
Selaginella
Selaginella
gymnosperms
monocots
Selaginella
dicots
C-terminal extension
no extension

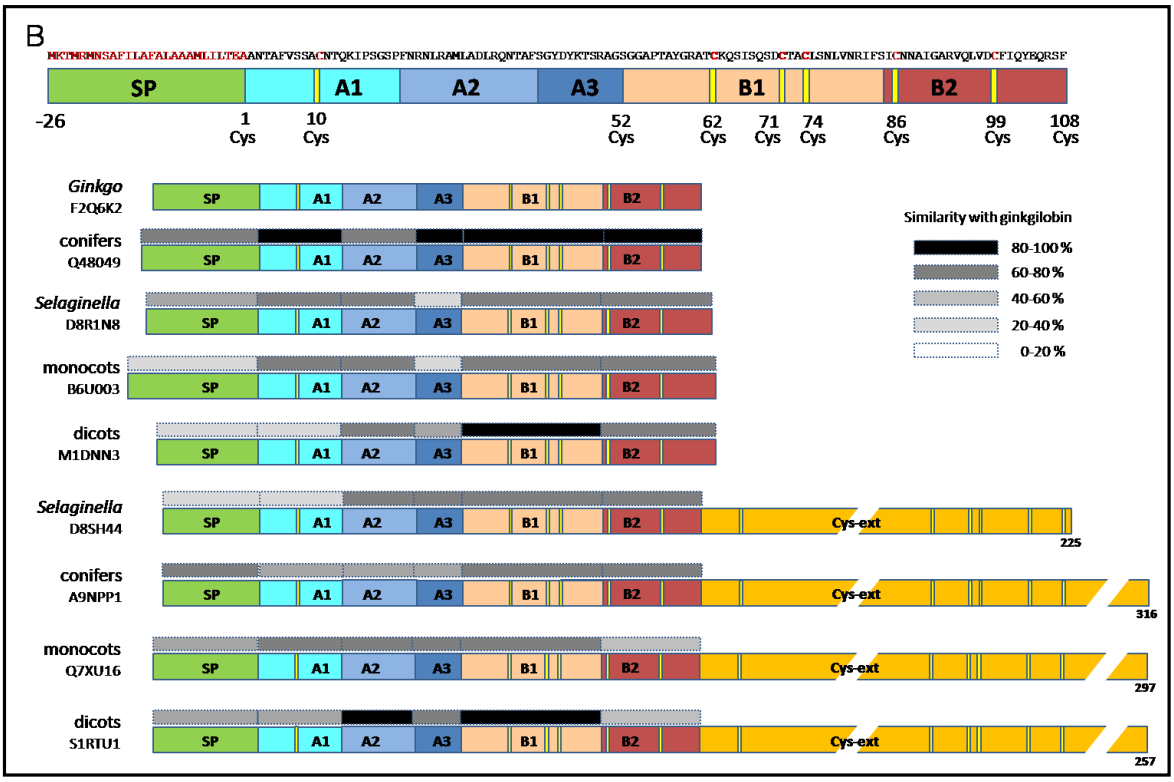

Figure 3.1 Phylogeny and domain structure of ginkbilobin-2 related proteins. (A) Evolutionary relationship between 55 ginkbilobin-2 related protein sequences inferred by Neighbor-Joining method. Values next to the branches represent the percentage of replicate trees in which the associated taxa clustered together in the bootstrap test (based on 500 replicates). The tree is drawn to scale, with branch lengths in the same units as those of the evolutionary distances used to infer the phylogenetic tree. The evolutionary distances were computed using the Poisson correction method and are in the units of the number of amino acid substitutions per site. All positions containing gaps and missing data were eliminated from the dataset (complete deletion option) leaving a total of 89 positions in the final dataset. The Swissprot accessions are given along with the genus name. (B) Domain structure of ginkbilobin-2 related protein sequences. SP predicted signal peptide, followed by subdomains A1-3, and subdomains B1-2, and in some of the proteins an additional long cysteine-rich C-terminal extension (Cys-ext). The conservation of the individual domains with ginkbilobin-2 is indicated by the shaded boxes based on similarity at the amino-acid level. The yellow lines represent conserved cysteine signatures.

3.2 Generation of transgenic cell lines and localization studies of ginkbilobin-2 fusion proteins

3.2.1 Modification of the Buschmann method for *Agrobacterium*-mediated transformation of BY-2 cells

In order to achieve the cellular localization and functions of ginkbilobin-2, we generated cell lines overexpressing full length and truncated variations of ginkbilobin-2 in this study. First, we used the Gateway® cloning system to construct the expressing vectors. Then, the protocol for transient *Agrobacterium*-mediated transformation of BY-2 cells developed by Buschmann *et al.* (2011) was applied for transforming BY-2 cells with a few modifications which improved the efficiency of transformation. First and most importantly, the cocultivation temperature was decreased to 22°C instead of 27°C which produced higher transient transformation rate in BY-2 cells (see Fig. 3.2). Fullner and Nester (1996) and Dillen *et al.* (1997) suggested that there was a difference in temperature for optimal bacteria propagation and effective plant transformation. Second, mixture of cells and *Agrobacteria* were not directly placed on the MS Paul agar surface but on a layer of filter paper in between instead to avoid the mechanical wounding caused by transferring the cells when using a sterile spatula. By doing that, the transformed cells will stay close to each other and are able to generate rapidly enough calli to overcome the selection pressure.

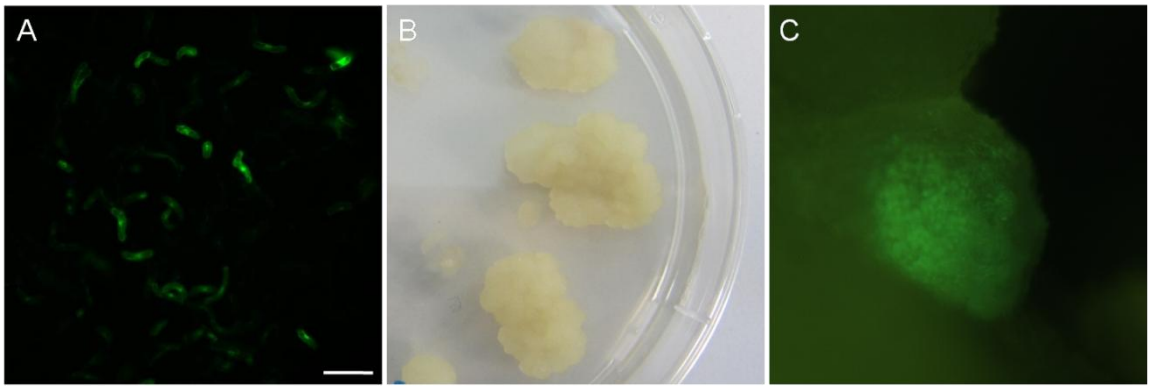

Fig. 3.2 (A) Transient transformants (sudomain A1-GFP) of BY-2 cells 3 days after cocultivation on solid Paul agar surface (Scale bar 200 µm). (B) Transformed calli appeared 3 weeks after incubation on MS agar medium supplied with 300 mg l^{-1} cefotaxime and 100 mg l^{-1} kanamycin. (C) Transformed calli under the fluorescent microscope.

3.2.2 Localization of full-length ginkbilobin-2 and its individual domains

To achieve more information about cellular functions of ginkbilobin-2, the subcellular localization of the full-length protein and specific truncations were tested by expressing GFP fusions in tobacco BY-2 cells, either transiently (by biolistics) or in a stable manner (using binary vectors based on the GATEWAY® cloning strategy). Since the N-terminus harboured a predicted signal peptide of 26 amino acids (using the on line software SignalP 4.1 server), we first tested a fusion of GFP C-terminal to this putative signal motif. Upon expression, this construct showed up small fluorescent vesicles (Figure 3.3 A) that were moving along with the cytoplasmic strands and also decorated the nuclear rim, which indicated that the signal peptide was functional and designated GFP for secretion.

In the next step, the full-length sequence of ginkbilobin-2 (including the signal motif) was investigated. Due to the presence of the signal peptide and potential steric hindrance, GFP was fused either in N- or in C-terminal position of the full-length ginkbilobin-2 coding sequence including the signal peptide. The C-terminal fusion of full-length ginkbilobin-2 (Figure 3.3 B) produced the same pattern as the signal peptide alone suggesting that the signal peptide was functional in committing its cargo for the secretory pathway. However, when GFP was fused to the N-terminus of full-length ginkbilobin-2 (including the signal peptide), this fusion exhibited a different pattern (Figure 3.3 C) as it visualized filamentous structures that tethered the nucleus by transvacuolar strands to a cortical meshwork, a morphology and organization that is characteristic for plant actin. To test whether this deviant localization of GFP-ginkbilobin-2 was caused by GFP masking the signal peptide, we fused GFP C-terminally of full-length ginkbilobin-2, but truncated the signal motif (ΔSP). Again, this construct visualized

filamentous structures (Figure 3.3 D) leading to the evidence that ginkbilobin-2 – if not sequestered from the cytoplasm by means of the N-terminal signal peptide – will tether to a filamentous network that might be actin.

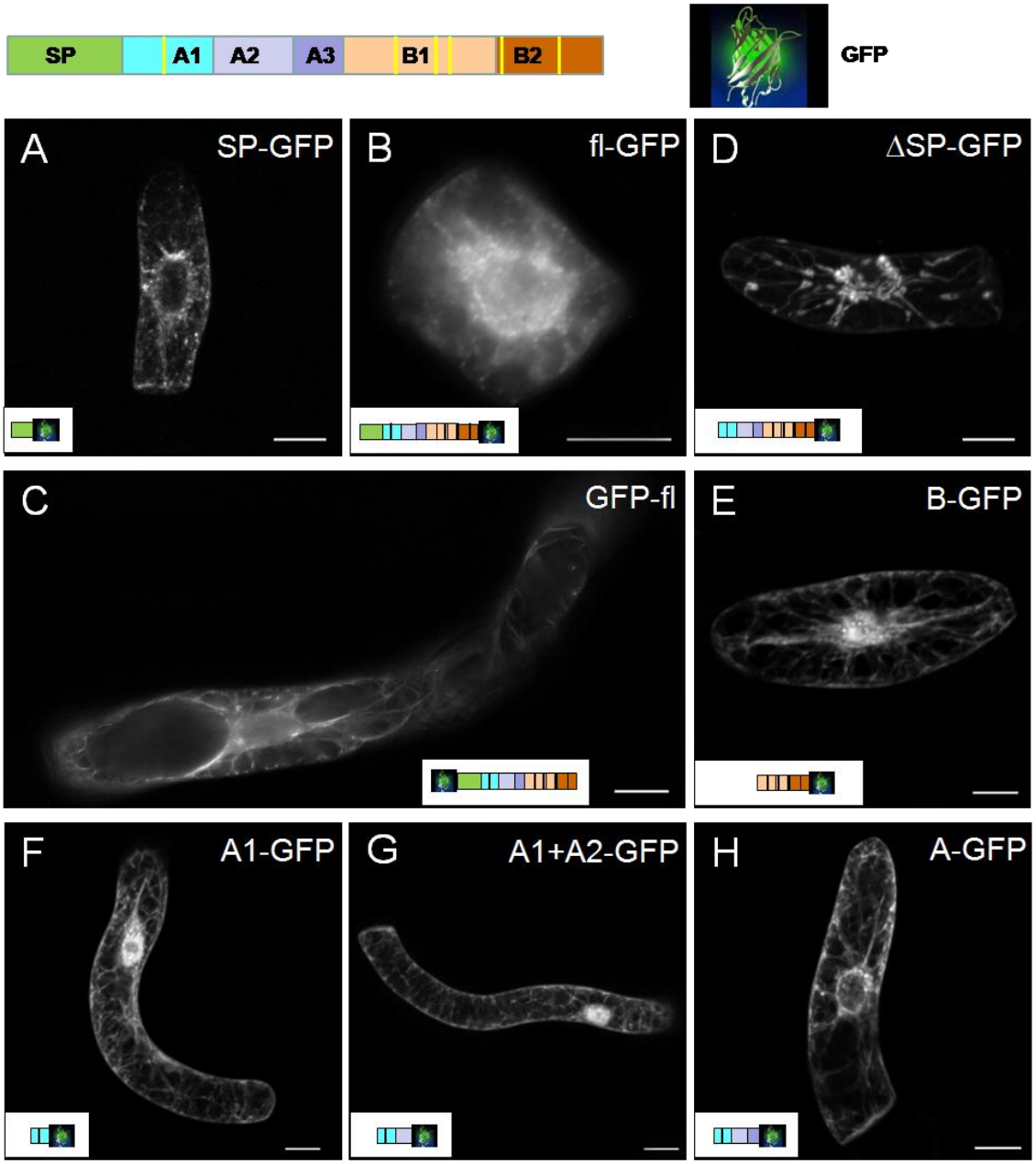

Figure 3.3 Localization of GFP fusion constructs of full-length or truncated ginkbilobin-2 upon transient expression in tobacco BY-2 cells. The structure of the constructs used is shown schematically. (A) Signal peptide upstream of GFP. (B) Full-length ginkbilobin-2 including the signal peptide upstream of C-terminally fused GFP. (C) Full-length ginkbilobin-2 including the signal peptide downstream of N-terminally fused GFP. (D) Ginkilobin-2 lacking the signal peptide upstream of C-terminally fused GFP. (E) Subdomain B upstream of C-terminally fused GFP. (F)

Subdomain A1 upstream of C-terminally fused GFP. (G) Subdomains A1+A2 upstream of C-terminally fused GFP. (H) Subdomains A1+A2+A3 upstream of C-terminally fused GFP. Scale bar 20 µm.

In the next step, we asked, which of the subdomains confers this specific localization. Thus, various subdomains or combinations thereof were tested for their localization. Subdomain B (Figure 3.3 E) that contains the specific cysteine signature was at first sight localized in a manner similar to the full-length protein with truncated signal peptide (Figure 3.3 D). However, a closer look reveals that the strands labelled by this construct are much broader and widen near the cell cortex into triangles, which is the pattern observed for the structure of the cytoplasmic strands in these vacuolated cells. This indicates that the filamentous localization of the full-length protein (Figure 3.3 C) is not conferred by domain B. Therefore, domain A was put under closer scrutiny: the entire domain A marked, in addition to cytoplasmic strands, filaments that were much more slender (Figure 3.3 H). When domain A was divided into subdomains A1 and A2, these thin strands became more prominent (Figure 3.3 G), and when everything was truncated down to subdomain A1 alone (Figure 3.3 F), a rich system of fine filaments became manifest that was congruent with the pattern observed for the full-length protein with truncated signal peptide. These filaments converged to the nuclear envelope and emanated from rod-like, sometimes more punctate structures at the nuclear rim. This pattern is reminiscent of the actin cytoskeleton in those cells. This truncation study assigns the specific localization of ginkbilobin-2 to subdomain A1.

3.2.3 Ginkbilobin-2 domains targeting to actin

To get insight into the cellular nature of the filamentous structures visualized by ginkbilobin-2, the different constructs described above were transiently expressed in a stable actin maker line expressing FABD2-RFP either via biolistic or via *Agrobacterium*-mediated transformation. The signal peptide alone (Figure 3.4

A1-3) as well as a fusion of GFP placed at the C-terminus of full-length ginkbilobin-2 (Figure 3.4 B1-3) produced vesicles that were moving along the actin filaments. In contrast, when GFP was fused to the N-terminal of the full-length ginkbilobin-2 (Figure 3.4 C1-3), filamentous structures were seen that matched exactly with actin filaments. Next, we want to test whether the differential localization of C-terminal (Figure 3.4 B1-3) versus N-terminal (Figure 3.4 C1-3) GFP fused to full length ginkbilobin-2 was caused by masking of the signal peptide, when GFP was fused at the N-terminus. We thus generated a construct, where GFP was placed at the C-terminus of full-length ginkbilobin-2, but where the signal peptide was truncated. This construct (ΔSP, Figure 3.4 D1-3) visualized a subset of actin filaments. Exemplarily for the subdomains we tested subdomain A1 (Figure 3.4 E1-3), which also colocalized with actin filaments.

To verify whether the localization of subdomain A1 was dependent on actin filaments, 1 µM of latrunculin B was used to treat subdomain A1 for 30 min. Latrunculin B is commonly used to disrupt the actin cytoskeleton net work (Spector *et al.*, 1983) and indeed we find that the filamentous structures visualized by the GFP fusion with subdomain A1 (Figure 3.3 F, P. 30) were completely eliminated and replaced by vesicular structures (Figure 3.5 A). The same was true for ginkbilobin-2 with GFP fused C-terminally but devoid of the signal peptide (Figure 3.5 B). As a control, the actin marker line GF11 was subjected to the same treatment and found to be devoid of any actin filaments, demonstrating that the treatment is efficient to eliminate actin microfilaments (Figure 3.5 C). A stable line of subdomain A1 in fusion with GFP showed the same filamentous structures as already seen in the transient transformants (compare Figure 3.3 and 3.4). To verify that these filaments represent actin filaments, the stable transformants were stained with TRITC-phalloidin, a dye known to bind to polymeric actin (Kakimoto and Shibaoka, 1987). The resulting images (Figure 3.5 D1-3) showed that the GFP fusion of subdomain A1 (Figure 3.5 D1) colocalized with the TRITC-phalloidin labelled actin (Figure 3.5 D2).

These data show that ginkilobin-2 – if not recruited for secretion by the signal peptide – binds to actin filaments, and that subdomain A1 is functionally equivalent to the full-length protein with respect to this actin-binding activity.

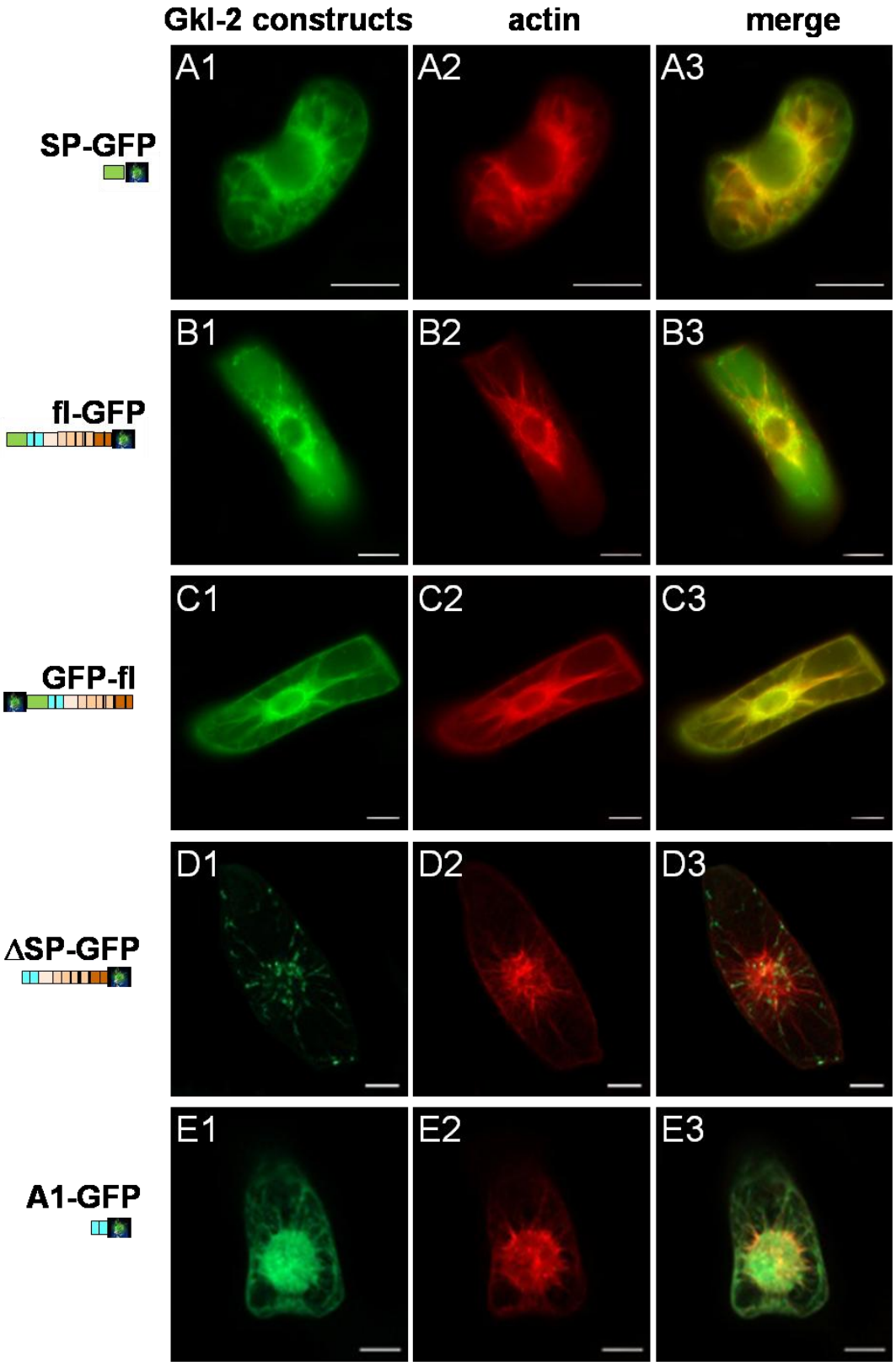

Figure 3.4 Localization patterns observed for expression of ginkbilobin-2 subdomains fused with GFP in the background of the actin marker line RFP-FABD2. (1) showing the GFP signal, (2) the RFP signal, and (3) the merge of both signals. The schematic sketch shows the structure of the respective construct. (A) Signal peptide upstream of C-terminally fused GFP. (B) Full-length ginkbilobin-2 including the signal peptide upstream of C-terminally fused GFP. (C) Full-length ginkbilobin-2 downstream of N-terminally fused GFP. (D) Ginkilobin-2 lacking the signal peptide upstream of C-terminally fused GFP (NSP). (E) Subdomain A1 upstream of C-terminally fused GFP. Scale bar 20 µm.

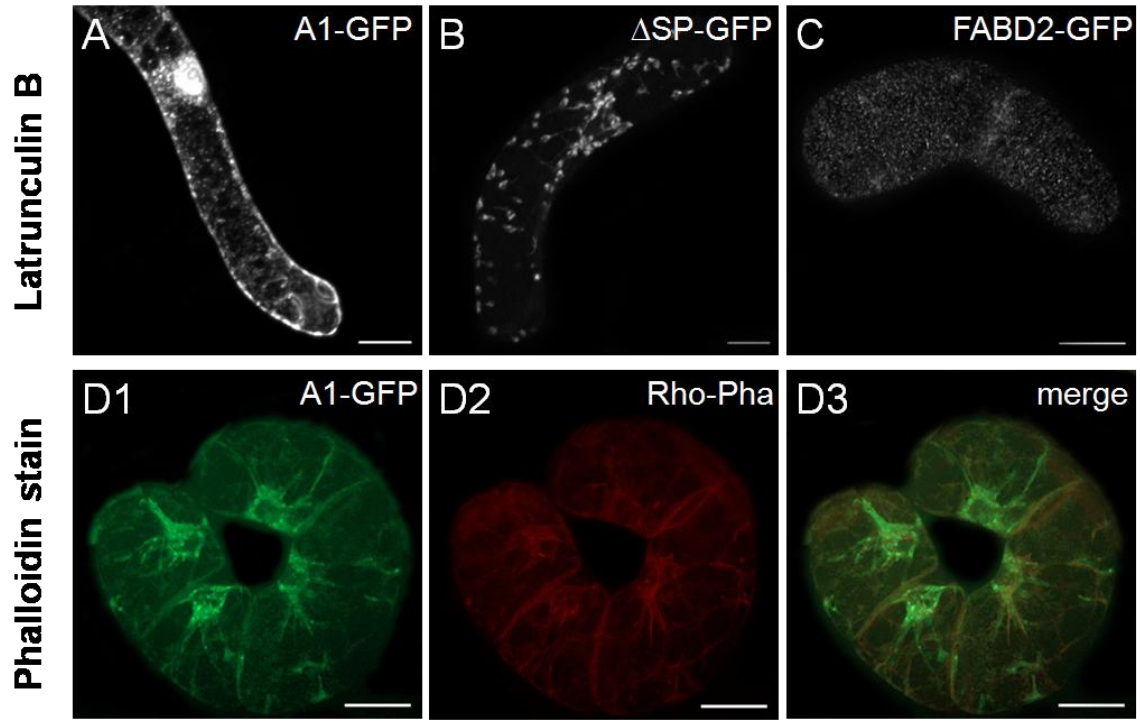

Figure 3.5 The filamentous signal visualized by the subdomain A1 of ginkbilobin-2 is caused by actin. (A) Subdomain A1 upstream of C-terminally fused GFP after treatment with 1 µM of latrunculin B for 30 min. (B) Ginkbilobin-2 lacking the signal peptide upstream of C-terminally fused GFP (ΔSP) treated with 1 µM of latrunculin B for 30 min. (C) Actin signal in the GF-11 line after treatment with 1 µM of latrunculin B for 30 min. (D) Labelling of actin filaments in a stable transformant expressing subdomain A1 upstream of C-terminally fused GFP using TRITC-phalloidin. The GFP signal is shown in (1), the phalloidin signal in (2), the merge of both signals in (3). Scale bar 20 µm.

3.3 Stable transformants of truncated variations of ginkbilobin-2

3.3.1 Subdomain A1 is sufficient to modulate nuclear positioning

To see whether the association of ginkbilobin-2 with actin would alter any actin-dependent cellular responses, different stable overexpression lines were generated in tobacco BY-2 via *Agrobacterium*-mediated transformation and phenotyped. Stable transformants were obtained for subdomains A1, B, and full-length ginkbilobin-2 without the signal peptide (ΔSP, also abbreviated as NSP for “non-signal peptide”). Subdomain A1 localized along transvacuolar actin cables and in rod-like punctate structures adjacent to the nuclear rim (Figure 3.5 D1-3, Figure 3.6 A1-3). For the lines overexpressing NSP or subdomain B (Figure 3.6 B and 3.6 C), only weak expression could be obtained that was localized in the same pattern as seen for the transiently transformed cells (Figure 3.3 E and 3.3 D). This indicates that higher stable expression of these two transgenes might impair viability, such that during the course of cultivation only the weak expressors had persisted. Stably transformed calli of C-terminal fused GFP of full length ginkbilobin-2 image showed small vesicles all over the cell, while the C-terminal fusion of the signal peptide with GFP accumulated in vesicles in some part of the cell (see the figures of fl-GFP and SP-GFP in Appendix 5.10, P. 85).

Premitotic nuclear positioning is a trait that depends on a perinuclear array of actin filaments (Durst *et al.*, 2014) that move and tether the nucleus in concert with microtubules and plant specific minus-directed KCH-kinesins (Kühn *et al.*, 2013). We therefore measured nuclear positioning on day 3 after subcultivation and observed that nuclear positioning was significantly delayed in the overexpressor of subdomain A1 (Figure 3.6 D) and NSP, compared to the non-transformed BY-2 control. In contrast, overexpression of subdomain B did not cause such a delay. The comparison of the isolated subdomain A1 with the NSP construct (that also harbours subdomain A1, but did not produce a stronger effect) and with subdomain B demonstrates that subdomain A1 is necessary and

sufficient to confer an inhibition on nuclear positioning.

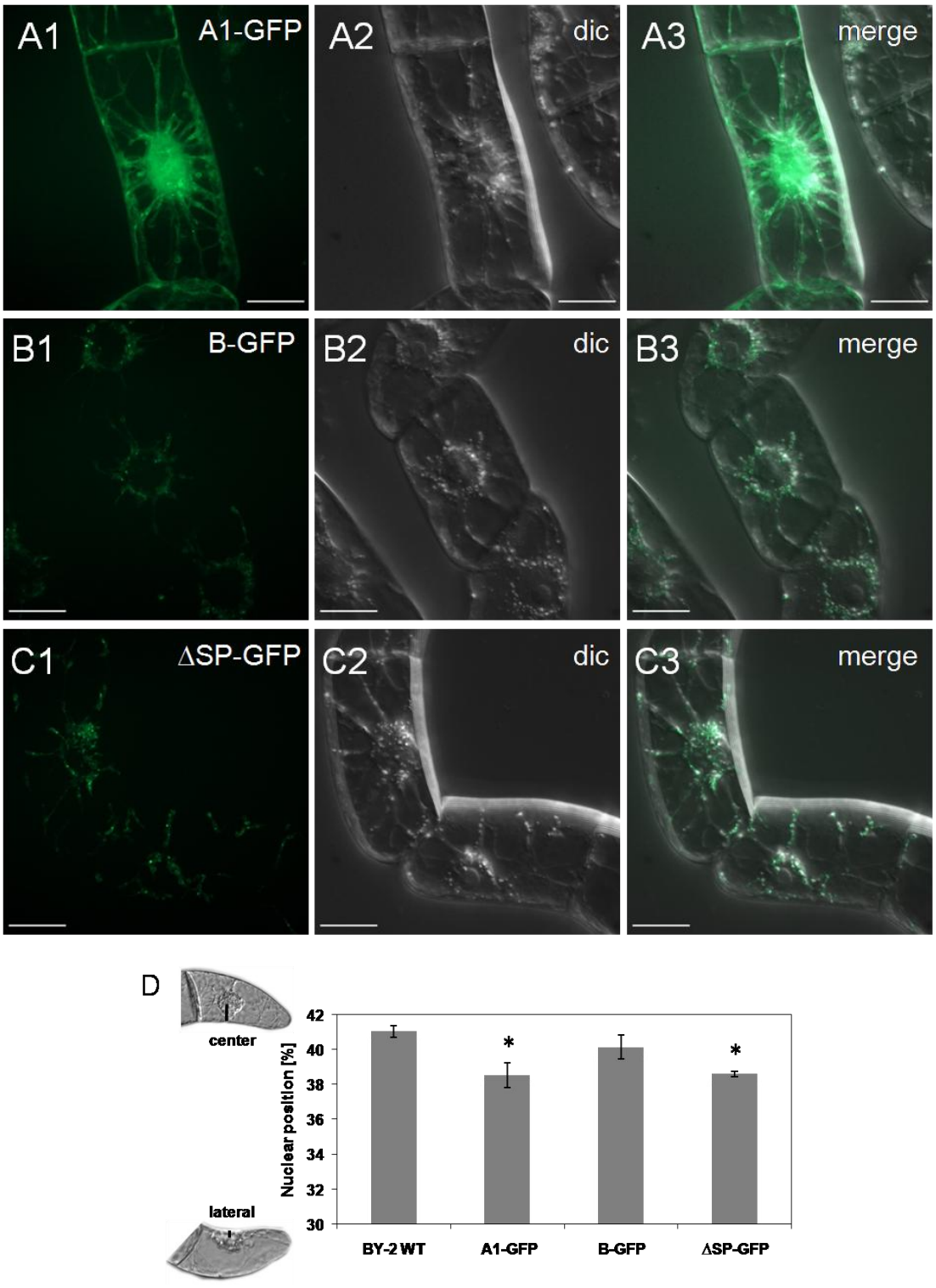

Figure 3.6 Phenotypes of stable transformants and the nuclear positioning. Phenotypes of stable transformants for C-terminal GFP-fusions with subdomain A1 (A), subdomain B (B), or the ΔSP construct, i.e. ginkbilobin without signal peptide (C). In (A-C), GFP is shown in (1), dic in (2),

merge of the two channels in (3). Scale bar 20 µm. (D) Nuclear positioning in the stable transformants shown in (A-C) as compared to the non-transformed control. A value of 30% indicates that the nucleus is completely lateral, whereas a value of 50% indicates that the nucleus has moved exactly into the cell center. Values represent means and standard errors from 1500 individual cells collected from three independent experimental series. Asterisks represent differences with the control that are significant at the 95% confidence level (Student's *t*-test).

3.3.2 Subdomain A1 restored the cell synchrony and inhibited elongation of IAA treated cells

The cell division of BY-2 cell line is partially synchronized and the synchrony can be disturbed by auxin transport inhibitor of 1-N-naphthylphthalamic acid (NPA) and auxin indole-3-acetic acid (IAA) (Maisch and Nick, 2007). To confirm subdomain A1 was actin bundling and to better understand the role of actin in auxin-dependent patterning, the stably transformed cell lines subdomain A1, B, NSP and BY-2 WT were incubated in the presence of 10 µM NPA and 2 µM IAA for 4 days to check the cell numbers per file. The nontransformed and transformed cells both exhibited peaks of files of two, four and six, and the even numbers were more frequent than the uneven numbers. For BY-2 WT (Figure 3.7 A) and NSP (Figure 3.7 D), after the treatment of IAA and NPA, files consisting of 4 cells decreased and files consisting of 1 cell increased. Hence, cell division was delayed in the presence of IAA and NPA, whereby treatment with 2 µM IAA had a stronger inhibitory on cell division than that of 10 µM NPA. Similar to the WT, in cells overexpressing Subdomain A1 (Figure 3.7 B), files consisting of 4 cells decreased and files consisting of 1 cell increased in the presence of IAA and NPA. However, the frequencies of files consisting of 4 cells were equal after addition of IAA and NPA. Subdomain A1 restored the synchrony in the presence of IAA compared with BY-2 WT and NSP. For Subdomain B, we did not see any significant changes of synchrony in the presence of Both IAA and NPA. Comparing the frequencies of transformed cells and that of nontransfromed cells (Figure 3.7 E), files consisting of 4 cells decreased and files consisting of 1 cell increased. Thus the cell divisions of the transformed cells were delayed.

After 7 days incubation in the presence of 10 µM NPA and 2 µM IAA, cell length and width were measured (Figure 3.7 F). The cell widths were similar with or without IAA or NPA. However, we observed a significant change of cell length. BY-2 WT and NSP overexpressing cells became shorter in the addition of NPA and IAA compared with the untreated samples. In conclusion, both cell division and cell elongation were affected. In cells overexpressing subdomain A1 and subdomain B, cell elongation was a little elevated in the presence of NPA, while it was inhibited in the presence of IAA.

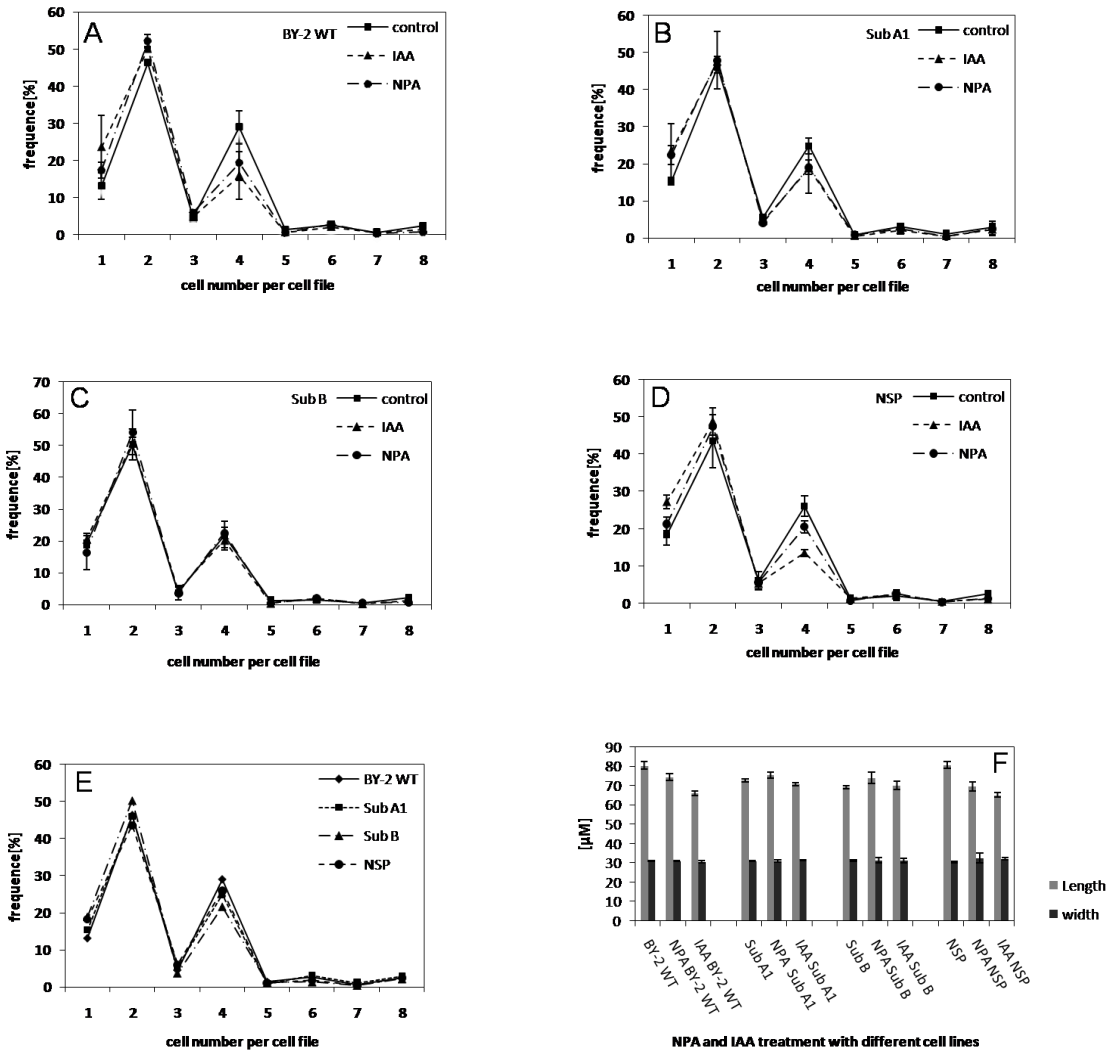

Figure 3.7 Effect of NPA and IAA on division pattern and cell length and width. (A-D) Frequency distribution over cell number per file of BY-2 WT, Subdomain A1, B, NSP overexpressing cells with or without 10µM NPA and 2µM IAA treatment for 7days. (E) Frequency distribution over cell

number per file of 7-day-old BY-2 WT, Subdomain A1, B and NSP cells. (F) 7-day-old cell length and width with or without 10µM NPA and 2µM IAA treatment. Values represent means and standard errors from 1500 individual cells collected from three independent experimental series.

3.4 Synthetic and partial ginkgilobin-2 peptides conjugated to a cell-penetrating peptide

3.4.1 Localization of ginkbilobin-2 subdomain conjugates in BY-2 cells

The attempt to generate stable overexpression cell line of the GFP-fusions with ginkbilobin-2 fragments was only partially successful, because the signal observed in the transformants was relatively low (see Figure 3.6 A-C) compared to the signal conferred by transient expression (see Figure 3.3). This indicates that overexpression of these transgenes impinges on viability, such that weaker expressors are favoured over stronger expressors. The stringency of antibiotic selection (100 mg l^{-1} kanamycin) was already at the maximum – further increase of stringency would therefore cause sublethality even of transformed cells. We therefore employed a different strategy: The cell-penetrating peptide (CPP) BP100 can carry functional cargoes into plant cells (Eggenberger *et al.*, 2011), which allows to administer a defined quantity of the function at any defined point in time. Therefore, various subdomains of ginkbilobin-2 were coupled with rhodamine B (RhB) as a fluorescent reporter and conjugated with BP100 by chemical synthesis, and then introduced into BY-2 WT cells. Since the previous experiments had shown that the actin-binding activity can be mainly attributed to subdomain A, we synthesized conjugates for subdomains A1, A2, and A3, respectively. Our specific aim here was to identify which of the three subdomains are responsible for binding to actin.

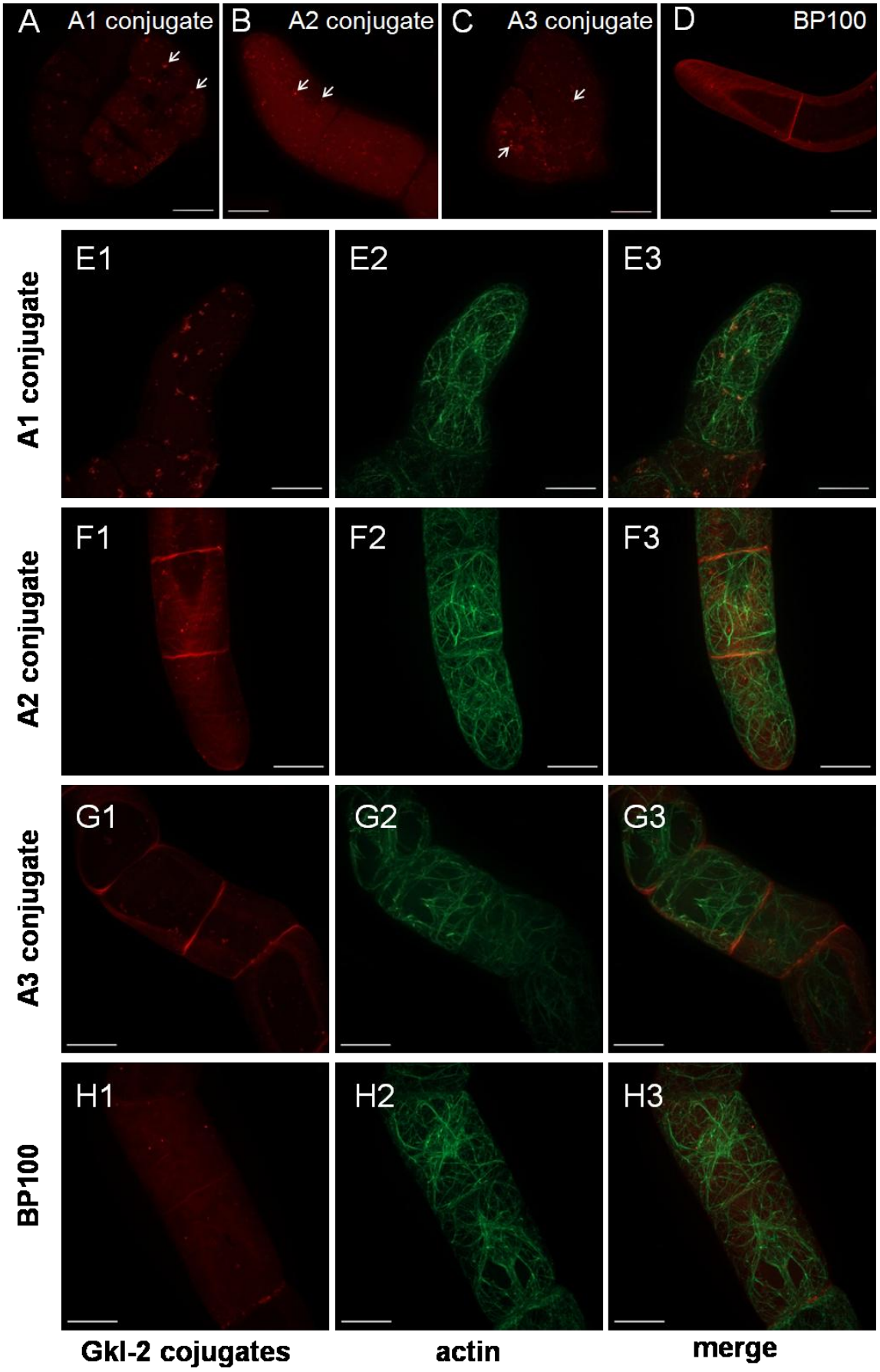
A
A1 conjugate
B
A2 conjugate
C
A3 conjugate
D
BP100
E1
E2
E3
F1
F2
F3
G1
G2
G3
H1
H2
H3
A1 conjugate
A2 conjugate
A3 conjugate
BP100
Gkl-2 cojugates
actin
merge

Figure 3.8 Localization of the peptide conjugates in BY-2 cells. Introduction of ginkbilobin-2 peptide conjugates with the cell-permeating peptide BP100 and rhodamine B as a fluorescent reporter into non-transformed cells of BY-2 (A-D), or into the actin-marker line GF11 expressing the actin-binding domain 2 of plant fimbrin in fusion with GFP (E-H). (A), (E) Subdomain A1. (B), (F) Subdomain A2. (C), (G) Subdomain A3. (D), (H) Unconjugated BP100. Panels (1E-1H) show the rhodamine signal, (2) the actin signal, and (3) the merge of both signals, respectively. Arrows show the punctate structures. Scale bar 20 µm.

Preparatory experiments demonstrated that treatment with the subdomain-CPP conjugates caused rapid cell death, if the concentration exceeded 1 µM. To follow uptake microscopically, we thus used 0.5 µM of the ginkbilobin-2 subdomain-CPP conjugates as well as the non-conjugated BP100 and incubated non-transformed BY-2 WT cells for 24 hours to test the uptake by spinning-disc microscopy. Confocal sections near the central plane of the cell demonstrated clearly that the fluorescent marker was present in the cytoplasm (Figure 3.8 A-D). For the conjugates with subdomain A1, A2, and A3, the signal was forming punctate structures. Some of these dots seemed to be aligned like beads on a string (Figure 3.8 A-C, shown with arrows). RhB coupled with BP100 alone was also transferred into the cytoplasm but produced diffuse labelling throughout the cytoplasm and was also bound along the cross wall (Figure 3.8 D). To get more insight into the localization of the peptides, the stable actin marker cell line GF-11 was incubated with the conjugates. The structures visualized by the subdomain A1 conjugate (Figure 3.8 E1) were associated with the transvacuolar actin cables. The fluorescence of the actin cables also appeared somewhat discontinuous. A similar outcome was observed for the subdomain A3 (Figure 3.8 G1-3). In contrast, for subdomain A2 and the non-conjugated BP100 (Figure 3.8 F, H), the RhB signal did not colocalize with actin filaments, which also were of contiguous appearance. Here, also a considerable fraction of the RhB signal was associated with the cross-walls.

3.4.2 Cell death can be induced by actin-binding ginkbilobin-2 peptides in fusion with BP100

We analyzed the cell-death response triggered by the conjugates in more detail, by employing the uptake of the non-permeable dye Evan's Blue as readout for mortality. A dose-response of mortality, scored 1 h after addition of the conjugates, showed a threshold at 1 µM and saturation (with 100% mortality) from 2 µM (Figure 3.9 A). As a control, we tested the unconjugated BP100 carrier but observed only a minor induction of mortality (saturating at around 25% from 2 µM), demonstrating that the high mortality is caused by the ginkbilobin peptide cargo and not by the carrier itself. Since the concentration range between threshold and saturation was very narrow at 1 h, this makes it difficult to see potential differences between the peptides. We therefore followed the time course of mortality for a concentration of 1 µM (Figure 3.9 B). Here, mortality developed most rapidly for the A1 and A3 conjugates, whereas A2 produced a weaker effect, and the BP100 carrier alone did not cause significant mortality, even after incubation for 24 h. Thus, those conjugates that decorated actin cables (A1 and A3), were also effective in inducing cell death, whereas the A2 conjugate that did not decorate actin cables, was also a less efficient trigger of cell death.

To gain insight of the progression of cell death, we traced the details of the cellular response of 4-day-old GF-11 treated with 2 µM subdomain A1 conjugate under the microscope for 8 min (Figure 3.9 C). Following that short time, the cell shrinked and the cables of the transvacuolar actin were destroyed rapidly. Simultaneously, the rhodamine labelled conjugated peptide went inside of the cell immediately around the nucleus (Figure 3.9 C second panel RBA1) due to the damaged cell membrane. In addition, some stress vesicles appeared in the 6-day-old GF-11 cells if grown in the presence of 0.5 µM A1 conjugate incubated for 24 hours (Figure 3.9 D 1-4).

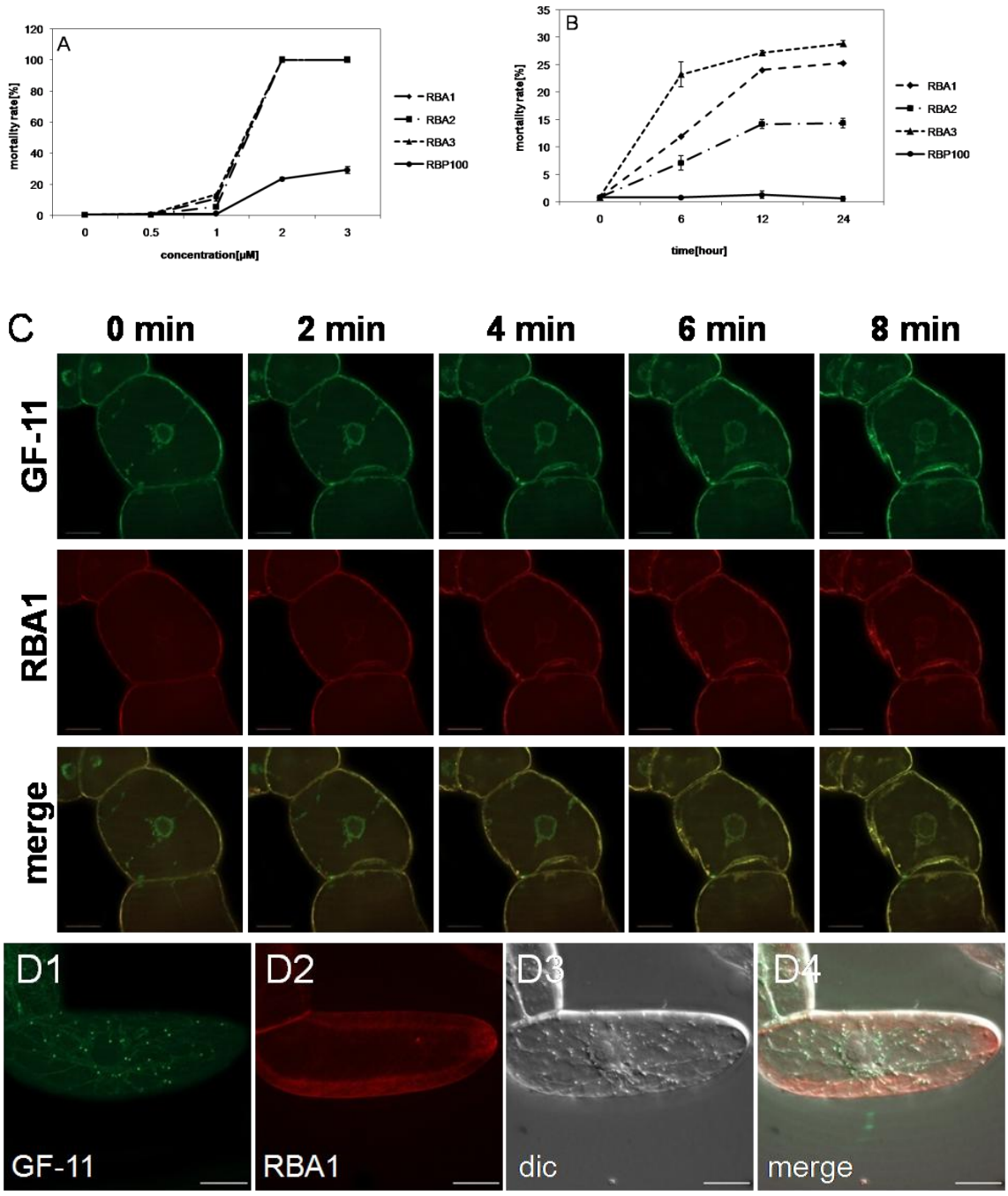

Figure 3.9 Peptide conjugates induced cell mortality in BY-2 cells. (A), (B) Mortality induced in non-transformed BY-2 cells upon incubation with the ginkbilobin-2 peptide conjugates and the non-conjugated BP100 carrier. (A) Dose response of mortality over the concentration of the conjugate with subdomain A1 (RBA1, diamonds), subdomain A2 (RBA2, squares), subdomain A3 (RBA3, triangles), or unconjugated BP100 (RBP100, circles) for a treatment of 1 hour. (B) Time course of mortality for treatment with 1 µM of the same conjugates as in (A). Data represent mean values and standard errors from three independent experimental series comprising a population of more than 3000 cells for each curve. (C) Detailed GF-11 cell death in addition of 2µM subdomain A1 conjugate (RBA1). First panel shows GFP of GF11, second panel shows

rhodamine B signal of RBA1, third panel shows merge of the two channels. (D) Cellular response of GF-11 cells over RBA1 treatment of 24 hours. (1) represents GFP, (2) represents rhodamine signal, (3) represents dic channel, (4) represents merge of the all three channels. Scale bar 20 µm.

3.4.3 Cellular uptake of conjugated peptides of ginkbilobin-2

According to the cell mortality results described above, the time point of uptake by 3-day-old BY-2 WT cells was tracked using 0.5 µM subdomain conjugates (A1, A2 and A3) and unconjugated BP100 at 6, 12 and 24 hours by spinning-disc microscopy. Confocal sections near the central plane of the cell demonstrated clearly that the fluorescent marker was present in the cytoplasm (Figure 3.10 A-D). The uptake was increased with the time course. For the conjugates with subdomain A1, A2, and A3 (Figure 3.10 A-C), the signal was forming punctate structures and bound along the cross wall after being incubated for 24 hours, whereas the cell uptake at 6 and 12 hours showed a diffuse label throughout the cytoplasm and was also bound along the cross wall. RhB coupled to BP100 alone was also transferred into the cytoplasm but only produced a homogeneous fluorescent labelled pattern without any punctate structures even for 24 hours incubation (Figure 3.10 D). And these peptoid-filled vesicles of subdomain A1 conjugates at 24 hours observed in the cell were attached to actin which was already shown in Figure 3.8 E.

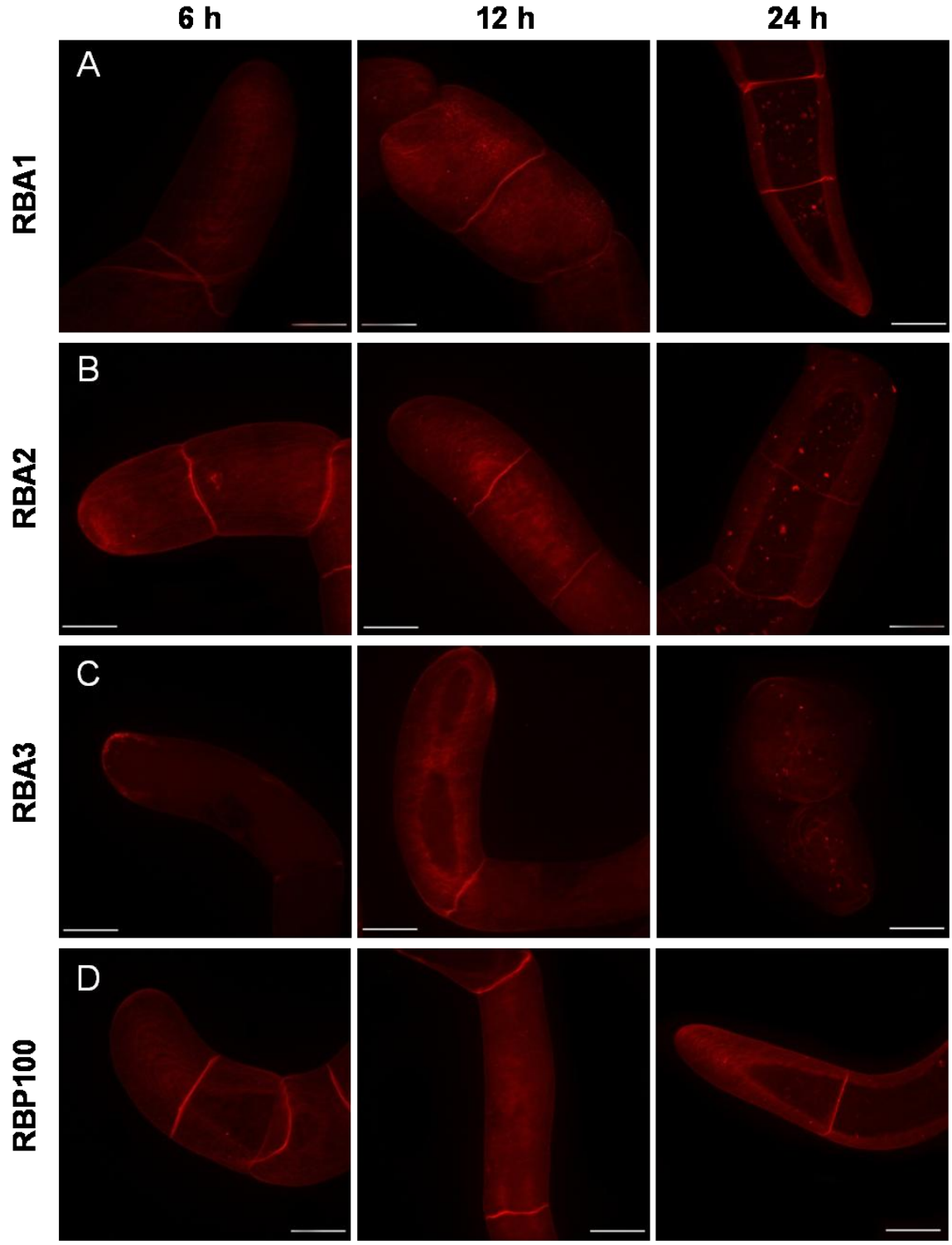

Figure 3.10 Visualization of BY-2 cell uptake at different time points. Introduction of ginkbilobin-2 peptide conjugates with the cell-permeating peptide BP100 and rhodamine B as fluorescent reporter into BY-2 WT cells. (A) Sudomain A1 (RBA1). (B) Sudomain A2 (RBA2). (C) Sudomain A3 (RBA3). (D) Unconjugated BP100 (RBP100). Scale bar 20 µm.

3.4.4 Actin bundled treated with peptide conjugates of ginkbilobin-2 in GF11 cell line

To find out the detailed cellular response, 2 µM conjugated ginkbilobin-2 peptides and unconjugated BP100 were delivered into the 4-day-old stable actin marker cell line GF11. Following 20 min visualization under the spinning-disc microscope, it became evident that actin was bundled under treatment of conjugated peptides of ginkbilobin-2 subdomain A1, A2 and A3 (Figure 3.11 A-C) with subdomains A1 and A3 (Figure 3.11 A and C) being the more potent one than subdomain A2 (Figure 3.11 B). The result was consistent with the finding that cell mortality is increase in subdomain A1 and A3 overexpressing cells (Figure 3.9 A and B). BP100 coupled with Rhodamine B only (Figure 3.11 D) and the control GF11 without any treatment (Figure 3.11 E) did not exhibit any actin bundle. Therefore bundling of actin can be understood as a stress signal that indicates the struggle against toxic peptides.

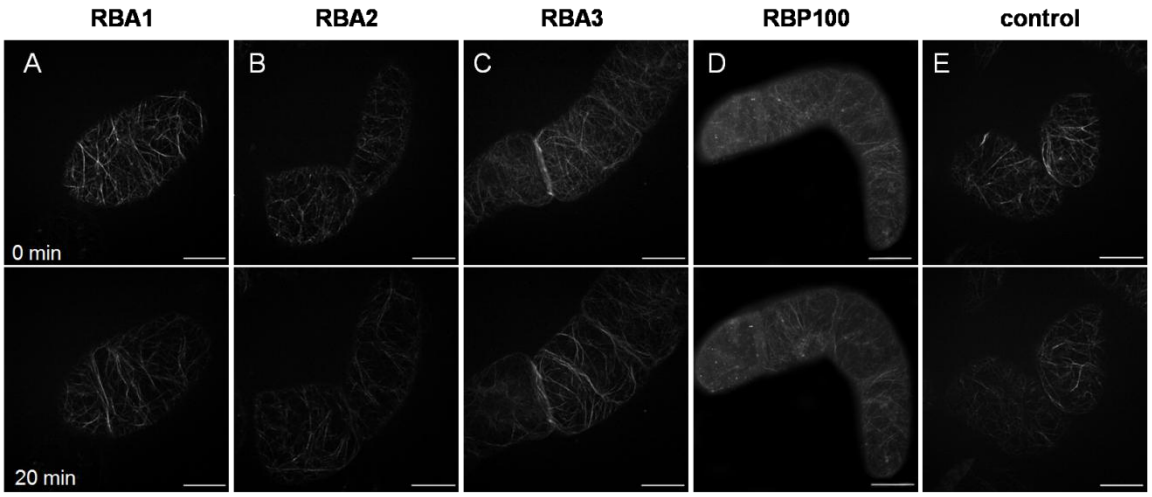

Figure 3.11 Stress response of actin filaments to subdomain conjugates of ginkbilobin-2. GF11 cell response to subdomain conjugates over 20 min. (A) Subdomain A1 conjugate (RBA1). (B) subdomain A2 conjugate (RBA2). (C) Subdomain A3 conjugate (RBA3). (D) Unconjugated BP100 (RBP100). (E) Control GF11 cells without treatment. Scale bar 20 µm.

3.4.5 Phytotropins and actin drugs affect the uptake of conjugated peptides

Conjugated peptides in fusion with BP100 were seen to accumulate in a highly heterogenous pattern. Even neighbouring cells of a cell file could differ in their uptake. This observation was correspondence with the doctoral thesis of Dr. Kai Eggenberger (2010).

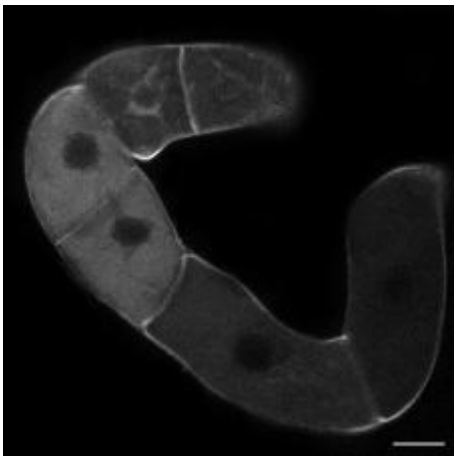

Figure 3.12 Distribution of BP100 in a tobacco BY-2 cell file after 24 hours of incubation. Scale bar 20 µm.

The amount of BP100 that had accumulated over 24 hours varied greatly between individual cells of a file as shown in figure 3.12. In this file, the two cells from the right clearly had accumulated the least within the cell file, while the next two cells had accumulated the most. And the other conjugated peptides fused with BP100 had the similar heterogenous pattern (data not shown).

The different uptake of the cells could be affected by auxin transport (doctoral thesis of Dr. Kai Eggenberger, 2010). To verify the conjugated peptides in fusion of BP100 were affected by auxin transport, tobacco BY-2 WT and GF-11 cells were pretreated with auxin efflux inhibitor 1-N-naphthylphthalamic acid (NPA), the naturally occurring auxin 3-indole-acetic acid (IAA), actin inhibitor latrunculin B and phalloidin. Following that, the cell mortality incubated with the peptide conjugates was recorded.

The effect of phytotropins and actin drugs on actin organization is showed in Figure 3.13. The overexpression of the actin-binding domain GF11 induced a strong reorganization of the actin cytoskeleton in the cell cortex (Figure 3.13 A-D 0 min). The presence of 2 µM IAA led to a debundling of actin and numerous fine

cortical actin filaments were observed (Figure 3.13 A 10 min). In the presence of 10 µM NPA, the cortical actin filaments were heavily bundled over 10 min (Figure 3.13 B). Latrunculin B blocks actin association and dissociation, which binds and irreversibly sequesters G-actin, led to an elimination of actin filaments into rods (Figure 3.13 C). Phalloidin decreases the rate of actin dissociation which causes increase of F-actin, and more actin filaments were associated with plasma membrane (Figure 3.13 D).

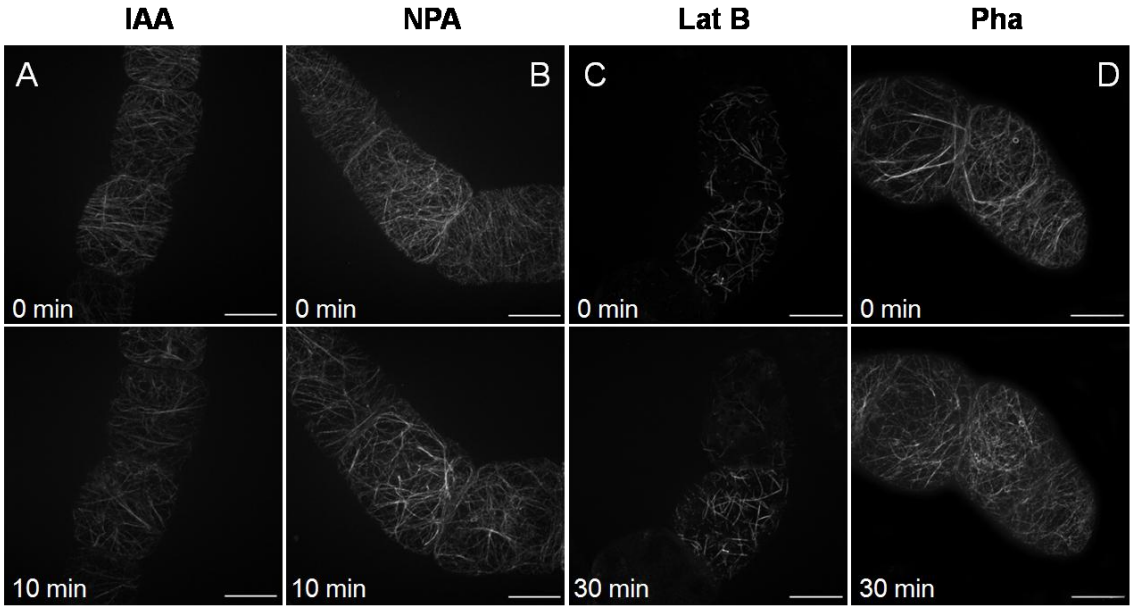

Figure 3.13 Effect of phytotropins and actin drugs on actin organization. GF-11 cell line was incubated with phytotropins (IAA and NPA) for 10 min and actin drugs (latrunculin B and phalloidin) for 30 min. (A) IAA treatment. (B) NPA treatment. (C) Latrunculin B treatment. (D) Phalloidin treatment. Scale bar 20 µm.

Following the pretreatment with the inhibitors above, the various subdomain conjugated peptides of ginkbilobin-2 and unconjugated BP100 were added, and immediately viewed the following 30 min under the microscope. The actin filaments were heavily bundled except the Lat B pretreated GF11 cells which was irreversible compared to the control with unconjugated BP100 (see the figures in appendix 5.11, P. 85). After incubation of BY-2 cells with the peptides for 6 hours, cell mortality was counted. The uptake of the conjugated peptides after

preincubation with the previously mentioned drugs was reduced compared to the untreated cells coinciding with decreased cell mortality to varying degrees from 2.3% to 15.15% (Table 3.1). However, the cell mortality of GF11 cells which overexpress actin-binding domain 2 of plant fimbrin was higher compared to BY-2 WT cells.

Table 3.1 Effect of inhibitors on uptake of conjugated peptides. The cell mortality and the variation of the cell mortality treated with the peptide conjugates in company with/without the inhibitor were shown in the table. NPA: 1-N-naphthylphthalamic acid, IAA: 3-indole-acetic acid, Lat B: latrunculin B.

Mortality (%)/ change (%) / Inhibitor / CPPS	BY-2 WT control	GF-11 control	GF-11 pretreated with IAA	GF-11 pretreated with NPA	GF-11 pretreated with Lat B	GF-11 pretreated with Phalloidin
RBA1	11.91	11.35/±0.00	7.35/-4	8.4/-2.95	4.7/-6.65	7.85/-3.5
RBA2	7.11	9.55/±0.00	5.85/-3.7	6.9/-2.65	1.95/-7.6	2.75/-6.8
RBA3	23.23	34.55/±0.00	26/-8.55	19.4/-15.15	27.15/-7.4	24.2/-10.35
RBP100	0.79	3.5/±0.00	1.2/-2.3	1.05/-2.45	1.15/-2.35	0.85/-2.65

3.5 Summary

Seeds of *Ginkgo biloba* contain high levels of the antifungal protein ginkbilobin (Wang and Ng, 2000) that exhibits sequence similarity to embryo-abundant proteins mainly from gymnosperms, and a homology with the extracellular domain of angiosperm cysteine-rich receptor-like kinases (Sawano *et al.*, 2007; Liu *et al.*, 2010). To get access to putative functions of ginkbilobin-2, we did a phylogenetic tree and alignment. The conservation of the cysteine signatures along with numerous other motifs of the ginkbilobin-2 domain throughout the evolution of vascular plants suggests that these motifs confer important biological functions. Alignments showed that the isolated subdomains (A1, A2, A3, B1 and B2) had additional homologues, and subdomains A1 was homology to CLASP-N-like/armadillo fold proteins which mediate interactions between actin filaments and microtubules.

With these putative speculations, we generated various cell lines overexpressing either full length or truncated ginkbilobin-2 with GFP tags for subsequent works. And during the process of establishing transgenic cell lines, the transformation procedure of the Buschmann method (Buschmann *et al.*, 2011) was modified which improved the performance in transforming tobacco BY-2 cells. Microscopic studies demonstrated that there was a signal peptide (26aa) at the N-terminus of ginkbilobin-2 and the localization of subdomain A1 might be related to actin filaments. To verify the pattern of subdomain A1, it was cotransformed with stable actin marker cell line FABD2-RFP and the two constructs were colocalizing. To further confirm the relation with actin, latrunculin B was used to eliminate the actin of subdomain A1 transformants and the phenotypes of the stable transformants treated with auxin were also studies. All the findings demonstrated that subdomain A1 labelling actin filaments.

In the last part, we employed a strategy based on chemical engineering using synthetic peptides comprising different parts of ginkbilobin-2 conjugated with the cell-permeating peptide BP100 and rhodamine B. We observed that higher amount of subdomain A1, A2 and A3 conjugates induced a rapid and efficient cell death. And the binding of subdomain A1 motives to actin filaments was monitored. The uptake of cell-penetrating peptide BP100 was reported to be driven by auxin transport (doctoral thesis of Dr. Kai Eggenberger, 2010). To gain insight of the mechanism, phytotropins and actin drugs were preincubated with the cells, and it demonstrated that the cell mortality treated with the peptide conjugates fused with BP100 was decreased compared to the untreated ones. This finding supports that the uptake is affected by auxin transport.

According to these findings, we conclude that ginkbilobin can interfere with the actin cytoskeleton of the target cell to activate an evolutionary conserved apoptotic pathway. However, a completed understanding about the function in vivo is still far from being accomplished.

4. Discussion

Fungi are an extremely diverse group of organisms with around 250,000 species and widely distributed in every ecosystem. Plants have evolved a variety of potent defence mechanisms, such as reinforcement of cell walls, hypersensitive responses (HR), and synthesis of secondary metabolites or antifungal proteins (Hammond-Kosack and Jones, 1996; Selitrennikoff, 2001; Wallace, 2004). So far, hundreds of antifungal proteins have been discovered in plants and are classified into different groups, such as thaumatin-like proteins, defensins, cyclophilins, ribosome-inactivating proteins, pathogenesis-related proteins, chitin-binding proteins and so on (Selitrennikoff, 2001). In the plant life cycle, the period of the seed germination is especially vulnerable for pathogen attack because pathogens could invade to seed storage tissues through the ruptured seed coats. Thus many plant seeds must contain antimicrobial proteins to protect their nutritious tissues from invaders. An antifungal protein ginkbilobin-2 isolated from the endosperm of *Ginkgo* seeds inhibits the growth of plant and human pathogenic fungi such as *Fusarium oxysporum* and *Candida albicans*. Interestingly, ginkbilobin-2 does not show any sequence similarity to other antimicrobial proteins such as cyclophilin, defensin, miraculin and thaumatin-like proteins (Sawano *et al.*, 2007).

What is the mechanism of this novel antifungal protein? In the following sections, we will discuss the findings from the results. First, the potential functions of ginkbilobin-2 will be discussed based on the previous work. In the second part, the advantages and cell responses in using the cell-penetrating carrier BP 100 to introduce functional cargoes (ginkbilobin-2 subdomains) into BY-2 cells are described. And based on these findings, we propose a working model on the function of ginkbilobin-2. Finally, the outlook is given, the remaining questions and the future work that should be answered and conducted.

4.1 Potential functions of ginkbilobin domains

4.1.1 Antifungal protein ginkbilobin

The plant receptor-like kinases (RLKs) play crucial roles in stress response and cellular processes. The cysteine-rich RLKs are a newly classified member with a C-X_8-C-X_2-C motif and are involved in plant defence responses, being induced by pathogen attack (Czernic *et al.*, 1999). But the mechanism of the novel antifungal protein is not clear. To understand the function of ginkbilobin, we did sequence homology analysis. From the alignment, we found that subdomain A1 was similar to a CLASP-N-like/armadillo fold protein which linked actin filaments to microtubule plus-ends, and it performed a couple of different functions related to connecting different proteins. Thus domain A1 might be responsible for the binding to actin filaments. The tertiary structure of ginkbilobin-2 has been solved based on crystallization and is composed of two α-helices and a β-sheet composed of five strands, which form a compact single-domain architecture comprising the α-helices and the β-strands (Miyakawa *et al.*, 2009). One of the α-helices produced by subdomain A2 constitutes a positively charged surface. This positively charged surface of subdomain A2 was suggested to interact with the (negatively charged) fungal surface, which might cause membrane permeabilization analogous to the case of sapecin, an insect defensin (Takeuchi *et al.*, 2004). Subdomain B contains a specific and conserved cysteine signature (C-X_8-C-X_2-C) that is also characteristic of so-called DUF-26 homologues, a subgroup of the extensive receptor-like kinase superfamily of angiosperms. This subgroup of cysteine-rich receptor-like kinases is involved in plant defence to pathogen attack (Czernic *et al.*, 1999). The conserved cysteine signature forms three disulfide bridges that are likely to contribute to the structural stability of ginkbilobin (Miyakawa *et al.*, 2009), and by functional analogy might act in pathogen recognition. The functional context of this putative pathogen recognition is certainly different: in *Ginkgo biloba*, the B-domain would target the actin-binding subdomain A1 to the pathogen, whereas in the context of the cysteine-rich

receptor-like kinases of angiosperms, the recognition of the pathogen would trigger an intracellular kinase cascade culminating in the activation of defence genes and, in the case of a biotrophic pathogen, programmed cell death.

4.1.2 Ginkbilobin binds to actin

To prove the predicted function of the protein, gateway vectors of the full length and partial cDNA of ginkbilobin-2 were constructed and transferred into BY-2 WT cells. We found that small vesicles accumulated along the cytoplasmic strands showed in C-terminal GFP fusion with the signal peptide (Figure 3.3 A, P. 30) and with full-length ginkbilobin-2 (Figure 3.3 B, P. 30). GFP fused to the N-terminus of full-length ginkbilobin-2 exhibited a different pattern to that of the C-terminal one, which labelled actin filaments (Figure 3.3 C, P. 30). So we confirmed that there was a signal peptide at the N-terminus of ginkbilobin-2, and the N-terminal fusion with GFP hided the function of the signal peptide. To identify the domain that accounts for actin binding, we constructed gateway vectors of various subdomains. Subdomain A1, A1+A2, A1+A2+A3 and full length without signal peptide (NSP/ΔSP) all exhibited the same actin like pattern, so domain A1 was destined to bind to actin (Figure 3.3 D, F, G and H, P. 30).

To further prove the localization of the subdomains, we colocalized the various domains with the stable actin marker line FABD2. Subdomain A1 was colocalizing with actin filaments (Figure 3.4 E, P. 33) and full length without signal peptide (NSP) colocalized with a certain subpopulation of actin filaments (Figure 3.4 D, P. 33). Latrunculin B treatment and TRITC-phalloidin actin staining of transformed BY-2 cells further confirmed that subdomain A1 is related to actin. Lat B was used as a tool to impair and eliminate the fine meshwork of actin filaments specifically, and the damaged and punctuated structures suggested that subdomain A1 and NSP labelled actin filaments (Figure 3.5 A-C, P. 34). Rhodamine-phalloidin actin staining showed that subdomain A1 (the filamentous structures labelled by GFP) and the rhodamine fluorescence were completely congruent (Figure 3.5 D, P. 34),

demonstrating that subdomain A1-GFP fusion protein labelled actin filaments. Since ginkbilobin-2 was cytoskeleton associated, we measured the nuclear movement of the stably transformed cell lines overexpressing subdomain A1, B and NSP. The nuclear position of 3-day-old subdomain A1 and NSP cells were significantly different compared to BY-2 WT, which were much closer to the plasma membrane, while for BY-2 WT it was closer to the center (Figure 3.6 D, P. 36). The delay of the nuclear movement feed back to a microtubule or actin cytoskeleton dependent process. Actin and tubulin are abundant cytoskeletal proteins of eukaryotic cells that play major roles in cytoplasmic organization and motility in both interphase and mitotic cells. Nuclear positioning in many cells is a microtubule dependent process, while some cases of nuclear positioning is involved in the actin cytoskeleton. In animal cells, the nuclear movement is tightly associated with a microtubule organizing center (MTOC) such as a centrosome or spindle pole body (SPB) or moves along microtubules like other cellular organelles (Reinsch and Gonczy, 1998; Starr and Fridolfsson, 2010; Metzger *et al.*, 2012). Plant nuclei move rapidly and farther along an actin filament cytoskeleton (Chytilova *et al.*, 2000). In plant cells, nuclei move large distances along the actin filaments, often undergoing shape changes when they move (Traas *et al.*, 1987; Chytilova *et al.*, 2000). They move more rapidly than animal nuclei by a unique mechanism involving actin and a myosin motor that enables rapid and long-distance nuclear movement and nuclear positioning in response to environmental stimuli (Van Bruaene *et al.*, 2003; Tamura *et al.*, 2013). The spatial correspondence between the distribution of actin filaments and microtubules indicates cooperation between both cytoskeleton elements in generating the motive force for nuclear migration (Lloyd *et al.*, 1987; Meindl *et al.*, 1994). So we concluded that the continuous bundling of actin filaments was the reason for the delayed nuclear movement of subdomain A1 and NSP.

The BY-2 cell line (Nagata *et al.*, 1992; Nagata and Kumagai, 1999) grows in simple files that exhibit basic characteristics of pattern formation, like clear axis

and polarity of cell division and growth. Hence, this system provides a good approach to study spatial aspects of cell division and detect fluctuations of hormone levels during cell division (Redig *et al.*, 1996). Actin is involved in auxin-dependent patterning. The state of actin filaments will be changed by auxin transport (Waller *et al.*, 2002; Nick, 2006; Maisch and Nick, 2007). Cell division was synchronized in cell lines with characteristic peaks of frequency two, four and six per cell file in BY-2 cells. After the treatment with IAA and NPA, frequencies of four cells per file of all the cell lines decreased and one cells per file increased, suggesting that the division of the cells was postponed (Figure 3.7 B, P. 38). For subdomain A1 (Figure 3.7 B, P. 38), the frequencies of files consisting of four cells were equal in the presence of IAA or NPA, while the cell frequencies of four cells per file of BY-2 WT treated with IAA were lower than that of NPA treated (Figure 3.7 A, P. 38). Therefore, subdomain A1 restored the synchrony in the presence of IAA compared with BY-2 WT. The results was consistent with Maisch who reported in 2007 that the constitutively bundled actin as well as the impaired synchrony of cell division depends on polar auxin transport, and the synchrony restored in the presence of IAA as the massive actin bundles are replaced by finer detached microfilaments. Previous studies of maize and rice coleoptiles demonstrate that IAA induced a dissociation of actin bundles and a formation of fine microfilament strands. The auxin response to actin involves changes in the bundling of actin filaments, with bundled actin being characteristic for a situation that auxin was depleted (Waller *et al.*, 2002; Holweg *et al.*, 2004). The cell length and width of cells overexpressing subdomain A1 was not changed after being treated with auxin. However, in the case of BY-2 WT, the cells became shorter in the presence of auxin (Figure 3.7 F, P. 38). It might be the bundling of actin balanced the increased auxin transport.

In conclusion, the binding of ginkbilobin to actin was mediated by the subdomain A1 (Figure 3.3, 3.4 and 3.5, P. 30, 33, 34), and it was necessary and sufficient for the delay of premitotic nuclear positioning (Figure 3.6 D, P. 36) and also restored

the synchrony in the presence of IAA (Figure 3.7 B, P. 38).

4.2 Advances in chemical engineering using functional cargoes

4.2.1 BP100 – a novel cell-penetrating carrier

Introduction of exogenous genes into plant cells is invaluable in various applications for basic plant science (Chilton, 2005). The *Agrobacterium*-mediated method (Broothaerts *et al.*, 2005) and particle bombardment (Boynton *et al.*, 1988) are two practical methods for delivering new genes into plant cells. Nevertheless, they all suffer from several limitations such as low yield in cell delivery, limitation of transgene sizes, risk of gene damage, restriction to applicable plant species and the requirement of expensive equipment (Miranda *et al.*, 1992). Therefore, new gene transformations systems are needed to explore for plant gene study. Cell-penetrating peptides which could be used successfully for the intracellular delivery of molecules offer a promising tool for noninvasive delivery. Cell-penetrating peptides have common features that are short, amphipathic and net positively charged. And these peptides offer advantages over the traditional transformation techniques due to the efficiency for a wide range of cell types (Lindgren *et al.*, 2000). In the last few decades, several cell-penetrating peptides have been demonstrated to pass through the plasma membrane of eukaryotic cells, and the mechanism is still under investigation. Peptide taken up into cells often involves the formation of a channel, either in the plasma membrane or in the endosomes. Pore formation in the plasma membrane like such caused by insect defensins will provoke cell death (Hoffmann *et al.*, 1996). In contrast for these cell-penetrating peptides, the translocation is reported to be receptor and energy independent and partially driven by endocytosis (Zorko and Langel, 2005). Zorko and Langel (2005) have constructed a hypothetical translocation diagram for CPPs, based on the known processes that occur during internalization (Figure 4.1). The uptake of CPP is a multistep process. The first step is the interaction of the cationic CPP molecules with the exposed negatively charged parts of the

phospholipid layer of the cell surface. After the internalization, the CCPs with the fusion proteins or peptides are either bound to cell intracellular structures or free in the cytoplasma. The uptake of the labelled CPPs in or at the cell membrane can be detected by confocal microscopy. The peptidolytic degradation of CPP exists in the cell which has been confirmed (Pooga *et al.*, 1998; Elmquist *et al.*, 2001), and finally, it will be released from the cell.

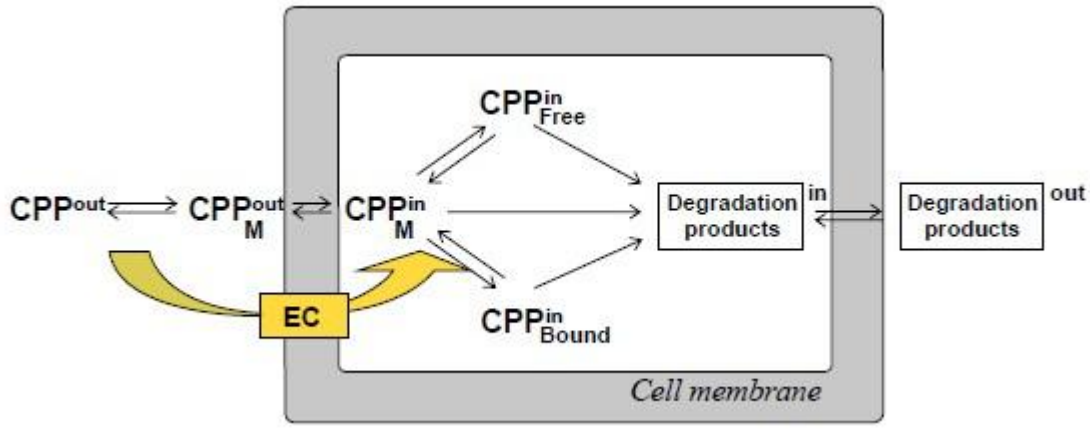

Figure 4.1 Simplified kinetic scheme for cell-penetrating peptide (CPP) internalization. In and out represent the CPP inside and outside the cell; M represents membrane bound CPP; Free means non-bound CPP (for instance in cytosol); Bound means the CPP that is interacting with inner cell structures (like intracellular membranes, proteins, etc); Degradation products means proteolytic cleavage of the CPP in the cell; EC denotes endocytosis. Cited from (Zorko and Langel, 2005).

Cell-penetrating peptides as delivery vehicles also have some undesirable side effects such as toxic effects on cell membranes or cell components and limitation of coupling large cargo (Zorko and Langel, 2005). BP100 (KKLFKKILKYL-amide) (Ferre *et al.*, 2009) as a cell-penetrating carrier shares common features with other CPPs, and BP100 has minimal toxic effects. In this study, 1µM of BP100 was sufficient to shuttle cargoes into BY-2 cells and did not show toxicity (Figure 3.8 and 3.9, P. 40, 43).

4.2.2 BP100 leading functional cargoes into plant cells

CPPs as delivery agents could rapidly translocate useful cargoes into living cells.

Various types of cargoes such as proteins (Pooga *et al.*, 2001), peptides (Taylor *et al.*, 2000; Villa *et al.*, 2000), fragments of DNA (Chen *et al.*, 2007), small molecules (Violini *et al.*, 2002) and liposomes (Tseng *et al.*, 2002) have been attached to CPPs and introduced into the cell. Cargoes (proteins or peptides) and CPPs are normally conjugated in tandem as fusion proteins (Lin *et al.*, 1995; Lin *et al.*, 1996; Rojas *et al.*, 1998). We have shown in previous work (Eggenberger *et al.*, 2011) that BP100 can be used as an efficient cell-penetrating carrier to enter living plant cells. This tool can be exploited for chemical engineering, by conjugating specific peptides that bind to specific cellular targets as cargo to BP100. As a proof of principle, the actin-binding peptide Lifeact had been successfully introduced into tobacco cells using BP100 and used to visualize the perinuclear actin network. Those earlier experiments by Eggenberger *et al.* (2011) have shown that Lifeact coupled to BP100 can be introduced into BY-2 cells and binds to the actin microfilaments, while Lifeact without BP100 can also be taken up by the cells but the Lifeact has no function that only localizes in the cytoplasm. Cell-penetrating peptides (CPPs) are short cationic peptides with an amphiphilic character that interact with the negatively charged cell surface and can finally pass through the hydrophobic lipid bilayer without causing any permanent damage. Although short cationic sequences with an amphiphilic nature seem to be required in CPPs to enable their membrane passage, the mechanism of this bilayer penetration is still unclear (Fischer *et al.*, 2004; Pujals *et al.*, 2006; Fonseca *et al.*, 2009). However, irrespective of the still enigmatic mechanism of uptake, the current work demonstrates that CPPs can be successfully used to introduce functional cargoes (in this case subdomain A1 of ginkbilobin) into living plant cells to obtain a specific cellular response namely programmed cell death (Figure 3.9, P. 43). However, lower amount of domain A1 conjugates could target to certain subpopulation of actin filaments (Figure 3.8, P. 40).

Monitoring the cellular uptake of the conjugated peptides of the various domains over 24 hours, we found that the uptake was increased over the time. Up to 24

hours, punctate structures appeared within the cell, while at the time point 6 and 12 hours, we only observed the diffuse rhodamine label throughout the cytoplasm (Figure 3.10, P. 45). In order to gain the mechanism of the internalization of BP100, we used actin drugs (Lat B and phalloidin) and phytotropins (IAA and NPA) to pretreat the cells. It has been reported in previous studies that the role of endocytosis in uptake of CPP is not negligible (Leifert and Whitton, 2003; Vives *et al.*, 2003). It has been shown that the internalization of protegrin derived SynB peptides and Tat derived CPPs into living cells is related to endocytotic processes (Drin *et al.*, 2003; Richard *et al.*, 2003). In plants, actin filaments drive the receptor-mediated endocytosis (Engqvist-Goldstein and Drubin, 2003; Baluska *et al.*, 2004). So we pretreated the BY-2 cells with Lat B and phalloidin, and it was shown that the death rate was decreased compared to not pretreated cells in the presence of BP100-subdomain conjugates (Table 3.1, P. 49), which was consistent with the previous work by Kai Eggenberger (2010, doctoral thesis). And the findings demonstrated that the internalization of BP100 carrier was mediated by actin filaments. It has already been confirmed that cell division and cell elongation was controlled by different auxin signalling pathways (Campanoni and Nick, 2005), and we have discussed above that the dynamic of actin filaments will be changed by auxin transport. We found that cell uptake of BP100 conjugates within a cell file was heterogenous (Figure 3.12, P. 47). This suggests that the uptake of BP100 was dependent on auxin transport. The cells pretreated with phytotropins (IAA and NPA) decreased the cell death rate in the presence of BP100-subdomain conjugates afterwards compared to not pretreated cells (Table 3.1, P. 49). These results indicated that the uptake of BP100 by the living plant cells was partially driven by actin mediated endocytosis.

4.3 Actin as a deadly switch

Our observations indicate a role of actin reorganization for the induction of programmed cell death, a phenomenon progressively emerging for eukaryotic

cells in general (for reviews see Gourlay and Ayscough, 2005; Franklin-Tong and Gourlay, 2008) that has also been demonstrated for plant cells (reviewed in Smertenko and Franklin-Tong, 2011). For instance, the bundling of actin cables in cells of the embryonic suspensor not only heralds ensuing cell death, but has been shown to be necessary and sufficient to initiate apoptosis in this system (for review see Smertenko and Bozhkov, 2014). We also could demonstrate in suspension cells of grapevine and tobacco that cell death triggered by bacterial Harpin elicitors is heralded by a rapid and specific reorganization of the actin cytoskeleton: The cortical actin filaments subtending the cell membrane detach, and the entire actin skeleton contracts into dense cables towards the nucleus (Qiao *et al.*, 2010, response of *Vitis rupestris*, to Harpin N; Guan *et al.*, 2013, response of tobacco BY-2 to Harpin Z). Moreover, the grapevine phytoalexin resveratrol, which seems to be crucial for resistance to biotrophic pathogens, can induce a similar actin response, which is later followed by programmed cell death (Chang *et al.*, 2011). In this study, we also observed that the actin filaments were bundled when the cell was treated with BP100-subdomain conjugated peptides over 20 min (Figure 3.11, P. 46), and some cells monitored under the microscope shrinked and died rapidly showing a destroyed actin cytoskeleton (Figure 3.9 C, P. 43). Additionally stress vesicles along actin filament were observed in the post cycling cells incubated with subdomain peptide conjugates (Figure 3.9 D, P. 43).

Based on the functional study conducted in the present work, a working model for the biological function of ginkbilobin can be proposed: The actin-bundling activity of subdomain A1 is prevented in the producer cell by efficient secretion of the protein by virtue of its N-terminal signal peptide. Upon secretion, ginkbilobin could be targeted through the B-domain to microbial surfaces and delivers there the actual “killer”, i.e. subdomain A1. The polar growth of fungal hyphae depends on the actin cytoskeleton (Pruyne and Bretscher, 2000a, b) sustaining very intensive recycling of membraneous material at the hyphal tip including numerous membrane fusion and separation events (Ayscough *et al.*, 1997). These events

are highly dependent on actin turnover and therefore represent a very sensitive target for compounds with antifungal activity. When ginkbilobin binds to the hyphal tip, it is expected to enter the cell as consequence of intensive membrane recycling events and will eventually come into contact with actin filaments to bind and interfere with their dynamicity. As a consequence, polar growth is arrested. Moreover, suppression of actin dynamicity can induce apoptotic cell death also in fungi, a phenomenon known in the literature as ‘actin-mediated apoptosis’ (Gourlay *et al.*, 2004; Gourlay and Ayscough, 2005, 2006). The antifungal activity of ginkbilobin has been demonstrated by plate inhibition assays (Wang and Ng, 2000; Sawano *et al.*, 2007) for different fungi such as *Fusarium oxysporum*, *Trichoderma reesei*, or *Candida albicans*. Unfortunately, the cellular mechanism of growth inhibition has not been addressed in those studies.

Based on this working model, the antifungal activity of ginkbilobin would exploit an evolutionarily conserved and ancient mechanism to control cell death via restricting actin dynamics. Later, by a functional shift in higher plants, the functional modules of ginkbilobin seemed to have been recruited for different purposes; the cysteine signature of the B-domain was integrated into receptor-like kinases such that microbial binding could be linked with defence signalling. Therefore, the A-domain became dispensable and was lost in most proteins except for some protective proteins of the seeds (the homologues harbouring the long C-terminal extension). Future work will be dedicated to analyse the cellular response of fungal hyphae to ginkbilobin and its functional subdomains.

4.4 Conclusion

According to the analysis and the experiments above, we could conclude that there was a signal peptide at the N-terminus of ginkbilobin-2, followed by an actin binding domain subdomain A1; subdomain A2 which formed a negative charged surface could be a transmembrane domain; subdomain A3 was similar to

bacterial surface protein without any predicted function. And the C-terminal part is the cysteine rich receptor-like domain (domain B) forming three disulfide bonds that involved in ligand binding. The cysteine-rich receptor-like kinases in *Arabidopsis* are induced by pathogen infection and convey hypersensitive reaction, which is a typical programmed cell death (Czernic *et al.*, 1999). In our current study, we found that subdomain A1, A2 and A3 coupled with cell-penetrating carrier BP100 could induce actin bundling of BY-2 cells and with higher concentration it would provoke cell death. However, the cell death rate was decreased after preincubating with actin drugs and auxin. Therefore it was clearly demonstrated that the mechanism of the uptake of CPP-BP100 was related to endocytosis. All these findings from this study support the above proposed model – ginkbilobin after secretion will recognize and bind to the actin of fungal hyphae and trigger actin-mediated apoptosis.

4.5 Outlook

Antifungal proteins have been isolated from diverse organisms, including animals, insects, plants and fungi. The mechanisms of these proteins are manifold including fungal cell wall polymer degradation, membrane channel and pore formation, damage of cellular ribosomes, inhibition of DNA synthesis and inhibition of the cell cycle (Selitrennikoff, 2001). New antifungal proteins with unknown mode of actions are being discovered permanently. To get insight in the function of these proteins, we need bio-techniques to translocate the genes into cells. Membranes of eukaryotic cells form a serious barrier for delivering the target molecules into the cells. To overcome this problem, many efforts have been conducted using viral vectors; however, it has several side effects like gene damage or disorder. And now newly synthesised cell-penetrating peptides which could be internalized into the cells without permanent damage have been well developed and used for scientific purpose. In this study, it became clear that CPP BP100 can be used as a novel tool for rapid gene delivery into plant cells.

However, the mechanism of its translocation into cells needs further exploration. And it also could be used in future studies to construct antifungal assays to enquire fungal hyphae response to ginkbilobin and its subdomains.

References

An, L.H., Wang, B.J. and Ji, C.J. (2007) Review of reproductive characters in *Ginkgo* and *Cycads*. *Acta Bot Boreal-occident Sin*, **27**, 2339-2345.

Ayscough, K.R., Stryker, J., Pokala, N., Sanders, M., Crews, P. and Drubin, D.G. (1997) High rates of actin filament turnover in budding yeast and roles for actin in establishment and maintenance of cell polarity revealed using the actin inhibitor latrunculin-A. *J Cell Biol*, **137**, 399-416.

Badosa, E., Ferre, R., Planas, M., Feliu, L., Besalu, E., Cabrefiga, J., Bardaji, E. and Montesinos, E. (2007) A library of linear undecapeptides with bactericidal activity against phytopathogenic bacteria. *Peptides*, **28**, 2276-2285.

Baluska, F., Samaj, J., Hlavacka, A., Kendrick-Jones, J. and Volkmann, D. (2004) Actin-dependent fluid-phase endocytosis in inner cortex cells of maize root apices. *J Exp Bot*, **55**, 463-473.

Banerjee, R.D. and Sen, P. (1980) Antibiotic activity of pteridophytes. *Eco. Botany* **34**, 284-298.

Bassilana, M. and Arkowitz, R.A. (2006) Rac1 and Cdc42 have different roles in *Candida albicans* development. *Eukaryot Cell*, **5**, 321-329.

Bernard, P. and Couturier, M. (1992) Cell killing by the F plasmid CcdB protein involves poisoning of DNA-topoisomerase II complexes. *J. Mol. Biol.*, **226**, 735-745.

Boynton, J.E., Gillham, N.W., Harris, E.H., Hosler, J.P., Johnson, A.M., Jones, A.R., Randolph-Anderson, B.L., Robertson, D., Klein, T.M., Shark, K.B. and et al. (1988) Chloroplast transformation in Chlamydomonas with high velocity microprojectiles. *Science*, **240**, 1534-1538.

Brogden, K.A. (2005) Antimicrobial peptides: pore formers or metabolic inhibitors in bacteria? *Nat Rev Microbiol*, **3**, 238-250.

Broothaerts, W., Mitchell, H.J., Weir, B., Kaines, S., Smith, L.M., Yang, W., Mayer, J.E., Roa-Rodriguez, C. and Jefferson, R.A. (2005) Gene transfer to plants by diverse species of bacteria. *Nature*, **433**, 629-633.

Buschmann, H., Green, P., Sambade, A., Doonan, J.H. and Lloyd, C.W. (2011) Cytoskeletal dynamics in interphase, mitosis and cytokinesis analysed through *Agrobacterium*-mediated transient transformation of tobacco BY-2 cells. *New Phytol*, **190**, 258-267.

Bushman, W., Thompson, J.F., Vargas, L. and Landy, A. (1985) Control of directionality in lambda site specific recombination. *Science*, **230**, 906-911.

Campanoni, P., Blasius, B. and Nick, P. (2003) Auxin transport synchronizes the pattern of cell division in a tobacco cell line. *Plant Physiol*, **133**, 1251-1260.

Campanoni, P. and Nick, P. (2005) Auxin-dependent cell division and cell elongation. 1-Naphthaleneacetic acid and 2,4-dichlorophenoxyacetic acid activate different pathways. *Plant Physiol*, **137**, 939-948.

Casamayor, A. and Snyder, M. (2002) Bud-site selection and cell polarity in budding yeast. *Curr Opin Microbiol*, **5**, 179-186.

Chang, X., Heene, E., Qiao, F. and Nick, P. (2011) The phytoalexin resveratrol regulates the initiation of hypersensitive cell death in Vitis cell. *PLoS One*, **6**, e26405.

Chen, C.P., Chou, J.C., Liu, B.R., Chang, M. and Lee, H.J. (2007) Transfection and expression of plasmid DNA in plant cells by an arginine-rich intracellular delivery peptide without protoplast preparation. *FEBS Lett*, **581**, 1891-1897.

Chen, Z. (2001) A superfamily of proteins with novel cysteine-rich repeats. *Plant Physiol*, **126**, 473-476.

Chilton, M.D. (2005) Adding diversity to plant transformation. *Nat Biotechnol*, **23**, 309-310.

Chugh, A. and Eudes, F. (2008) Study of uptake of cell penetrating peptides and their cargoes in permeabilized wheat immature embryos. *FEBS J*, **275**, 2403-2414.

Chytilova, E., Macas, J., Sliwinska, E., Rafelski, S.M., Lambert, G.M. and Galbraith, D.W. (2000) Nuclear dynamics in *Arabidopsis thaliana*. *Mol Biol Cell*, **11**, 2733-2741.

Czernic, P., Visser, B., Sun, W., Savoure, A., Deslandes, L., Marco, Y., Van Montagu, M. and Verbruggen, N. (1999) Characterization of an Arabidopsis thaliana receptor-like protein kinase gene activated by oxidative stress and pathogen attack. *Plant J*, **18**, 321-327.

Diamond, B.J., Shiflett, S.C., Feiwel, N., Matheis, R.J., Noskin, O., Richards, J.A. and Schoenberger, N.E. (2000) *Ginkgo biloba* extract: mechanisms and clinical indications. *Arch Phys Med Rehabil*, **81**, 668-678.

Dillen, W., De Clercq, J., Kapila, J., Zambre, M., Van Montagu, M. and Angenon, G. (1997) The effect of temperature on *Agrobacterium tumefaciens*-mediated gene transfer to plants. *the Plant J.*, **12**, 1459-1463.

Drin, G., Cottin, S., Blanc, E., Rees, A.R. and Temsamani, J. (2003) Studies on the internalization mechanism of cationic cell-penetrating peptides. *J Biol Chem*, **278**, 31192-31201.

Drubin, D.G., Miller, K.G. and Botstein, D. (1988) Yeast actin-binding proteins: evidence for a role in morphogenesis. *J Cell Biol*, **107**, 2551-2561.

Durst, S., Hedde, P.N., Brochhausen, L., Nick, P., Nienhaus, G.U. and Maisch, J. (2014) Organization of perinuclear actin in live tobacco cells observed by PALM with optical sectioning. *J Plant Physiol*, **171**, 97-108.

Eggenberger, K., Mink, C., Wadhwani, P., Ulrich, A.S. and Nick, P. (2011) Using the peptide BP100 as a cell-penetrating tool for the chemical engineering of actin filaments within living plant cells. *Chembiochem*, **12**, 132-137.

Elmquist, A., Lindgren, M., Bartfai, T. and Langel, U. (2001) VE-cadherin-derived

cell-penetrating peptide, pVEC, with carrier functions. *Exp Cell Res*, **269**, 237-244.

Engqvist-Goldstein, A.E. and Drubin, D.G. (2003) Actin assembly and endocytosis: from yeast to mammals. *Annu Rev Cell Dev Biol*, **19**, 287-332.

Fawell, S., Seery, J., Daikh, Y., Moore, C., Chen, L.L., Pepinsky, B. and Barsoum, J. (1994) Tat-mediated delivery of heterologous proteins into cells. *Proc Natl Acad Sci U S A*, **91**, 664-668.

Ferre, R., Badosa, E., Feliu, L., Planas, M., Montesinos, E. and Bardaji, E. (2006) Inhibition of plant-pathogenic bacteria by short synthetic cecropin A-melittin hybrid peptides. *Appl Environ Microbiol*, **72**, 3302-3308.

Ferre, R., Melo, M.N., Correia, A.D., Feliu, L., Bardaji, E., Planas, M. and Castanho, M. (2009) Synergistic effects of the membrane actions of cecropin-melittin antimicrobial hybrid peptide BP100. *Biophys J*, **96**, 1815-1827.

Fields, G.B. and Noble, R.L. (1990) Solid phase peptide synthesis utilizing 9-fluorenylmethoxycarbonyl amino acids. *Int J Pept Protein Res*, **35**, 161-214.

Finer, J.J., Vain, P., Jones, M.W. and McMullen, M.D. (1992) Development of the particle inflow gun for DNA delivery to plant cells. *Plant Cell Rep*, **11**, 323-328.

Fischer, R., Kohler, K., Fotin-Mleczek, M. and Brock, R. (2004) A stepwise dissection of the intracellular fate of cationic cell-penetrating peptides. *J Biol Chem*, **279**, 12625-12635.

Fischer, R., Zekert, N. and Takeshita, N. (2008) Polarized growth in fungi--interplay between the cytoskeleton, positional markers and membrane domains. *Mol Microbiol*, **68**, 813-826.

Fonseca, S.B., Pereira, M.P. and Kelley, S.O. (2009) Recent advances in the use of cell-penetrating peptides for medical and biological applications. *Adv Drug Deliv Rev*, **61**, 953-964.

Frahm, J.P. (2004) Recent development of Commercial products from *Bryophytes*. *The Bryologist*, **107**, 277-283.

Franklin-Tong, V.E. and Gourlay, C.W. (2008) A role for actin in regulating apoptosis/programmed cell death: evidence spanning yeast, plants and animals. *Biochem J*, **413**, 389-404.

Friedman, W.E. (1993) The evolutionary history of the seed plant male gametophyte. *Trends Ecol Evol*, **8**, 15-21.

Fullner, K.J. and Nester, E.W. (1996) Temperature affects the T-DNA transfer machinery of Agrobacterium tumefaciens. *J Bacteriol*, **178**, 1498-1504.

Gourlay, C.W. and Ayscough, K.R. (2005) Identification of an upstream regulatory pathway controlling actin-mediated apoptosis in yeast. *J Cell Sci*, **118**, 2119-2132.

Gourlay, C.W. and Ayscough, K.R. (2006) Actin-induced hyperactivation of the Ras signaling pathway leads to apoptosis in *Saccharomyces cerevisiae*. *Mol Cell Biol*, **26**, 6487-6501.

Gourlay, C.W., Carpp, L.N., Timpson, P., Winder, S.J. and Ayscough, K.R. (2004) A role for the actin cytoskeleton in cell death and aging in yeast. *J Cell Biol*, **164**, 803-809.

Guan, X., Buchholz, G. and Nick, P. (2013) The cytoskeleton is disrupted by the bacterial effector HrpZ, but not by the bacterial PAMP flg22, in tobacco BY-2 cells. *J Exp Bot*, **64**, 1805-1816.

Hammond-Kosack, K.E. and Jones, J.D. (1996) Resistance gene-dependent plant defense responses. *Plant Cell*, **8**, 1773-1791.

Hancock, R.E. and Sahl, H.G. (2006) Antimicrobial and host-defense peptides as new anti-infective therapeutic strategies. *Nat Biotechnol*, **24**, 1551-1557.

Hardie, D.G. (1999) PLANT PROTEIN SERINE/THREONINE KINASES: Classification and Functions. *Annu Rev Plant Physiol Plant Mol Biol*, **50**, 97-131.

Harris, S.D. (2006) Cell polarity in filamentous fungi: shaping the mold. *Int Rev Cytol*, **251**, 41-77.

Hartley, J.L., Temple, G.F. and Brasch, M.A. (2000) DNA cloning using in vitro site-specific recombination. *Genome Res.* , **10**, 1788-1795.

Herve, C., Dabos, P., Galaud, J.P., Rouge, P. and Lescure, B. (1996) Characterization of an *Arabidopsis thaliana* gene that defines a new class of putative plant receptor kinases with an extracellular lectin-like domain. *J Mol Biol*, **258**, 778-788.

Hoffmann, J.A., Reichhart, J.M. and Hetru, C. (1996) Innate immunity in higher insects. *Curr Opin Immunol*, **8**, 8-13.

Holweg, C., Susslin, C. and Nick, P. (2004) Capturing in vivo dynamics of the actin cytoskeleton stimulated by auxin or light. *Plant Cell Physiol*, **45**, 855-863.

Hornsey, I.S. and Hide, D. (1974) The production of antimicrobial compounds by British marine algae: Ⅰ. Antibiotic-producing marine algae. *Br. Phycol. J.* , **9**, 353-361.

Huang, X., Xie, W. and Gong, Z. (2000) Characteristics and antifungal activity of a chitin binding protein from *Ginkgo biloba*. *FEBS Lett*, **478**, 123-126.

Huckaba, T.M., Gay, A.C., Pantalena, L.F., Yang, H.C. and Pon, L.A. (2004) Live cell imaging of the assembly, disassembly, and actin cable-dependent movement of endosomes and actin patches in the budding yeast, *Saccharomyces cerevisiae*. *J Cell Biol*, **167**, 519-530.

Jacobs, B.P. and Browner, W.S. (2000) Ginkgo biloba: a living fossil. *Am J Med*, **108**, 341-342.

Johnston, G.C., Prendergast, J.A. and Singer, R.A. (1991) The *Saccharomyces cerevisiae* MYO2 gene encodes an essential myosin for vectorial transport of vesicles. *J Cell Biol*, **113**, 539-551.

Jones, J.D. and Dangl, J.L. (2006) The plant immune system. *Nature*, **444**, 323-329.

Kühn, S., Liu, Q., Eing, C., Frey, W. and Nick, P. (2013) Nanosecond electric pulses affect a plant-specific kinesin at the plasma membrane. *J Membr Biol*, **246**, 927-938.

Kakimoto, T. and Shibaoka, H. (1987) Actin filaments and microtubules in the preprophase band

and phragmoplast of tobacco cells. *Protoplasma* **140**, 151-156.

Kaksonen, M., Sun, Y. and Drubin, D.G. (2003) A pathway for association of receptors, adaptors, and actin during endocytic internalization. *Cell*, **115**, 475-487.

Karimi, M., Inze, D. and Depicker, A. (2002) GATEWAY vectors for *Agrobacterium*-mediated plant transformation. *Trends Plant Sci*, **7**, 193-195.

Karpova, T.S., Moltz, S.L., Riles, L.E., Guldener, U., Hegemann, J.H., Veronneau, S., Bussey, H. and Cooper, J.A. (1998) Depolarization of the actin cytoskeleton is a specific phenotype in *Saccharomyces cerevisiae*. *J Cell Sci*, **111 (Pt 17)**, 2689-2696.

Karpova, T.S., Reck-Peterson, S.L., Elkind, N.B., Mooseker, M.S., Novick, P.J. and Cooper, J.A. (2000) Role of actin and Myo2p in polarized secretion and growth of *Saccharomyces cerevisiae*. *Mol Biol Cell*, **11**, 1727-1737.

Klotz, J. and Nick, P. (2012) A novel actin-microtubule cross-linking kinesin, NtKCH, functions in cell expansion and division. *New Phytol*, **193**, 576-589.

Kobayashi, S., Chikushi, A., Tougu, S., Imura, Y., Nishida, M., Yano, Y. and Matsuzaki, K. (2004) Membrane translocation mechanism of the antimicrobial peptide buforin 2. *Biochemistry*, **43**, 15610-15616.

Kohlmeyer, J. (1971) Fungi from the *Sargasso Sea*. *Mar. Biol.*, **8**, 344-350.

Kohorn, B.D., Lane, S. and Smith, T.A. (1992) An Arabidopsis serine/threonine kinase homologue with an epidermal growth factor repeat selected in yeast for its specificity for a thylakoid membrane protein. *Proc Natl Acad Sci U S A*, **89**, 10989-10992.

Kubanek, J., Jensen, P.R., Keifer, P.A., Sullards, M.C., Collins, D.O. and Fenical, W. (2003) Seaweed resistance to microbial attack: a targeted chemical defense against marine fungi. *Proc Natl Acad Sci U S A*, **100**, 6916-6921.

Kubler, E. and Riezman, H. (1993) Actin and fimbrin are required for the internalization step of endocytosis in yeast. *EMBO J*, **12**, 2855-2862.

Leifert, J.A. and Whitton, J.L. (2003) "Translocatory proteins" and "protein transduction domains": a critical analysis of their biological effects and the underlying mechanisms. *Mol Ther*, **8**, 13-20.

Lin, L.C., Kuo, Y.C. and Chou, C.J. (2000) Cytotoxic biflavonoids from *Selaginella delicatula*. *J Nat Prod*, **63**, 627-630.

Lin, Y.Z., Yao, S.Y. and Hawiger, J. (1996) Role of the nuclear localization sequence in fibroblast growth factor-1-stimulated mitogenic pathways. *J Biol Chem*, **271**, 5305-5308.

Lin, Y.Z., Yao, S.Y., Veach, R.A., Torgerson, T.R. and Hawiger, J. (1995) Inhibition of nuclear translocation of transcription factor NF-kappa B by a synthetic peptide containing a cell membrane-permeable motif and nuclear localization sequence. *J Biol Chem*, **270**, 14255-14258.

Lindgren, M., Hallbrink, M., Prochiantz, A. and Langel, U. (2000) Cell-penetrating peptides.

Trends Pharmacol Sci, **21**, 99-103.

Liu, J., Y.H., W., Q., W., Z.Z., L. and A.G., G. (2010) Purification and Gene Cloning of an Antimicrobial Protein from Seeds of Ginkgo biloba L. *J. Agric. Biotech.*, **18**, 246-253.

Lloyd, C.W., Pearce, K.J., Rawlins, D.J., Ridge, R.W. and Shaw, P.J. (1987) Endoplasmic microtubules connect the advancing nucleus to the lip of legume root hairs, but F-actin is involved in basipetal migration. *Cell Motil. Cytoskel*, **8**, 27-36.

Maisch, J., Fiserova, J., Fischer, L. and Nick, P. (2009) Tobacco Arp3 is localized to actin-nucleating sites in vivo. *J Exp Bot*, **60**, 603-614.

Maisch, J. and Nick, P. (2007) Actin is involved in auxin-dependent patterning. *Plant Physiol*, **143**, 1695-1704.

Meindl, U., Zhang, D. and Hepler, P.K. (1994) Actin microfilaments are associated with the migrating nucleus and the cell cortex in the green alga *Micrasterias*. Studies on living cells. *J Cell Sci*, **107 (Pt 7)**, 1929-1934.

Metzger, T., Gache, V., Xu, M., Cadot, B., Folker, E.S., Richardson, B.E., Gomes, E.R. and Baylies, M.K. (2012) MAP and kinesin-dependent nuclear positioning is required for skeletal muscle function. *Nature*, **484**, 120-124.

Miranda, A., Janssen, G., Hodges, L., Peralta, E.G. and Ream, W. (1992) *Agrobacterium tumefaciens* transfers extremely long T-DNAs by a unidirectional mechanism. *J Bacteriol*, **174**, 2288-2297.

Miyakawa, T., Miyazono, K., Sawano, Y., Hatano, K. and Tanokura, M. (2009) Crystal structure of ginkbilobin-2 with homology to the extracellular domain of plant cysteine-rich receptor-like kinases. *Proteins*, **77**, 247-251.

Mundry, M. and Stutzel, T. (2006) Morphogenesis of leaves and cones of male short-shoots of *Ginkgo biloba* L. *Flora*, **199**, 437-452.

Nagata, T. and Kumagai, F. (1999) Plant cell biology through the window of the highly synchronized tobacco BY-2 cell line. *Methods Cell Sci*, **21**, 123-127.

Nagata, T., Nemoto, Y. and Hasezawa, S. (1992) Tobacco BY-2 cell line as the "Hela" cell in the cell biology of higher plants. *Int. Rev. Cytol.*, **132**, 1-30.

Nick, P. (2006) Noise yields order--auxin, actin, and polar patterning. *Plant Biol (Stuttg)*, **8**, 360-370.

Nick, P., Heuing, A. and B., E. (2000) Plant chaperonins: a role in microtubule-dependent wall formation? . *Protoplasma*, **211**, 234-244.

Numata, K. and Kaplan, D.L. (2010) Silk-based delivery systems of bioactive molecules. *Adv Drug Deliv Rev*, **62**, 1497-1508.

Olyslaegers, G. and Verbelen, J.P. (1998) Improved staining of F-actin and colocalization of mitochondria in plant cells. *J. Microsc.*, **192**, 73-77.

Parihar, P., Parihar, L. and Bohra, A. (2010) In vitro antibacterial activity of fronds (leaves) of some important pteridophytes. *J. Microbiol. Antimicrob.*, **2**, 19-22.

Phillips, A.J., Crowe, J.D. and Ramsdale, M. (2006) Ras pathway signaling accelerates programmed cell death in the pathogenic fungus *Candida albicans*. *Proc Natl Acad Sci U S A*, **103**, 726-731.

Phillips, A.J., Sudbery, I. and Ramsdale, M. (2003) Apoptosis induced by environmental stresses and amphotericin B in *Candida albicans*. *Proc Natl Acad Sci U S A*, **100**, 14327-14332.

Ponce de Leon, I. and Montesano, M. (2013) Activation of Defense Mechanisms against Pathogens in Mosses and Flowering Plants. *Int J Mol Sci*, **14**, 3178-3200.

Pooga, M., Hallbrink, M., Zorko, M. and Langel, U. (1998) Cell penetration by transportan. *FASEB J*, **12**, 67-77.

Pooga, M., Kut, C., Kihlmark, M., Hallbrink, M., Fernaeus, S., Raid, R., Land, T., Hallberg, E., Bartfai, T. and Langel, U. (2001) Cellular translocation of proteins by transportan. *FASEB J*, **15**, 1451-1453.

Pringle, J.R., Bi, E., Harkins, H.A., Zahner, J.E., De Virgilio, C., Chant, J., Corrado, K. and Fares, H. (1995) Establishment of cell polarity in yeast. *Cold Spring Harb Symp Quant Biol*, **60**, 729-744.

Pruyne, D. and Bretscher, A. (2000a) Polarization of cell growth in yeast. *J Cell Sci*, **113 (Pt 4)**, 571-585.

Pruyne, D. and Bretscher, A. (2000b) Polarization of cell growth in yeast. I. Establishment and maintenance of polarity states. *J Cell Sci*, **113 (Pt 3)**, 365-375.

Pujals, S., Fernandez-Carneado, J., Lopez-Iglesias, C., Kogan, M.J. and Giralt, E. (2006) Mechanistic aspects of CPP-mediated intracellular drug delivery: relevance of CPP self-assembly. *Biochim Biophys Acta*, **1758**, 264-279.

Qiao, F., Chang, X.L. and Nick, P. (2010) The cytoskeleton enhances gene expression in the response to the Harpin elicitor in grapevine. *J Exp Bot*, **61**, 4021-4031.

Redig, P., Shaul, O., Inze, D., Van Montagu, M. and Van Onckelen, H. (1996) Levels of endogenous cytokinins, indole-3-acetic acid and abscisic acid during the cell cycle of synchronized tobacco BY-2 cells. *FEBS Lett*, **391**, 175-180.

Reinsch, S. and Gonczy, P. (1998) Mechanisms of nuclear positioning. *J Cell Sci*, **111 (Pt 16)**, 2283-2295.

Rensing, S.A., Ick, J., Fawcett, J.A., Lang, D., Zimmer, A., Van de Peer, Y. and Reski, R. (2007) An ancient genome duplication contributed to the abundance of metabolic genes in the moss Physcomitrella patens. *BMC Evol Biol*, **7**, 130.

Richard, J.P., Melikov, K., Vives, E., Ramos, C., Verbeure, B., Gait, M.J., Chernomordik, L.V. and Lebleu, B. (2003) Cell-penetrating peptides. A reevaluation of the mechanism of cellular uptake. *J Biol Chem*, **278**, 585-590.

Riquelme, M., Fischer, R. and Bartnicki-Garcia, S. (2003) Apical growth and mitosis are independent processes in *Aspergillus nidulans*. *Protoplasma*, **222**, 211-215.

Rojas, M., Donahue, J.P., Tan, Z. and Lin, Y.Z. (1998) Genetic engineering of proteins with cell membrane permeability. *Nat Biotechnol*, **16**, 370-375.

Sano, T., Higaki, T., Oda, Y., Hayashi, T. and Hasezawa, S. (2005) Appearance of actin microfilament 'twin peaks' in mitosis and their function in cell plate formation, as visualized in tobacco BY-2 cells expressing GFP–fimbrin. *Plant Journal*, **44**, 595–605.

Sawano, Y., Miyakawa, T., Yamazaki, H., Tanokura, M. and Hatano, K. (2007) Purification, characterization, and molecular gene cloning of an antifungal protein from *Ginkgo biloba* seeds. *Biol Chem*, **388**, 273-280.

Schott, D., Ho, J., Pruyne, D. and Bretscher, A. (1999) The COOH-terminal domain of Myo2p, a yeast myosin V, has a direct role in secretory vesicle targeting. *J Cell Biol*, **147**, 791-808.

Selitrennikoff, C.P. (2001) Antifungal proteins. *Appl Environ Microbiol*, **67**, 2883-2894.

Shai, Y. (1999) Mechanism of the binding, insertion and destabilization of phospholipid bilayer membranes by alpha-helical antimicrobial and cell non-selective membrane-lytic peptides. *Biochim Biophys Acta*, **1462**, 55-70.

Sharma, B.D. and Vyas, M.S. (1985) Ethanobotanical studies on the fern and fern allies of Rajasthan. *Bull. of Bot. Survey of India*, **27**, 90-91.

Shaw, F.J.F. (1908) A contribution to the anatomy of *Ginkgo biloba*. *New Phytol*, **7**, 85-92.

Shen, G., Pang, Y., Wu, W., Deng, Z., Liu, X., Lin, J., Zhao, L., Sun, X. and Tang, K. (2005) Molecular cloning, characterization and expression of a novel Asr gene from *Ginkgo biloba*. *Plant Physiol Biochem*, **43**, 836-843.

Shiu, S.H. and Bleecker, A.B. (2001) Plant receptor-like kinase gene family: diversity, function, and signaling. *Sci STKE*, **2001**, re22.

Shiu, S.H., Karlowski, W.M., Pan, R., Tzeng, Y.H., Mayer, K.F. and Li, W.H. (2004) Comparative analysis of the receptor-like kinase family in Arabidopsis and rice. *Plant Cell*, **16**, 1220-1234.

Simeoni, F., Morris, M.C., Heitz, F. and Divita, G. (2003) Insight into the mechanism of the peptide-based gene delivery system MPG: implications for delivery of siRNA into mammalian cells. *Nucleic Acids Res*, **31**, 2717-2724.

Skalamera, D. and Heath, M.C. (1998) Changes in the cytoskeleton accompanying infection-induced nuclear movements and the hypersensitive response in plant cells invaded by rust fungi. *Plant J*, **16**, 191-200.

Smertenko, A. and Bozhkov, P. (2014) The Life and Death Signalling Underlying Cell Fate Determination During Somatic Embryogenesis. In *Applied Plant Cell Biology*, pp. 131-178.

Smertenko, A. and Franklin-Tong, V.E. (2011) Organisation and regulation of the cytoskeleton in

plant programmed cell death. *Cell Death Differ*, **18**, 1263-1270.

Snell, V. and Nurse, P. (1994) Genetic analysis of cell morphogenesis in fission yeast--a role for casein kinase II in the establishment of polarized growth. *EMBO J*, **13**, 2066-2074.

Spector, I., Shochet, N.R., Kashman, Y. and Groweiss, A. (1983) Latrunculins: novel marine toxins that disrupt microfilament organization in cultured cells. *Science*, **219**, 493-495.

Starr, D.A. and Fridolfsson, H.N. (2010) Interactions between nuclei and the cytoskeleton are mediated by SUN-KASH nuclear-envelope bridges. *Annu Rev Cell Dev Biol*, **26**, 421-444.

Stein, J.C., Howlett, B., Boyes, D.C., Nasrallah, M.E. and Nasrallah, J.B. (1991) Molecular cloning of a putative receptor protein kinase gene encoded at the self-incompatibility locus of Brassica oleracea. *Proc Natl Acad Sci U S A*, **88**, 8816-8820.

Takeuchi, K., Takahashi, H., Sugai, M., Iwai, H., Kohno, T., Sekimizu, K., Natori, S. and Shimada, I. (2004) Channel-forming membrane permeabilization by an antibacterial protein, sapecin: determination of membrane-buried and oligomerization surfaces by NMR. *J Biol Chem*, **279**, 4981-4987.

Tamura, K., Iwabuchi, K., Fukao, Y., Kondo, M., Okamoto, K., Ueda, H., Nishimura, M. and Hara-Nishimura, I. (2013) Myosin XI-i links the nuclear membrane to the cytoskeleton to control nuclear movement and shape in *Arabidopsis*. *Curr Biol*, **23**, 1776-1781.

Taylor, C.T., Furuta, G.T., Synnestvedt, K. and Colgan, S.P. (2000) Phosphorylation-dependent targeting of cAMP response element binding protein to the ubiquitin/proteasome pathway in hypoxia. *Proc Natl Acad Sci U S A*, **97**, 12091-12096.

Thevelein, J.M. (1992) The RAS-adenylate cyclase pathway and cell cycle control in *Saccharomyces cerevisiae*. *Antonie Van Leeuwenhoek*, **62**, 109-130.

Thevelein, J.M., Gelade, R., Holsbeeks, I., Lagatie, O., Popova, Y., Rolland, F., Stolz, F., Van de Velde, S., Van Dijck, P., Vandormael, P., Van Nuland, A., Van Roey, K., Van Zeebroeck, G. and Yan, B. (2005) Nutrient sensing systems for rapid activation of the protein kinase A pathway in yeast. *Biochem Soc Trans*, **33**, 253-256.

Toda, T., Uno, I., Ishikawa, T., Powers, S., Kataoka, T., Broek, D., Cameron, S., Broach, J., Matsumoto, K. and Wigler, M. (1985) In yeast, RAS proteins are controlling elements of adenylate cyclase. *Cell*, **40**, 27-36.

Tomiyama, K., Sato, K. and Doke, N. (1982) Effect of cytochalasin B and colchicine on hypersensitive death of potato cells infected by incompatible race of Phytophthora infestans. *Ann. Phytopathol. Soc. Jpn.*, **48**, 228-230.

Torralba, S., Raudaskoski, M., Pedregosa, A.M. and Laborda, F. (1998) Effect of cytochalasin A on apical growth, actin cytoskeleton organization and enzyme secretion in *Aspergillus nidulans*. *Microbiology*, **144 (Pt 1)**, 45-53.

Traas, J.A., Doonan, J.H., Rawlins, D.J., Shaw, P.J., Watts, J. and Lloyd, C.W. (1987) An actin network is present in the cytoplasm throughout the cell cycle of carrot cells and associates with the dividing nucleus. *J Cell Biol*, **105**, 387-395.

Tseng, Y.L., Liu, J.J. and Hong, R.L. (2002) Translocation of liposomes into cancer cells by cell-penetrating peptides penetratin and tat: a kinetic and efficacy study. *Mol Pharmacol*, **62**, 864-872.

Unnamalai, N., Kang, B.G. and Lee, W.S. (2004) Cationic oligopeptide-mediated delivery of dsRNA for post-transcriptional gene silencing in plant cells. *FEBS Lett*, **566**, 307-310.

Van Bruaene, N., Joss, G., Thas, O. and Van Oostveldt, P. (2003) Four-dimensional imaging and computer-assisted track analysis of nuclear migration in root hairs of *Arabidopsis thaliana*. *J Microsc*, **211**, 167-178.

van der Geer, P., Hunter, T. and Lindberg, R.A. (1994) Receptor protein-tyrosine kinases and their signal transduction pathways. *Annu Rev Cell Biol*, **10**, 251-337.

Villa, R., Folini, M., Lualdi, S., Veronese, S., Daidone, M.G. and Zaffaroni, N. (2000) Inhibition of telomerase activity by a cell-penetrating peptide nucleic acid construct in human melanoma cells. *FEBS Lett*, **473**, 241-248.

Violini, S., Sharma, V., Prior, J.L., Dyszlewski, M. and Piwnica-Worms, D. (2002) Evidence for a plasma membrane-mediated permeability barrier to Tat basic domain in well-differentiated epithelial cells: lack of correlation with heparan sulfate. *Biochemistry*, **41**, 12652-12661.

Vives, E., Richard, J.P., Rispal, C. and Lebleu, B. (2003) TAT peptide internalization: seeking the mechanism of entry. *Curr Protein Pept Sci*, **4**, 125-132.

Wade, D., Andreu, D., Mitchell, S.A., Silveira, A.M., Boman, A., Boman, H.G. and Merrifield, R.B. (1992) Antibacterial peptides designed as analogs or hybrids of cecropins and melittin. *Int J Pept Protein Res*, **40**, 429-436.

Wadhwani, P., Afonin, S., Ieronimo, M., Buerck, J. and Ulrich, A.S. (2006) Optimized protocol for synthesis of cyclic gramicidin S: starting amino acid is key to high yield. *J Org Chem*, **71**, 55-61.

Wadhwani, P., Burck, J., Strandberg, E., Mink, C., Afonin, S. and Ulrich, A.S. (2008) Using a sterically restrictive amino acid as a 19F NMR label to monitor and to control peptide aggregation in membranes. *J Am Chem Soc*, **130**, 16515-16517.

Wadhwani, P., Strandberg, E., van den Berg, J., Mink, C., Burck, J., Ciriello, R.A. and Ulrich, A.S. (2014) Dynamical structure of the short multifunctional peptide BP100 in membranes. *Biochim Biophys Acta*, **1838**, 940-949.

Walker, J.C. (1994) Structure and function of the receptor-like protein kinases of higher plants. *Plant Mol Biol*, **26**, 1599-1609.

Wallace, R.J. (2004) Antimicrobial properties of plant secondary metabolites. *Proc Nutr Soc*, **63**, 621-629.

Waller, F., Riemann, M. and Nick, P. (2002) A role for actin-driven secretion in auxin-induced growth. *Protoplasma*, **219**, 72-81.

Wang, H. and Ng, T.B. (2000) Ginkbilobin, a novel antifungal protein from *Ginkgo biloba* seeds with sequence similarity to embryo-abundant protein. *Biochem Biophys Res Commun*, **279**, 407-411.

Wang, X., Zafian, P., Choudhary, M. and Lawton, M. (1996) The PR5K receptor protein kinase from *Arabidopsis* thaliana is structurally related to a family of plant defense proteins. *Proc Natl Acad Sci U S A*, **93**, 2598-2602.

Weinberger, F. (2007) Pathogen-induced defense and innate immunity in macroalgae. *Biol Bull*, **213**, 290-302.

Wendland, J. and Philippsen, P. (2001) Cell polarity and hyphal morphogenesis are controlled by multiple rho-protein modules in the filamentous ascomycete *Ashbya gossypii*. *Genetics*, **157**, 601-610.

Wu, Y. and Zhou, J.M. (2013) Receptor-like kinases in plant innate immunity. *J Integr Plant Biol*, **55**, 1271-1286.

Yang, L., Harroun, T.A., Weiss, T.M., Ding, L. and Huang, H.W. (2001) Barrel-stave model or toroidal model? A case study on melittin pores. *Biophys J*, **81**, 1475-1485.

Yeaman, M.R. and Yount, N.Y. (2003) Mechanisms of antimicrobial peptide action and resistance. *Pharmacol Rev*, **55**, 27-55.

Zhang, G.G., Jing, Y., Zhang, H.M., Ma, E.L., Guan, J., Xue, F.N., Liu, H.X. and Sun, X.Y. (2012) Isolation and cytotoxic activity of selaginellin derivatives and biflavonoids from *Selaginella tamariscina*. *Planta Med*, **78**, 390-392.

Zhang, Z. (1998) Current progress in the studies on reproductive biology of *Ginkgo biloba*. *Chin Bot Bull*, **14**, 6-12.

Zhang, Z., Clayton, S.C., Cui, K. and Lee, C. (2013) Developmental synchronization of male and female gametophytes in *Ginkgo biloba* and its neck mother cell division prior to fertilization. *Physiol Plant*, **147**, 541-552.

Zorko, M. and Langel, U. (2005) Cell-penetrating peptides: mechanism and kinetics of cargo delivery. *Adv Drug Deliv Rev*, **57**, 529-545.

5. Appendix

5.1 Improved RNA extraction

5.1.1 RNA extraction buffer and instruments preparation

Extraction buffer: 2.5% CTAB (W/V), 100 mmol l^{-1} Tris-HCl (pH 8.0), 25 mmol l^{-1} EDTA (pH 8.0), 2 mol l^{-1} NaCl, 0.5 g l^{-1} Spermidine, 2% PVP (Sigma MW.40000). Before the extraction, 2% (v/v) β-mercaptoethanol and 1.5 mg ml^{-1} Proteinase K (Merk, Germany) was added to the extraction buffer. The extraction buffer was prepared freshly every time before use. After fully mixed, the extraction buffer was incubated at 42°C of water bath. Tris-HCl solution was prepared with the autoclaved DEPC-H_2O, the other solutions were treated with 0.1% DEPC-H_2O overnight then autoclaved. Mortars and tweezers were packed with silver paper, and sterilized in the oven at 180°C for 6 h. Tips and 2 ml reaction tubes were treated with 0.1% DEPC-H_2O overnight then autoclaved.

5.1.2 Total RNA extraction

500 µl preheated extraction buffer was pipetted into a 2 ml reaction tube. The powder of grinded seeds with liquid nitrogen was immediately transferred into the reaction tube, vortexed vigorously for 2 min, incubated at 45°C for 90 min and mixed it every 10 min. 0.5 ml water-saturated phenol: chloroform: isoamyl alcohol 25:24:1 was added, vortexed vigorously for 2 min, then centrifuged at 4°C, 14000 g, 5 min. 0.5 ml supernatant was pipetted to another 2 ml reaction tube. 1 ml Trizol was added, vortexed for 2 min and then incubated on the ice for 5 min. 0.3 ml chloroform was added, vortexed and kept for 5 min at room temperature, then centrifuged at 4°C, 14000 g, 10 min. 0.75 ml supernatant was pipetted to another 2 ml reaction tube, 1/4 volume 10 mol l^{-1} LiCl added, vortexed for 1 min, then kept at 4°C overnight. The following day, the samples were centrifuged at 4°C, 14000 g, 15min. The supernatant was discarded, 2 mol l^{-1} LiCl 1ml were added to suspend and rinse precipitate, and centrifuged again and the supernatant was discarded. The precipitate dissolved with 600 µl sterilized water (treated with 0.1% DEPC-H_2O), equal volume chloroform added, vortexed and incubated at room temperature for 5min, then centrifuged at 4°C, 14000 g, 10 min. 0.5 ml supernatant was transferred to another 2 ml reaction tube. 2.5 times volume (1.25 ml) ethanol and 50 µl (1/10 volume) 3 mol l^{-1} NaAc (PH 5.2) was added, vortexed vigorously for 1 min, and incubated at -20°C for 1h. Following the last step, the samples were centrifuged at 4°C, 14000 g, 1 min. The supernatant was discarded, 1ml 70% ethanol was added to suspend and rinse the precipitate. The samples were centrifuged shortly, the supernatant were discarded, the

precipitate was dried at the room temperature for 2 min, and last 10 µl sterilized water (treated with 0.1% DEPC-H_2O) was added to dissolve completely.

5.2 Coding sequence of the genes under investigation

Full length of ginkbilobin-2 (GenBank: DQ496113.1)

MKTMRMNSAFILAFALAAAMLILTEAANTAFVSSACNTQKIPSGSPFNRNLRAMLADLRQNT
AFSGYDYKTSRAGSGGAPTAYGRATCKQSISQSDCTACLSNLVNRIFSICNNAIGARVQLVD
CFIQYEQRSF

Signal peptide of ginkbilobin-2

MKTMRMNSAFILAFALAAAMLILTEA

Full length without signal peptide (NSP, ΔSP)

ANTAFVSSACNTQKIPSGSPFNRNLRAMLADLRQNTAFSGYDYKTSRAGSGGAPTAYGRAT
CKQSISQSDCTACLSNLVNRIFSICNNAIGARVQLVDCFIQYEQRSF

Subdomain A1

ANTAFVSSACNTQKIPSGSPF

Subdomain A1+A2

ANTAFVSSACNTQKIPSGSPFNRNLRAMLADLRQNTAF

Subdomain A1+A2+A3

ANTAFVSSACNTQKIPSGSPFNRNLRAMLADLRQNTAFSGYDYKTSRAGSGG

Subdomain B

APTAYGRATCKQSISQSDCTACLSNLVNRIFSICNNAIGARVQLVDCFIQYEQRSF

5.3 Primer sequences for TA cloning and Gateway®-Cloning

Primers	Sequences (5'- 3')
Full length Fw **Signal peptide Fw**	GGGGACAAGTTTGTACAAAAAAGCAGGCTTCATGAAGAC TATGAGAATGAATTCGG
Full length Re N-terminal	GGGGACCACTTTGTACAAGAAAGCTGGGTCTTAGAAGCT

	CCTCTGCTCG
Full length Re C-terminal **Full length without SP Re** **Domain B Re**	GGGGACCACTTTGTACAAGAAAGCTGGGTCGAAGCTCC TCTGCTCGTATTG
Signal peptide Re C-terminal	GGGGACCACTTTGTACAAGAAAGCTGGGTCAGCTTCTGT AAGTATGAGCATGGC
Domain B Fw	GGGGACAAGTTTGTACAAAAAAGCAGGCTTCATGGCACC CACTGCCTACGG
Full length without SP Fw **Domain A1 Fw** **Domain A1+A2 Fw** **Domain A1+A2+A3 Fw**	GGGGACAAGTTTGTACAAAAAAGCAGGCTTCATGGCCAA TACAGCCTTCGTC
Domain A1 Re C-terminal	GGGGACCACTTTGTACAAGAAAGCTGGGTCAAATGGGCT GCCGCTTGG
Domain A1+A2 Re C-terminal	GGGGACCACTTTGTACAAGAAAGCTGGGTCGAAGGCAG TGTTTTGCCTC
Domain A1+A2+A3 Re C-terminal	GGGGACCACTTTGTACAAGAAAGCTGGGTCTCCTCCGCT TCCTGCAC

5.4 TA cloning technology overview

5.4.1 Ligation Protocol

Reaction component	**Volume**
2X Rapid Ligation Buffer, T4 DNA Ligase	5 µl
pGEM®-T Easy Vector (50 ng)	1 µl
A-tailing PCR product	3 µl
T4 DNA Ligase (3 Weiss units/µl)	1 µl
Final volume	10 µl

5.4.2 Transformation Protocol

1. Prepare two LB/100 µg ml^{-1} ampicillin/0.5 mM IPTG/ 80 µg ml^{-1} X-Gal plates for each ligation reaction. Equilibrate the plates to room temperature.

2. Centrifuge the tubes containing the ligation reactions to collect the contents at the bottom. Add 2 µl of each ligation reaction to a sterile 1.5ml reaction tube on ice.

3. Take reaction tube(s) of frozen DH 5α Competent Cells from storage and place in an ice bath until just thawed (about 5 min). Mix the cells by gently flicking the reaction tube. Avoid excessive pipetting, as the competent cells are extremely fragile.

4. Carefully transfer 50 µl of cells into each reaction tube prepared in Step 2.

5. Gently flick the reaction tubes to mix and place them on ice for 20 min.

6. Heat-shock the cells for 45–50 seconds in a water bath at exactly 42°C (do not shake).

7. Immediately return the reaction tubes to ice for 2 minutes.

8. Add 950 µl room-temperature LB medium to the reaction tubes containing cells transformed with ligation reactions.

9. Incubate for 1.5 h at 37°C with shaking (~150rpm).

10. Plate 100 µl of each transformation culture onto duplicate LB/ampicillin/IPTG/X-Gal plates. If a higher number of colonies is desired, the cells may be pelleted by centrifugation at 1,000 × g for 10 min, resuspended in 200 µl of LB medium, and 100 µl plated on each of two plates.

11. Incubate the plates overnight (16–24 hours) at 37°C. If 100 µl is plated, approximately 100 colonies per plate are routinely seen using competent cells that are 1×10^8 cfu/µg DNA. Longer incubations or storage of plates at 4°C (after 37°C overnight incubation) may be used to facilitate blue color development. White colonies generally contain inserts; however, inserts may also be present in blue colonies.

For more information concerning the TA-cloning technology, refer to the manual “pGEM®-T and pGEM®-T Easy Vector Systems” (promega: http://www.promega.com).

5.5 Gateway® recombination reactions technology overview

The Gateway® technology (Invitrogen Corporation, Paisley, UK) uses the bacteriophage site-specific lambda recombination system to facilitate transfer of heterologous DNA sequences between vectors (Hartley *et al.*, 2000). The components of the lambda recombination sites (*att* sites) are modified to improve the specificity and efficiency of the system (Bushman *et al.*, 1985).

Two recombination reactions constitute the basis of this technology:

1. BP reaction: Facilitates recombination of an *attB* substrate (attB-PCR product) with an *attP* substrate (called “donor vector”) to create an *attL*-containing entry clone. This reaction is catalysed by BP Clonase™ II enzyme mix (Invitrogen).

2. LR reaction: Facilitates recombination of an *attL* substrate (called “entry clone”) with an *attR* substrate (called “destination vector”) to create an *attB*-containing expression clone. This reaction is catalysed by LR Clonase™ II enzyme mix (Invitrogen).

The presence of the *ccdB* gene within this system allows negative selection of the donor and destination vectors in E. coli following recombination and transformation. The CcdB protein interferes with E. coli DNA gyrase (Bernard and Couturier, 1992), thereby inhibiting growth of most *E. coli* strains. When recombination occurs (i.e. between an attB-PCR product and a donor vector or between an entry clone and a destination vector), the *ccdB* gene is replaced by the gene of interest. Cells that take up unreacted vectors carrying the *ccdB* gene or by-product molecules retaining the *ccdB* gene will fail to grow. This allows high-efficiency recovery of the desired clones. For more information concerning the Gateway® technology, refer to the manual “Gateway® Technology with Clonase™ II” (Invitrogen; http://www.invitrogen.com). This summary of the Gateway® technology was taken from the doctoral thesis of Dr. Jan Maisch (Botanical Institute I, KIT, Karlsruhe; Maisch, 2007).

5.6 Gateway® destination vector of ginkbilobin-2 maps

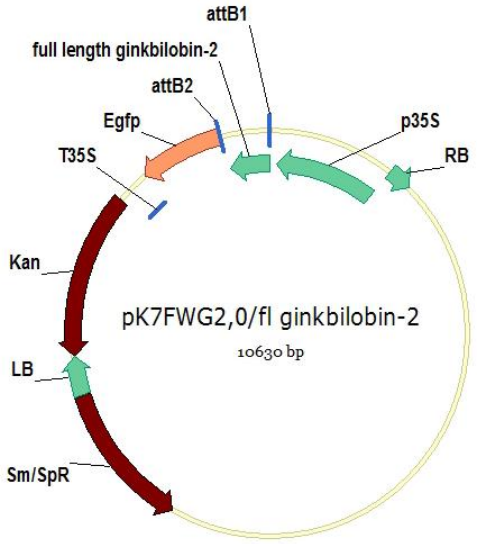
attB1
full length ginkbilobin-2
attB2
Egfp
T35S
p35S
RB
Kan
LB
Sm/SpR
pK7FWG2,0/fl ginkbilobin-2
10630 bp

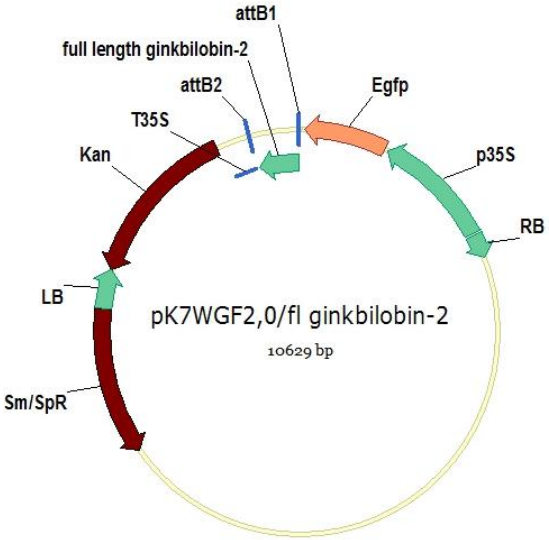
attB1
full length ginkbilobin-2
attB2
Egfp
T35S
p35S
RB
Kan
LB
Sm/SpR
pK7WGF2,0/fl ginkbilobin-2
10629 bp

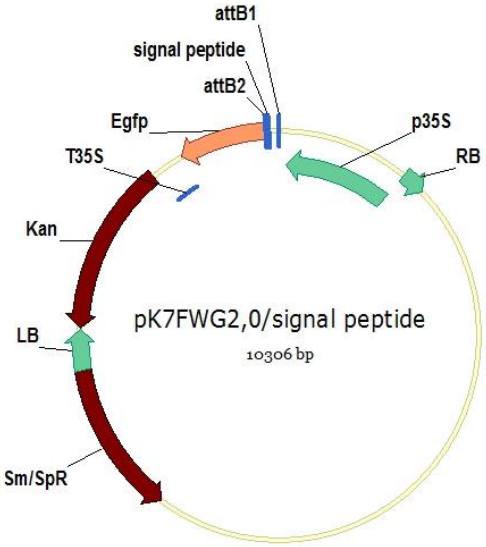
attB1
signal peptide
attB2
Egfp
p35S
T35S
RB
Kan
LB
Sm/SpR
pK7FWG2,0/signal peptide
10306 bp

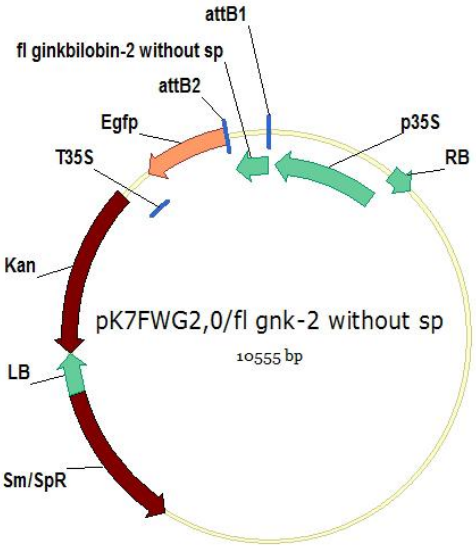
attB1
fl ginkbilobin-2 without sp
attB2
Egfp
p35S
T35S
RB
Kan
LB
Sm/SpR
pK7FWG2,0/fl gnk-2 without sp
10555 bp

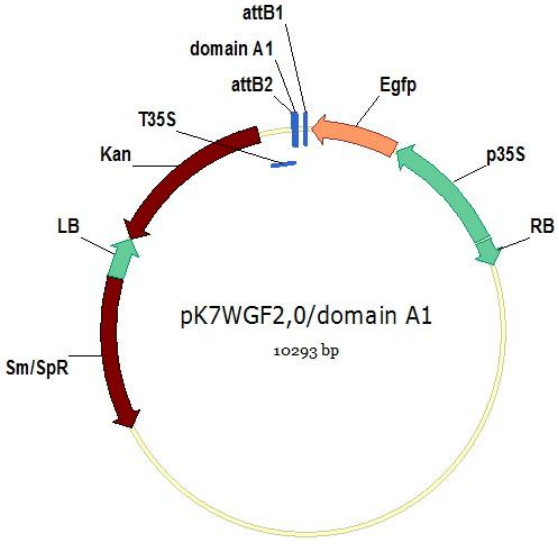
attB1
domain A1
attB2
Egfp
T35S
Kan
p35S
LB
RB
Sm/SpR
pK7WGF2,0/domain A1
10293 bp

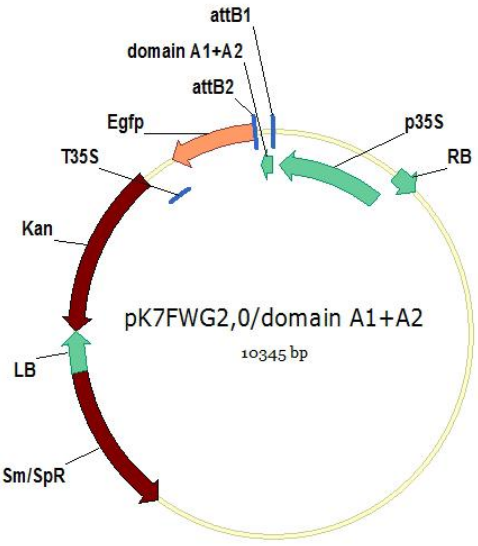
attB1
domain A1+A2
attB2
Egfp
p35S
T35S
RB
Kan
LB
Sm/SpR
pK7FWG2,0/domain A1+A2
10345 bp

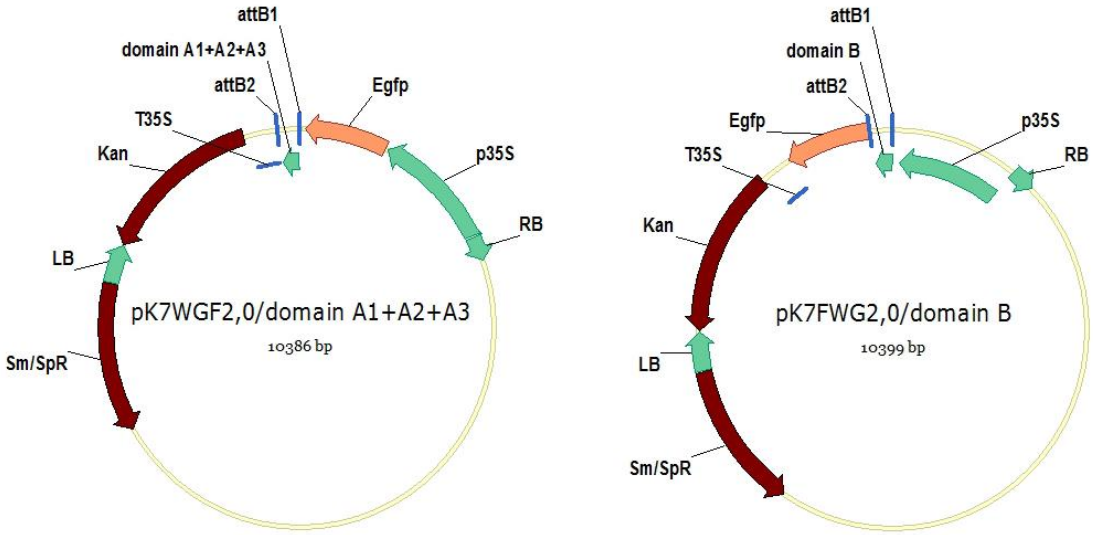

5.7 Preparation of DNA-coated gold particles for biolistic transformation

120 mg of gold particles (1.5-3.0 µm; Sigma-Aldrich) were suspended in 1 ml 50 % (v/v) sterile glycerol by mixing on a platform vortexer (Bender & Hobein, Zurich, Switzerland). Continuous agitation of the suspended gold particles was needed for uniform DNA precipitation onto gold particles maximizing uniform sampling. For each sample, 12.5 µl of gold suspension was removed to a 1.5 ml reaction tube.

While mixing vigorously, the following components were added successively: 1 µg of DNA, 12.5 µl of 2.5 M sterile $CaCl_2$, and 5 µl of 0.1 M sterile spermidine (Roth, Karlsruhe, Germany).

Following supplementary mixing for 3 minutes, the DNA-coated gold particles were spun down briefly, and the supernatant was discarded. Subsequently, the gold particles were washed with 125 µl of ice-cold absolute ethanol and resuspended in 40 µl of ice-cold absolute ethanol. DNA-coated gold particles were loaded onto the macrocarrier (BIO-RAD, Hercules, CA, USA) in 10 µl steps. Particle bombardment was performed immediately after complete evaporation of the ethanol.

This protocol was taken and modified from the doctoral thesis of Dr. Jan Maisch (Botanical Institute I, KIT, Karlsruhe; Maisch J., 2007).

5.8 Sequences of ginkbilobin-2 subdomain peptide conjugates

Peptide conjugates	Sequence
Rhodamine B- BP100-	RhB-(KKLFKKILKYL)-(ANTAFVSSACNTQKIPSGSPF)

subdomain A1 (RBA1)	
Rhodamine B- BP100-subdomain A2 (RBA2)	RhB-(KKLFKKILKYL)-(NLRAMLADLRQNTAF)
Rhodamine B- BP100-subdomain A3 (RBA3)	RhB-(KKLFKKILKYL)-(SGYDYKTSRAGSGG)
Rhodamine B- BP100 (RBP100)	RhB-(KKLFKKILKYL)

5.9 Alignment of ginkbilobin-2 subdomains with other homologous proteins

A4ZDL 6 represents the antifungal protein ginkbilobin-2.

Subdomain A1

```
>A4ZDL6_GNK2_GINBI      ANTAFVSSACNTQ-KIPSGSPF
>D0N3V3_PHYIT           VSKDGVSSS-ETQ-KIPAG PL
>H9HXS0_ATTCE           RDDSKTNSPTSTQSKIPSG PF
>E2B1J0_CAMFO        ATDENNPKTNSPTSTQLKIPSG PF
```

The three of the homologous protein are CLASP-N-like/armadillo fold, homology behind CLASP-N-domain. Phytophthora (DON3V3), leaf cutter ant (H9HXS0), carpenter ant (E2B1J0).

Subdomain A2

```
>A4ZDL6_GNK2_GINBI  NLRA---MLADLRQNTAF
>J2UWU2_9BURK       NLRAGDAMLADLRQ
>D7BA94_MEISD       NLRA---MLEDLR
>A4YNX5_BRASO       NLRERDAKLADLRQHAA
>H0TB79_9BRAD       NLRERDAKLADLRQHAA
>H0SFQ8_9BRAD       NLRERDAKLADLRQHAA
>H0RVR1_9BRAD       NLRERDAKLADLRQHAA
```

The six of the homologous proteins are located at the start of the histidine kinase. Herbaspirillum (J2UWU2), Meiothermus Silvanus (D7BA94), Bradyrhizobium (H0TB79, H0SFQ8, H0RVR1).

Subdomain B1

```
>A4ZDL6_GNK2_GINBI  APTAYGRATCKQSISQSDCTACLSNLVNRI
>B9S441_RICCO          AYGHAACNQNLTSSDCTACL
>B9H872_POPTR          AYGHAACNQNLTSSDCSSCL
>K7TJX4_MAIZE        TMYGVAQCRPDVSASDCTACLAAASSKLI
```

The homologous proteins are receptor-like kinase function envisaged. Ricinus communis (B9S441), Populus trichocarpa (B9H872), Maize DUF26 domain (K7TJX4).

Subdomain B2

```
>A4ZDL6_GNK2_GINBI  ICNAIGARV     QLD C FI      QYEQSF
>K7LJU0_SOYBN           ISARV     QLDGC YIH      YE
>K8YA55_STAAU           ISDRVIYSKQLD C FIIVKNNQYE
>D2P5U3_LISM2                       D C FV      QYEQ
>K0TNB8_THAOC             ARV     QLD C F
>B9S7M6_RICCO           AVAARV     QLNGCYF       HYE
```

Unknown soybean protein (K7LJU0), Staphylococcus several sequences linked with pathogenicity (K8YA55), Listeria protein (D2P5U3), Diatom protein (K0TNB8), Castor bean DUF26 domain kinase (B9S7M6).

5.10 Visualization of stable transformed calli of full length and signal peptide of ginkbilobin-2 with C-terminally fused GFP

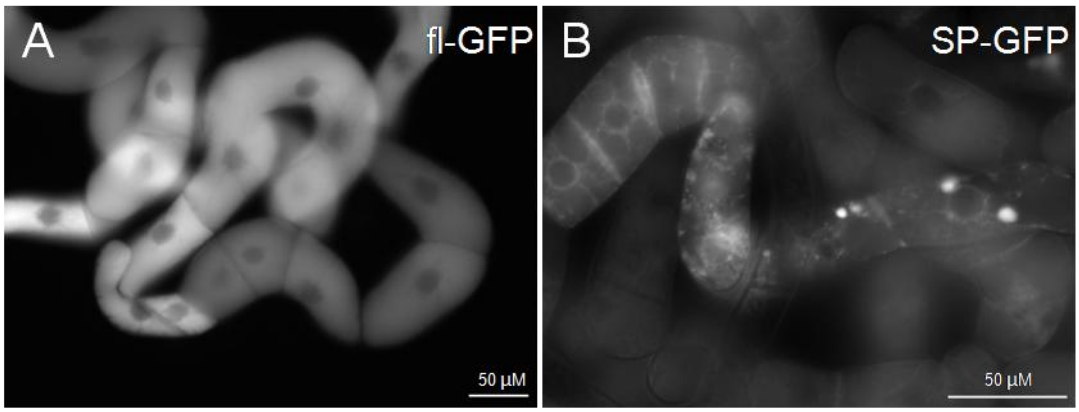

5.11 Actin organization to the conjugated peptides of ginkbilobin-2 pretreated with phytotropins and actin drugs

The following figures showed the actin response of 4-day-old GF11 cells incubated with 2 µM various subdomain conjugates A1, A2, A3 of ginkbilobin-2 (RBA1, RBA2, RBA3) and unconjugated BP100 (RBP100) over 30 min pretreated with phytotropins (2 M µM IAA and 10 µM NPA) for 10 min and and actin drugs (1 µM latrunculin B and 1 µM phalloidin) for 30 min. (A-D) Actin response in addition of RBA1, RBA2, RBA3 and RBP100 preincubated with IAA. (E-H) Actin response in addition of RBA1, RBA2, RBA3 and RBP100 preincubated with NPA. (I-L) Actin response in addition of RBA1, RBA2, RBA3 and RBP100 preincubated with latrunculin B. (M-P) Actin response in addition of RBA1, RBA2, RBA3 and RBP100 preincubated with phalloidin. Scale bar 20 µm.

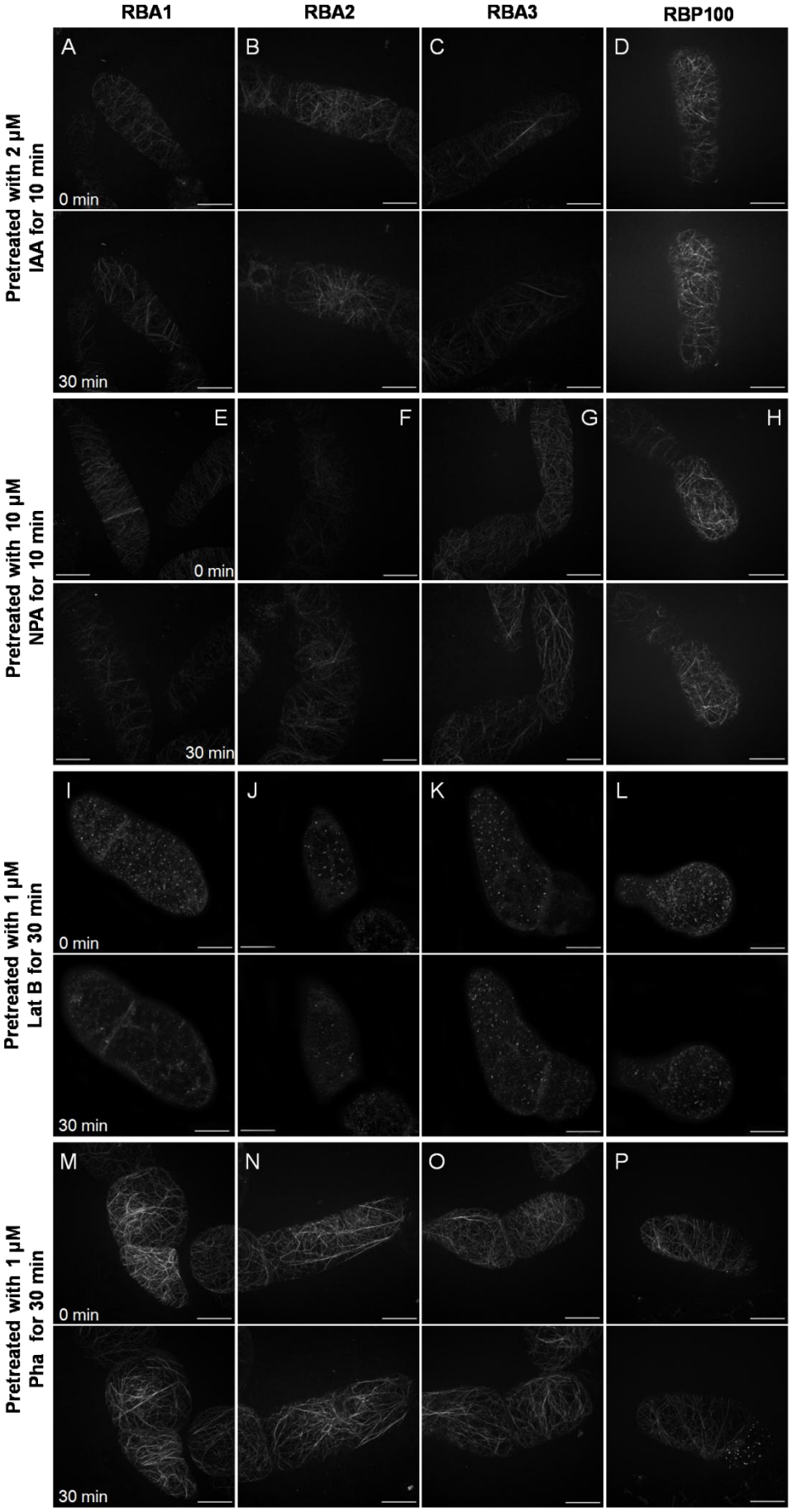
RBA1
RBA2
RBA3
RBP100
Pretreated with 2 µM IAA for 10 min
Pretreated with 10 µM NPA for 10 min
Pretreated with 1 µM Lat B for 30 min
Pretreated with 1 µM Pha for 30 min
A
B
C
D
E
F
G
H
I
J
K
L
M
N
O
P
0 min
30 min